The Term Structure of Macroeconomic Risks at the Effective Lower Bound

Guillaume Roussellet*

First version: January 2017 This version: May 2020

Abstract

This paper exploits the term structures of treasury yields to extract information about macroeconomic dynamics during the effective lower bound period (ELB). I introduce a new no-arbitrage macro-finance affine model jointly representing stochastic inflation trend and volatility with a short-term nominal yield that can be persistently stuck at its lower bound. The model consistently attributes movements in the long-end of treasury curves to the pricing of macroeconomic shocks, providing a tighter identification of inflation components. Estimation performed on U.S. real and nominal treasuries reveals that the ELB period coincides with lower inflation trend and elevated inflation volatility. These adverse inflation outcomes produce significant deflation fears, leading investors to be averse to tightening monetary policy shocks and justifying an ELB embrace by the monetary authority. Lifting off can have destabilizing effects depending on the anchoring of expectations of a binding ELB, leaving room for unconventional monetary policy effectiveness.

JEL Codes: C58, E43, G12

Key-words: Affine Term Structure Model, Zero Lower Bound, QTSM, TIPS, Liftoff Probabilities, Inflation Risk Premia.

*McGill University – Desautels School of Management, 1001 Sherbrooke St. West, Montreal QC H3A 1G5, Canada, guillaume.roussellet@mcgill.ca

1 Introduction

Short-term sovereign yields in the U.S. have shown an unprecedented behavior during the last decade being stuck at virtually zero for an exceptionally long period. This effective lower bound episode (ELB henceforth) represents a complete game-changer for both practitioners and researchers, since conventional monetary easing becomes unfeasible. Existing macroeconomic theories disagree on whether and how reaching the ELB can be destabilizing, generating either no change, a deflation spiral, or increased inflation volatility (see e.g. the debate between Cochrane (2017) and Christiano (2017)). The validation of these predictions constitutes an empirical challenge due to limited data, and most results rely on comparisons of simple statistics of macroeconomic variables pre- and post-ELB, with questionable robustness.

Traditional macro-finance term structure models have proved limited to explore this potential shift in macroeconomic and interest rate dynamics, mostly because they were developed pre-ELB. Although they are parsimonious and provide elegant pricing formulas, these affine models fail to reproduce a short-term interest rate bounded from below or its behavior, notably persistence, at the lower bound. A growing literature on ELB-consistent yield curve models had some success in addressing these shortcomings, losing at the same time the tractability and simplicity of traditional affine models, and showing limited flexibility in incorporating macroeconomic variables or stochastic volatility (see e.g. Black (1995) or Kim and Singleton (2012)).

In this paper, I investigate what sovereign Treasury curves reveal about macroeconomic dynamics at the effective lower bound. I propose a new way of jointly modeling sovereign yields with observable macroeconomic variables in a tractable, affine, and ELB-consistent framework. In my model, macroeconomic

dynamics are driven by both a slowly moving trend and stochastic volatility, both of which are priced by investors. These components have an explicit impact on the likelihood of a binding ELB and on the expected path of future short rates, while the current rate can be stuck at virtually zero. A particular feature of the model is that it does not assume an exogenous regime shift when the ELB starts binding, but rather uses information available throughout the sample to identify pricing relationships. By being able to provide an explicit link between macroeconomic trends and volatilities and sovereign yields even during the ELB, my model extends the traditional macro-finance affine models *à la* Ang and Piazzesi (2003).

I exploit the model to investigate the potential change in inflation dynamics when the economy reaches the ELB. Inflation shocks represent a natural interest since the primary target of monetary policymakers is to anchor inflation expectations and to curb inflation volatility. The model gathers unobserved inflation trend and volatility factors as well as two yield-specific latent factors that follow an autoregressive structure. Pricing targets consist of 1- to 10-year maturity nominal and real U.S. treasury yields observed monthly from 1990 to 2015.

The estimation provides three main takeaways. First, treasury yield curves uncover the existence of adverse inflation outcomes during the ELB period. Inflation trend and volatility filtered from the model show persistently large undershooting and overshooting, respectively, compared to the pre-ELB period. Extracting risk premium from the yield curves, I confirm investors that perceive these inflation outcomes as bad events. Inflation volatility is a key driver of the nominal term premium through the investors prices of risk. These premia grow with maturity, from virtually zero at the 1y maturity to between 100bps and 350bps during the ELB period for the 10y. This result contrasts

with low or negative term premia commonly implied by affine models, which can be an artifact of a fast model-implied mean-reversion from the ELB. In turn, the inflation trend decrease creates significant deflation fears at the short-end (−190bps), while long-term inflation premia remain small and slowly moving. Both short- and long-ends of nominal and real term structures contain significant information about inflation components, either through investors risk aversion or through the differential pricing of both assets.

Second, I provide evidence that the monetary policy response to "*embrace the ELB*" (Williams (2009)) and to delay the increase of short-term rates (i.e. the liftoff) was in line with investors perceptions. I find that investors attribute a high premium to lifting off early largely because of their fears of future adverse inflation outcomes. I derive the risk premium associated with a synthetic digital bond, paying off only if the economy is still at the ELB at maturity. This asset is considered a hedge, and its premium is negative. A further decomposition provides evidence that this fear is substantially driven by inflation trend and volatility shocks, a previously undocumented result which complements the findings of Breach et al. (2020). This has implications for monetary policy-makers. Because I obtain a significant risk premium associated with the liftoff event, I am able to show that investors prefer to delay the exit from the ELB. This translates into large discrepancies between the objective and risk-neutral expected liftoff date.

Third, a non-linear impulse-response analysis reveals that a tightening monetary policy shock produces more diverse and uncertain effects during a binding ELB period compared to normal times. When the ELB expectations become well-anchored in 2012, the effects on both inflation and financial outcomes reverse and gather a significant uncertainty as well. The main implication is that unconventional monetary policy episodes, through forward

guidance and large-scale asset purchases, can help mitigating the fears associated with the liftoff. I show that these shifts can be observed mostly for QE2 and around the start of calendar-based forward guidance. As such, unconventional monetary policies can have competing effects on long-term yields by lowering the expectation component but increasing the inflation risk premium.

This paper gathers both a modeling and an empirical innovation relative to the existing literature. First, for the former, the new term structure model introduced below combines tractability for pricing nominal and real Treasuries, for the joint dynamics of their yields with macroeconomic components, as well as the ability to enforce a sticky effective lower bound. In particular, the model obtains closed-form pricing formulas, forecasts of yields and of macroeconomic variables, and of liftoff probabilities thanks to its affine property. The latter is preserved by combining the non-negative gamma-zero process of Monfort et al. (2017) to represent the ELB-consistent short rate, with a standard quadratic term structure framework, which is known for its empirical performance (see Ahn, Dittmar, and Gallant (2002), Leippold and Wu (2007), or Andreasen and Meldrum (2018) for an ELB application).[1] The estimated model shows appealing empirical properties, with low pricing errors on both nominal and real term structures (3bps and 12bps on average, respectively) with only four factors, and generates a substantially higher probability to stay at the lower bound compared to a standard QTSM.

Other approaches have been considered to produce an ELB-consistent pricing framework. The shadow-rate approach enforces the ELB and constitutes an alternative to the present model, stepping outside the class of affine models

[1] Alternative ELB-consistent models include Filipovic, Larsson, and Trolle (2017) linear-rational term structure model, Feunou, Fontaine, Le, and Lundblad (2015) nearly arbitrage-free framework and Renne (2014) discrete states model.

(see e.g. Kim and Singleton (2012)).[2] These models usually pose a challenge at the estimation stage, since pricing has to be approximate and show limited flexibility.[3] Conversely, by staying in the affine world, my model can be estimated quickly even incorporating macroeconomic and yields forecasts, as well as proxies for liftoff probabilities, in the set of empirical targets. This strengthens the identification of the joint macroeconomic and financial dynamics at virtually no cost, a particularly important feature when yields show limited variability at the ELB.

Second, my paper contributes to a strand of empirical literature devoted to understanding the dynamics of inflation through the study of nominal and real treasuries. Numerous term structure models have been developed to extract inflation dynamics and inflation pricing from asset prices (see e.g. Barr and Campbell (1997), Evans (1998), or Anderson and Sleath (2001)). However, most papers either do not consider ELB-consistency (Haubrich et al. (2012) or Fleckenstein et al. (2017)), are focused on the estimation of the relative liquidity of real bonds (e.g. Grischenko and Huang (2013), Abrahams et al. (2016), or D'Amico et al. (2018)) or are focused on inflation dynamics pre-ELB binding period (see Ang et al. (2008) Adrian and Wu (2009), and Campbell et al. (2017)). In contrast, the empirical exercise in this paper focuses on the potential change of interdependence between inflation components and asset prices in and out of the ELB. As such, it builds on the insights of both Mertens

[2]Examples include and are not limited to Lemke and Vladu (2016), or Andreasen and Meldrum (2015) for yield-only models, Bauer and Rudebusch (2016), or Wu and Xia (2016) for macro-finance models. Carriero et al. (2018) employ a shadow rate model on nominal and real term structures jointly. Branger et al. (2016) incorporate a shadow rate in a long-run-risk model with inflation dynamics.

[3]Approximate estimation methods for SR models have been developed by Kim and Priebsch (2013), Priebsch (2013), Wu and Xia (2016) and Christensen and Rudebusch (2015). Computationally intensive algorithms are also provided by Andreasen and Meldrum (2011) and Pericoli and Taboga (2015).

and Williams (2018) and King (2019) that a non-linear model is needed to understand the shift implied by an economy stuck at the ELB.

Last, and importantly, this paper has implications for the macroeconomic literature looking at the relevance of the zero-lower bound for structural models (see Gali (2018) for a survey of New Keynesian models). Cochrane (2017) advocates that none of the stark predictions of standard macroeconomic models on inflation are validated during the ELB period, and proposes a new model based on fiscal theory. Debortoli, Gali, and Gambetti (2020) show the irrelevance of the ELB for macroeconomic impulse-responses through a time-varying VAR. In turn, papers looking at asset prices show that there is a significant link between inflation components and treasury curves (see e.g. Ehling, Gallmeyer, and Heyerdahl-Larsen (2018)), a moderate but significant change in inflation densities when the ELB is binding (see Mertens and Williams (2018)), or a change of correlation of inflation with stock returns (Gourio and Ngo (2020)) during the ELB. This paper contributes to this debate by trying to extract information about inflation dynamics from asset prices using a reduced-form model, hence not taking a stand on the structural assumptions underlying the above works.

The remainder of the paper is organized as follows. Section 2 presents the formulation and the properties of the term structure model. I present the identification strategy and estimation method in Section 3. Section 4 details the fitting results and the decomposition of the nominal yield curve and the economic implications of the model in terms of inflation risk. Section 5 focuses on a dynamic comparative analysis of inflation risk in and out of the ELB through an impulse response exercise and concludes by an event study around unconventional monetary policy episodes. Section 6 concludes.

2 A model for inflation risks and interest rates

I introduce the joint asset pricing model for nominal and real yields and observable macroeconomic factors. While I formulate it directly with inflation dynamics, a more general specification is presented in Online Appendix B.1. I specify the pricing factors physical dynamics and express the nominal pricing kernel such that all yields are closed-form functions of the factors. Importantly, the framework imposes a lower bound for the nominal term structure.

2.1 Inflation risks: central tendency and stochastic volatility

I assume that the dynamics of a $K \times 1$ vector of risk factors X_t are given by the following vector autoregression:

$$X_{t+1} = \mu + \Phi X_t + v_{t+1}\,, \tag{1}$$

where $v_{t+1} \overset{i.i.d.}{\sim} \mathcal{N}(0, \Sigma)$. This state vector contains three sets of variables, such that $X_{t+1} = \left(\pi^*_{t+1},\, \sigma_{t+1},\, y'_{t+1}\right)'$ where both π^*_{t+1} and σ_{t+1} are univariate and y_t is a vector of yield-specific risk factors of size $K_y \times 1$.

Inflation is defined as the year-on-year log-change of the CPI-U index, denoted by $\mathcal{I}_{t+1}$, such that $\pi_{t+1} = \log(\mathcal{I}_{t+1}/\mathcal{I}_{t-11})$. Inflation dynamics are driven by the first two elements of X_{t+1}, and the inflation rate is given by:

$$\pi_{t+1} = \bar{\pi} + \pi^*_t + \sigma_{t+1}\varepsilon^{\pi}_{t+1}\,, \tag{2}$$

where $\varepsilon^{\pi}_{t+1} \overset{i.i.d.}{\sim} \mathcal{N}(0,1)$, and is uncorrelated with v_{t+1}. Equation (2) has two key features drawn from the literature on modeling and forecasting inflation.

First, π_t^* is the time-varying component of expected inflation and can be interpreted as the inflation central tendency (or conditional mean, see e.g. Feunou and Fontaine (2014)), representing its low frequency fluctuations. Second, σ_{t+1} is the stochastic volatility of inflation thus reproducing its high frequency fluctuations.[4]

2.2 A ZLB-consistent short-rate specification

In this economy, there exists a riskless n-maturity nominal investment accessible to investors at time t at price $P_t^{(n)}$. The one-month riskless yield is known at t and given by $r_t = -\log P_t^{(1)}$. Assuming no-arbitrage, r_t cannot in principle become negative since investors would just hoard cash otherwise, thus is bounded by the zero lower bound (ZLB). In practice, there is an effective lower bound $\underline{r}$ (ELB) that can differ from zero and the observed yield evolves above this ELB. I use indifferently ELB or ZLB in the remainder of the paper. Figure 1, left panel, presents the time series of the one-year nominal yield, and emphasizes the important stickiness of the ELB, from 2009 to the end of our sample in 2015.

To reproduce these features, I assume that the short-term yield is given by:

$$r_t = \underline{r} + z_t \,, \tag{3}$$

where z_t is a univariate non-negative stochastic process whose dynamics are given by the autoregressive gamma-zero introduced by Monfort et al. (2017).

[4] Motivation for time-varying volatility and short- and long-run components of inflation can be found among others in Engle (1982), Stock and Watson (2007), Cogley, Primiceri, and Sargent (2010), or Garcia and Poon (2018).

These dynamics are defined through a mixing Poisson variable P_t, such that:

$$\mathsf{P}_t \,\big|\, (X_t,\, z_{t-1}) \sim \mathcal{P}\left(\alpha + \phi z_{t-1} + \kappa\beta' X_t + (\beta' X_t)^2\right) \quad \text{and} \quad z_t \,\big|\, \mathsf{P}_t \sim \Gamma\left(\mathsf{P}_t\,;\, c\right), \tag{4}$$

where ϕ, κ, c and α are positive scalars, β is of dimension $K \times 1$, and P_t is the degree of freedom of the gamma distribution.

I obtain three main implications from this specification. First, it is imperative that the Poisson intensity stays positive. A sufficient condition for this is that $\alpha = \frac{\kappa^2}{4}$. Second, z_t is (almost surely) equal to zero as long as the Poisson draw P_t are equal to zero. This allows the short-rate process r_t to reach its lower bound $\underline{r}$ and spend several periods there. Since the process X_t is persistent, the linear combination $\beta' X_t$ will typically be close to zero several months in a row. Even though I allow only one linear combination of the state vector to enter the Poisson intensity for parsimony, the specification is general enough such that inflation mean and volatility factors π_t^* and σ_t as well as yield-specific factors y_t all impact the current one-period yield. As noted by Andreasen and Meldrum (2018), this restriction turns out to be supported by data in a standard quadratic model and is barely restrictive. Last, the probabilities of reaching or getting away from the lower bound crucially depend on the current values of both inflation and yield-specific risk factors since the Poisson intensity involves the current values of the risk factors. The technical properties of the gamma-zero distribution are detailed in Appendix A.1.

To gain some insight about the short-rate dynamics, I consider a system where X_t consists only of the inflation trend π_t^* with zero mean, and where the ELB is zero. I parameterize the dynamics such that r_t has a persistence coefficient of 0.97, inflation trend is fairly persistent at $\Phi = 0.9$, its volatility is

18bps $\sqrt{\Sigma} = 0.18$, and inflation trend shocks impact the short rate positively.[5] I obtain the following decomposition:

$$r_t = \underbrace{0.97 r_{t-1} + 8.1\beta^2 \left(2.504 + \pi^*_{t-1} + 0.1\pi^{*^2}_{t-1}\right)}_{\text{Expectation: } \mathbb{E}_{t-1}(r_t)} + \underbrace{9\beta^2 \left[1 + 0.2\pi^*_{t-1}\right] v_t + \beta^2 \left[v_t^2 - 0.0324\right] + \varepsilon^z_t}_{\text{Shocks}}, \quad (5)$$

where ε^z_t a zero-mean martingale difference sequence conditionally on π^*_t and z_{t-1} uncorrelated with v_t. Equation (5) emphasizes interesting features coming out of our short-rate specification. First, inflation expectations above target ($\pi^*_{t-1} > 0$) tend to increase both policy rates forecasts and volatility. Thus, high inflation expectations tend to increase the policy response of the central bank to inflation expectation shocks (see Ang et al. (2011)). Second, the distribution of shocks to the short-rate is skewed by the presence of squared inflation trend shocks v_t^2, reflecting the fact that the policy rate is bounded from below. Third, the key parameter in Equation (5) is the inflation sensitivity β, which scales every term and controls the strength at which the central bank responds to inflation trend shocks with its policy rate.

The general short-rate specification resembles greatly the one used in quadratic term structure models (QTSM, see e.g. Ahn et al. (2002) or Breach et al. (2020)). This allows both inflation mean and volatility shocks to have time-varying impacts on the distribution of future yields. I view this as a desirable feature representing monetary policy shifts as in Ang et al. (2011). One key distinction of my model with respect to a standard QTSM is that it directly enables

[5] More specifically, the change of monotonicity of the quadratic function happens at $\pi^*_t = -5\%$. This imposes $-\frac{\kappa}{2\beta\rho} = -5 \iff \kappa = 9\beta$.

to identify periods when the lower bound $\underline{r}$ is binding, i.e. when realizations of z_t are equal to zero. I extensively exploit this feature in the empirical Section.

2.3 The pricing kernel

I assume that the pricing kernel of the representative investor M_t is given by an exponential-affine function of the shocks to the risk factors:

$$M_{t+1} = \exp\left(- r_t + \lambda_t' \, v_{t+1} + \lambda_r \, [r_{t+1} - \mathbb{E}_t(r_{t+1})] - \xi_t \right) \tag{6}$$

where $\mathbb{E}_t(\bullet)$ is the conditional expectation operator given the filtration spanned by the history of $\{X_t, \pi_t, z_t\}$, and ξ_t is the convexity adjustment such that $\mathbb{E}_t\left(M_{t+1}\right) = e^{-r_t}$ (see Appendix A.1 and Internet Appendix B.3 for their respective form). As in Duffee (2002), the prices of risk are in the essentially affine form:

$$\lambda_t = \lambda_0 + \lambda_1 X_t \, . \tag{7}$$

Equation (6) emphasizes that both inflation trend and volatility shocks are priced. As usual with this type of kernel, investors attribute a price λ_t to shocks v_{t+1}, and empirical estimates usually reflect that they fear positive inflation shocks. However, a second channel is at play when investors price unexpected shocks to the short rate. The latter is driven by squares of the Gaussian shocks v_{t+1}, and investors also price large deviations to their inflation components forecasts, whatever their sign (see also Appendix A.1). Such a channel is consistent with two-sided fears of inflation as documented for instance in Kitsul and Wright (2013).[6]

[6]Note that it is possible to impose that inflation risks are unspanned by the nominal yield curve through linear constraints on the prices of risk and on the parameters driving the joint dynamics of yield-specific and inflation factors (see Joslin et al. (2014))

Despite the non-linearities in the pricing kernel specification, I show in Appendix A.2 that it has a self-preserving structure hence the risk-neutral dynamics of the risk factors are given by:

$$X_{t+1} = \mu^{\mathbb{Q}} + \Phi^{\mathbb{Q}} X_t + v_{t+1}^{\mathbb{Q}}\,, \tag{8}$$

where $v_{t+1}^{\mathbb{Q}} \overset{i.i.d.}{\sim} \mathcal{N}\left(0, \Sigma^{\mathbb{Q}}\right)$ and:

$$\begin{aligned}
\mu^{\mathbb{Q}} &= \left(I_K - 2\frac{\lambda_r c}{1-\lambda_r c}\Sigma\beta\beta'\right)^{-1}\left(\mu + \Sigma\lambda_0 + \frac{\kappa\lambda_r c}{1-\lambda_r c}\Sigma\beta\right) \\
\Phi^{\mathbb{Q}} &= \left(I_K - 2\frac{\lambda_r c}{1-\lambda_r c}\Sigma\beta\beta'\right)^{-1}\left(\Phi + \Sigma\lambda_1\right) \\
\Sigma^{\mathbb{Q}} &= \left(I_K - 2\frac{\lambda_r c}{1-\lambda_r c}\Sigma\beta\beta'\right)^{-1}\Sigma\,.
\end{aligned} \tag{9}$$

The risk-neutral dynamics of the short-rate factor z_t is then given by:

$$z_t \,\big|\, X_t,\, z_{t-1} \overset{\mathbb{Q}}{\sim} \mathrm{ARG}_0\left(\alpha^{\mathbb{Q}} + \phi^{\mathbb{Q}} z_{t-1} + \kappa^{\mathbb{Q}}\beta^{\mathbb{Q}\prime} X_t + \left(\beta^{\mathbb{Q}\prime} X_t\right)^2\,;\, c^{\mathbb{Q}}\right)\,, \tag{10}$$

where $\alpha^{\mathbb{Q}}$, $\phi^{\mathbb{Q}}$ and $c^{\mathbb{Q}}$ are equal to their physical counterparts divided by $(1-\lambda_r c)$, and both $\kappa^{\mathbb{Q}}$ and $\beta^{\mathbb{Q}}$ are equal to their physical counterparts divided by $\sqrt{1-\lambda_r c}$.

2.4 Pricing the term structures

By no-arbitrage, the prices of nominal bonds of any maturity n are given by:

$$P_t^{(n)} = \mathbb{E}_t^{\mathbb{Q}}\left[\exp\left(-\sum_{i=0}^{n-1} r_{t+i}\right)\right]\,, \tag{11}$$

where $\mathbb{E}_t^{\mathbb{Q}}(\bullet)$ is the risk-neutral conditional expectation operator given the filtration spanned by the history of $\{X_t,\, \pi_t,\, z_t\}$. In contrast, inflation-protected securities (TIPS hereafter) are securities paying off at maturity the realized inflation from issuance to maturity. For any maturity n, their prices are given by:[7]

$$P_t^{(n)^*} = \mathbb{E}_t^{\mathbb{Q}}\left[\exp\left(-\sum_{i=0}^{n-1} r_{t+i}\right)\frac{\mathcal{I}_{t+n}}{\mathcal{I}_t}\right], \tag{12}$$

where $\mathcal{I}_t$ is the CPI-U index. Despite the non-Gaussian structure of the framework, I show in Appendix A.2 that the risk-neutral dynamics of inflation, of the risk factors and of the short-rate obtained in the previous Section define a so-called *affine (quadratic) term structure model* (ATSM-QTSM) where it is well-known that the pricing Equations (11) and (12) can be obtained through closed-form recursions:

$$\begin{aligned} P_t^{(n)} &= \exp\left(\mathcal{A}_n + \mathcal{B}_n' X_t + X_t' \mathcal{C}_n X_t + \mathcal{D}_n z_t\right), \\ P_t^{(n)^*} &= \exp\left(\mathcal{A}_n^* + \mathcal{B}_n^{*\prime} X_t + X_t' \mathcal{C}_n^* X_t + \mathcal{D}_n^* z_t\right). \end{aligned} \tag{13}$$

The explicit recursions are functions of the risk-neutral parameters and are detailed in Appendix A.3. Corresponding continuously-compounded nominal and real yields are given by $R_t^{(n)} := -\frac{1}{n}\log P_t^{(n)}$ and $R_t^{(n)^*} := -\frac{1}{n}\log P_t^{(n)^*}$, respectively, and are linear-quadratic combinations of the risk factors.

The fact that the model belongs to the class of QTSMs allows for several extremely useful features. Contrary to the shadow-rate model, I do not need to rely on any approximation or simulation technique to obtain the term structures since the pricing formulas are analytic (see for instance Wu and Xia

[7] I discuss the specifics of TIPS in the Section detailing the data, notably our treatment of the so-called inflation lag used to compute the actual payoff of TIPS.

(2016) or Christensen and Rudebusch (2015)). Second, the combination of physical and risk-neutral dynamics imply that forecasts of yields of all maturities at all horizons are obtained as closed-form linear-quadratic combinations of the risk factors (see Internet Appendix B.5). Although the previous properties are usually available in a standard QTSM, the gamma-zero distribution properties provide the conditional probabilities to stay at the ELB for any length n as a closed-form function of the factors:

$$\mathbb{P}_t\left(r_{t+1:t+n} = \underline{r}\right) = \exp\left(\mathcal{A}_n^{\mathbb{P},(\text{zlb})} + \mathcal{B}_n^{\mathbb{P},(\text{zlb})\prime} X_t + X_t' \mathcal{C}_n^{\mathbb{P},(\text{zlb})} X_t + \mathcal{D}_n^{\mathbb{P},(\text{zlb})} z_t\right), \tag{14}$$

where the loadings are given through closed-form recursions in Appendix A.4. These two points prove particularly useful in practice for improving the quality of the estimation through the use of forecast data, both for yields levels and liftoff probabilities (see e.g. Kim and Orphanides (2012)). I include both in the empirical application below.

3 Estimation Strategy

This section presents the estimation procedure for the macrofinance model. After detailing the observable data used for identifying the latent risk factors, I show that the model can be expressed in a linear-quadratic state-space form, thus facilitating the estimation through quadratic filtering methods.

3.1 Identification strategy and data

I consider monthly U.S. data from January 1990 to March 2015.We obtain the one-month nominal interest rate from Bloomberg (<*GB1M Index*>) and longer nominal zero-coupon yields for maturities of 1, 2, 3, 5, 7, and 10 years

from Gurkaynak et al. (2007). For TIPS, I compute liquidity-adjusted synthetic yields by subtracting zero-coupon inflation swap rates of maturities of 1, 2, 3, 5, 7, and 10 years obtained from Bloomberg (*<USSWITx Crncy>*, converted to continuous compounding) to the corresponding-maturity nominal bond (see Christensen and Gillan (2012) or Moench and Vladu (2018)).[8] The inflation-linked swap data starts in July 2004. I treat the months following Lehman failure – from September 2008 to February 2009 – as missing data since most movements on the TIPS interest rates during this period can likely be attributed to the disruption of the inflation-indexed market (see for instance D'Amico et al. (2018)). The year-on-year inflation rate is computed from the CPI-U series of the BLS database, and is lagged of 3 months to be consistent with the reference price index.

[Include Figure 1 and Table 1 about here.]

To better identify the joint dynamics of yields and inflation, I follow Kim and Orphanides (2012) and Chernov and Mueller (2012) adding two sets of survey forecasts in the observable variables. I obtain series of expected average inflation over the next 1 and 10 years and nominal yields forecasts for the 10-year maturity, respectively 3-months and 1-year ahead from the Philadelphia Fed database. All these surveys are quarterly. Last, I extract data about the probabilities of seeing no interest rate increase by the Fed between each date and one year ahead from the primary dealer survey conducted by the New York Fed. I collect information starting from January 2011. Details on

[8] Christensen and Gillan (2012) note that though not free from liquidity risk, inflation swaps are less likely to be affected by liquidity issues compared to TIPS (see also Fleckenstein et al. (2017)). For papers who focus on extracting the liquidity risk from TIPS data, see for instance Sack and Elasser (2004), Shen (2006), Gurkaynak et al. (2010), Grischenko and Huang (2013), Pflueger and Viceira (2013) or D'Amico et al. (2018). Fleckenstein et al. (2014) note that the TIPS bonds were also subject to large mispricing during the crisis.

these computations are provided in internet Appendix B.7. Time series and standard descriptive statistics of interest rates and inflation are presented in Figure 1 and in Table 1. Surveys and ZLB probability series are represented in Figure 2.

3.2 The state-space formulation

All the observables except two are closed-form linear-quadratic combinations of the state variables X_t and z_t. On the one hand, the probabilities to stay at the ZLB are exponential linear-quadratic functions of the states (see Equation (14)). I therefore take the natural logarithm of the probabilities data. On the other hand, inflation dynamics involve the i.i.d. shocks ε_t^π and the lag of π_t^* which are not readily included in our state variables VAR. I readily take care of this issue augmenting the states as $X_t^{(aug)} = (X_t', \varepsilon_t^\pi, \pi_{t-1}^*)'$ without changing their VAR structure. Again, the inflation rate becomes a linear-quadratic function of all states.

I now turn to the state-space formulation of the model. To fix ideas, consider that all our observables at time t are gathered in a vector denoted by $\mathcal{Y}_t^{(obs)}$. This vector contains all 13 yields, the inflation rate, 4 inflation and yields survey series and one ZLB log-probabilities series. I assume that all these observables except inflation are measured with errors, and write:

$$\mathcal{Y}_t^{(obs)} = \mathcal{A} + \mathcal{B}' X_t^{(aug)} + \mathcal{C}\,\mathrm{Vec}\left(X_t^{(aug)} X_t^{(aug)'}\right) + \mathcal{D}\, z_t + \eta_t\,, \tag{15}$$

where each element of η_t is independent and $\eta_{i,t} \overset{i.i.d.}{\sim} \mathcal{N}(0, \omega_i^2)$. For parsimony, I assume the the standard deviation of the measurement errors is the same across nominal yields on the one hand, across TIPS yields on the other hand, and calibrated to the average forecaster disagreement.

I consider 2 latent yield-specific factors y_t ($K_y = 2$). Without further assumptions, the latent factors can still be rotated and are not uniquely identified (see for instance Joslin et al. (2011)). I therefore impose several constraints on the parameters driving the dynamics of our risk factors. The conditional covariance matrix Σ is diagonal and the part corresponding to y_t is set to identity. I impose that the autoregressive matrix Φ is upper triangular so all factors can feedback on π_t^*. For identification, I also impose that the model-implied mean of π_t^* is null so that average inflation is given directly by $\bar{\pi}$.

Since the measurement equations (15) are linear-quadratic in the states and all states form an affine process, I can readily estimate the model using the *Quadratic Kalman filter* of Monfort et al. (2015). The method allows to take care of the quadratic part of the state-space model more efficiently than standard approximate non-linear filters such as the extended and unscented Kalman filters. The algorithm is detailed in internet Appendix B.6. I perform a first estimation with the previous constraints and set all non-significant parameters to zero for a second round, and repeat until all parameters are significant.

3.3 Estimates and fitting properties

The estimated parameters are presented on Tables 3 and 4 in the Appendix. Inflation central tendency has persistence of 0.89, and inflation volatility of 0.98. Estimates of β show that the central bank reacts to inflation trend shocks ($\beta_{\pi^*} = 0.05$) but not significantly to inflation volatility, thus caring primarily about medium/long-run inflation (see Table 4). Under the risk-neutral measure, inflation volatility has and receives feedback from all the other risk factors including inflation trend. It therefore plays a significant role

in the pricing of both nominal bonds and TIPS of long maturities through risk premia.

[Insert Table 2 and Figure 2 about here.]

The model is able to provide both a reasonable fit on the survey data, and an impressive fit on both term structures with only 4 factors. RMSEs range from 2bps to 5bps for nominal rates and from 6bps to 17bps for real rates (see Table 2). To put this in perspective, these fitting properties are comparable to the model of Abrahams et al. (2016), who use a 5-factor ATSM to fit both yield curves. In comparison, my model only has 4 factors, two of which are identified by inflation dynamics. Quadratic models are well-known to fit yields more efficiently than a pure linear model with the same number of factors (see e.g. Leippold and Wu (2007)). I also illustrate the skew in short-rates distributions by plotting their marginal densities on Figure 11 in the online Appendix.

Last, I check that both objective and risk-neutral dynamics are well-identified by performing the LPY tests of Dai and Singleton (2002) (see online appendix B.8 for details). It is well-known that models relying on positive processes have difficulties passing these tests (see e.g. Backus et al. (2001)). Conversely, Figure 10 and Table 6 of the technical Appendix show that both conditions cannot be rejected at the 5% level, thus validating my empirical estimates.

4 The destabilizing effects of reaching the ELB

This section explores the in-sample behavior of inflation components at the ELB and how they are priced by investors. Using nominal and real term structures with inflation data emphasizes that reaching the ELB leads to persistent

adverse inflation outcomes and generates large premia in real assets.

4.1 Inflation components at the lower bound

I first explore how inflation trend and volatility factors behave when the economy reaches the ELB. The filtered factors obtained both from inflation and bond yields are presented on Figure 3, along with the date at which the the ELB starts binding (vertical red line).

[Insert Figure 3 about here.]

Both inflation central tendency and volatility exhibit a large shift at the ELB. Inflation trend π_t^* mostly fluctuates around zero between 1990 and 2009, jumps to -4% in 2009 ($\overline{\pi} = 2.84\%$ so inflation forecast is -1.16%), and stays consistently in the negative territory afterwards. At the end of the sample, the filtered π_t^* is close to -3%, largely below its mean of 0. A similar phenomenon can be seen for inflation volatility, which is comprised below 1% before the ELB starts binding, but spikes up to 3% and stays elevated afterwards (see Figure 3).

The identification of inflation components through bond yields therefore reveals that the ELB episode in the U.S. resulted in persistent inflation shocks, where inflation stays below target with a large volatility during the five ELB-binding years included in the sample. These stylized facts are hard to identify using historical inflation data only, but can be efficiently unveiled by the ELB-consistent asset pricing model. The ELB-consistency is key to identify these features of inflation volatility, and explains why our estimates differ from the empirical evidence of Breach, D'amico, and Orphanides (2020).[9] Asset prices

[9]Note that the series of inflation volatility considered are the 1y inflation uncertainty while we have a monthly uncertainty estimate.

thus reveal that the predictions of benchmark new-Keynesian models cannot be completely invalidated by the data (see e.g. Debortoli, Gali, and Gambetti (2020)).

4.2 Asset pricing implications of the ELB

While the short-term nominal rate is stuck at the ELB, long-term rates continue to move in accordance with the state variables, including inflation shocks. Swanson and Williams (2014) argue that these long-term rates have been virtually unaffected by the ELB, possibly because of term premia responsiveness to news. Using a term structure model provides the ability to obtain such decomposition of long-term yields into the expected path of future short-term rates (*expectation component*) and the associated term premium, which is presented on the left-panel of Figure 4.

[Insert Figure 4 about here.]

The behavior of the 1-year maturity yield post-crisis reflects the persistence of the ELB-binding period. The 1-year and 10-year expectation components become, respectively, virtually null and below 100bps during that period. The latter is nearly constant through time, emphasizing the stability of investors expectations that short-term interest rates will remain low for a long period of time.

This leads most of the nominal yields fluctuations to be explained by the term premium that investors require to hold these bonds. Consistently with the term structure literature, this term premium is time-varying and upward sloping with maturity. During recessions, the short-term premium tends to go down while the 10-year term premium goes up if anything. This phenomenon

reflects the difference of uncertainty with respect to maturity: during recessions, the central bank is expected to push down interest rates creating low short-term uncertainty while the timing of recovery and the path of future interest rates is unclear. This is particularly blatant during the ELB period where the 1-year nominal risk premia component is null whereas most of the 10-year nominal term premium is consistently positive and volatile, fluctuating between 100bps and 350bps. Most of the responsiveness of the long-run yields during the ELB can therefore be attributed to fluctuations in the term premium.

Looking at the (normalized) factor loadings enables to investigate to which extent the fluctuations of nominal yields can be explained by inflation components. These loadings are presented on Figure 5, left panels.

[Insert Figure 5 about here.]

The main insight provided by Figure 5 is that inflation central tendency is nearly unpriced in the term structure of nominal yields, while inflation volatility is one of the most important factors to explain nominal yields' fluctuations, especially at medium-run maturities. For the 5-year yield for instance, the linear loading associated with σ_t is the most important, at par with that of the latent factor $y_{1,t}$, and ranks close second for the quadratic loadings (see left panel of Figure 5).

Since inflation volatility does not cause any of the other factors and β_σ is not significantly different from zero (see Table 3 and 4), its impact on bond yields can only go through its influence on the market prices of risk, thus nominal term premia. Therefore, heightened inflation volatility during the ELB period results in a widespread increase in risk premia since it fundamentally alters the way investors price financial and economic shocks. This importance

of inflation volatility for investors is hidden in asset prices, and can only be uncovered through a consistent macrofinance approach.

4.3 The price of inflation shocks at the ELB

By pricing not only nominal but also TIPS, the estimated model provides a deeper view on the pricing of inflation shocks at the ELB. In this Section, I analyze the decomposition of expectation and term premia components into inflation expectations and inflation risk premia (IRP).

Before detailing the empirical results, I briefly explain how to interpret inflation compensation components. Nominal bonds are exposed to high inflation since their cashflows are settled in dollar terms. Nominal bond yields therefore embed a term compensating investors for the risk of high inflation. Conversely, TIPS are completely immune to inflation fluctuations since their payoffs are set in consumption basket units. The *breakeven inflation rate* (BEI) – difference between matched-maturity nominal and TIPS yields – isolates the inflation compensation components of nominal bonds. By no-arbitrage, the BEI is equivalent to the fixed rate of a swap paying off the compounded inflation at maturity, a hedge against positive inflation shocks. The associated IRP will be positive whenever investors desire such a hedge (fear of high inflation) and negative whenever they desire the exposure (fear of deflation). I use this terminology in our analysis below, and present IRP time series on the right panel of Figure 4.

The empirical estimates contrast starkly with the patterns of nominal term premia. At the short-end, the BEI is very volatile and the ELB coincides with a surge in deflation fears where the IRP reaches an all time low of nearly -200bps. The post-2009 period shows a convergence to close-to-zero historical

values but the inflation risk premium stays consistently negative between 0 and −60bps. Conversely, the 10-year inflation premium component has a low volatility, and slowly fluctuates around 0. When the ELB hits, the long-run IRP also peaks down but to a moderate −60bps before converging to positive historical values. These moderate movements at the long-end provide evidence that long-term inflation expectations are well-anchored despite the ELB, and that there is low uncertainty around the level of the 10-year ahead compounded inflation rate. Economic agents are confident that the central bank will be able to stabilize inflation in the long-run and avoid a deflation spiral, although the persistent shock in inflation trend leads to a severe undershooting of inflation.

To understand the source of short-term deflation fears, I yet again provide the (normalized) estimated loadings of BEI for different maturities with respect to the different risk factors on Figures 5 and 6. Note that although quadratic terms are important for nominal bonds and TIPS, they are nearly irrelevant for the pricing of BEI.

[Insert Figure 6 about here.]

Figure 5 shows that inflation central tendency π_t^* is the primary driver of BEI, moving nearly one-for-one at the 1-year maturity. Thus, BEI rates go down during the ELB period mostly because of the persistent drop in the inflation central tendency component. This translates into the drop of the expected inflation component and of the IRP at the short-run maturity. Figure 6 further reveals that the short-term deflation fears are mostly related to the central tendency and the yield factors, and are if anything attenuated by the increased inflation volatility during the ELB period (1-year IRP estimates drop by 0.4% for a one standard deviation decrease in π_t^*, but increase by 0.2% for a one standard deviation increase in σ_t).

In the end, the analysis of nominal and real bond yields shows that reaching the ELB coincides with adverse inflation outcomes which are costly for investors. The fall of inflation trend creates high fear of deflation which translates into higher real rates in the economy, mostly for short and medium-run maturities. The increase of inflation volatility further increases the real and nominal term premium, driving medium and long-run yields upwards. I interpret both these components as slowing down the recovery since high real rates lead to underinvestment in the economy.

4.4 Discussion of the risk premium estimates

Fleckenstein et al. (2017) estimate a positive and stable 1-y inflation premium (IRP henceforth), contained between 0bps and 30bps on a 2009/2015 sample. In comparison, their 10-y inflation premium is very volatile, peaking at 80bps in January 2010 and going to negative territory at -35bps from early 2015 onwards. Haubrich et al. (2012) imposes risk premia estimates to be functions of the conditional volatility of interest rates only. This produces long-term real term premia and inflation risk premia that are roughly constant over time and consistently positive. Abrahams et al. (2016) produce obtain a 10-y IRP fluctuating between -40bps and 90bps from 2000 to 2014. Breach et al. (2020) find a 2y and 10y IRP negative during the ELB period (about -50bps) but more pronounced business cycle fluctuations. These existing studies attribute both a different sign and magnitude to IRP since they all gather different modeling features.

In comparison my model combines several of these features altogether such as including inflation expectations data and inflation stochastic volatility. The IRP estimates produced above shows time series behavior consistent

with Abrahams et al. (2016) and overall magnitudes consistent with Breach et al. (2020). The sign of my IRP estimates are particularly in line with the model-free estimates of Camba-Mendez and Werner (2017). However, the ELB constraint on nominal yields is unique to my framework and uncovers the particular pattern of a large dip and convergence detailed above, with a larger volatility for the short-run IRP.

To confirm the added value of the ELB-consistency in addition to the quadratic structure of my framework, I estimate a standard QTSM without the gamma-zero variable but with the same structure as presented in Section 2. In essence, the estimated QTSM is very close to the one in Andreasen and Meldrum (2018) or Breach, D'amico, and Orphanides (2020) but adding the ELB constraint. I replace Equations (3) and (4) by: $r_t = \underline{r} + \kappa\beta' X_t + (\beta' X_t)^2$ and impose that the price of risk associated with the short-term interest rate λ_r is equal to zero. I focus on the stickiness of the ELB for both models by simulating data using the estimated parameters from both models to compare the probabilities of obtaining interest rates below 25bps. The difference is striking: the Gamma-QTSM model implies a 28% probability to reach the ELB and a 30% probability to obtain a short-term interest rate below 25bps while the standard QTSM-implied probability for staying below 25bps is only 9%. This reflects on the decomposition of nominal rates: the standard QTSM-implied expected components are consistently higher and more volatile than for our model. This shows that the standard QTSM cannot generate enough persistence at the ELB. This complements the analysis of Andreasen and Meldrum (2018), showing that adding a gamma-zero variable to the standard QTSM can solve some of its inconsistencies during the ELB.

5 The impact of embracing the ELB

So far I have been able to identify realized inflation shocks during the ELB-binding period. In this section, I analyze the impact of the adverse ELB inflation outcomes on the monetary policy conducted by the Fed during the ELB episode. I find that embracing the ELB as a response helped containing bond term premia and deflation fears of investors, and that lifting off before the end of the sample would have resulted in increased economic uncertainty.

5.1 Investors willingness to stay at the ELB

From the aftermath of the recession onwards, monetary policymakers in the U.S. chose to "embrace the ELB" (Williams (2009)) by leaving short-term nominal rates to close to zero values for a substantial amount of time. From a theoretical perspective, it is natural to believe that this policy response was desirable with the Fed being as accommodating as possible, provided adverse inflation outcomes. My model provides empirical evidence of this feature, by extracting the risk premium associated with a binding lower bound in the future.

I construct the ELB risk premium as follows. For simplicity of exposition, consider that the effective lower bound parameter is null ($\underline{r} = 0$). Using the model estimates, I form the price of an ELB Arrow-Debreu security, providing \$1 if and only if the ELB binds between today and any date $t+n$ in the future. Such a price $P^{(n)}_{elb,t}$ is given by:

$$P^{(n)}_{elb,t} = \mathbb{E}^{\mathbb{Q}}_t \left[\exp\left(-\sum_{i=0}^{n-1} r_{t+i} \right) \times \mathbb{1}\left\{ r_{t+1:t+n} = 0 \right\} \right] = \mathbb{Q}_t \left[r_{t+1:t+n} = 0 \right] . \quad (16)$$

Equation (16) equates the price of the ELB Arrow-Debreu security with the

risk-neutral probability to stay at the ELB. In the model, these risk-neutral probabilities are obtained in closed-form and given by the risk-neutral counterpart of Equation (14) as:

$$\mathbb{Q}_t\left(r_{t+1:t+n}=0\right)=\exp\left(\mathcal{A}_n^{\mathbb{Q},(\text{zlb})}+\mathcal{B}_n^{\mathbb{Q},(\text{zlb})'}X_t+X_t'\mathcal{C}_n^{\mathbb{Q},(\text{zlb})}X_t+\mathcal{D}_n^{\mathbb{Q},(\text{zlb})}z_t\right). \tag{17}$$

Similarly, the price of this bond purging from the risk premium is given by the physical probability to stay at the ELB, i.e. $\mathbb{P}_t\left(r_{t+1:t+n}=0\right)$. These physical probabilities are the one fitted by the model consistently with the primary dealer survey data. The ELB risk premium can be defined as:

$$\text{RP}_{elb,t}^{(n)}=\frac{1}{n}\log\left(\frac{\mathbb{Q}_t(r_{t+1:t+n}=0)}{\mathbb{P}_t(r_{t+1:t+n}=0)}\right). \tag{18}$$

This risk premium is positive (negative) when staying at the ELB coincides with states of high (low) marginal utility. I thus interpret a negative risk premium as indicative of the desirability of a binding ELB in the future, or fear of lifting-off, as perceived by investors.

Figure 7 presents the time series of both physical and risk-neutral ELB probabilities for maturities of 1 and 5 years. The risk-neutral probabilities (grey line) are a direct outcome of the model, and present estimates nearly always below their physical counterparts (black lines), for both maturities. I translate these differences into the risk premium estimates using Equation (18) and represent them on the bottom-left panel.

[Insert Figure 7 about here.]

The negative ELB risk premium observed throughout most of the period indicates that investors mostly fear that the central bank will be lifting off in the short and medium run. This component goes as negative as -1 starting in

early 2009. The magnitude is comparable to what is found in the credit risk literature comparing risk-neutral and physical default probabilities of entities, but has opposite sign (Driessen (2004) finds a log-ratio of 0.75 for corporates, and Monfort et al. (2020) find 1.5 for some European sovereigns). This premium becomes positive for a few months before QE2, date at which the premium drops back to the negative territory for good. Consistently with the U.S. economic recovery, the 1y ELB risk premium becomes positive again in late 2014 as investors expect and desire the central bank to increase gradually interest rates.

There is thus a significant insurance premium charged by investors to stay at the ELB for a significant amount of time during the ELB-binding period. By keeping the economy in a low interest rate environment, monetary policymakers are in line with both investors expectations and fear or liftoff.

5.2 The inflation drivers of liftoff fears

In the model, the ELB insurance premium can be driven by the shocks of any of the state variables, including inflation components. The liftoff could therefore be seen as an adverse outcome because it coincides with adverse inflation trend and volatility shocks from the investors' perspective. I investigate below to which extent this is the case.

In the model, all the risk premium is generated by the prices of risk parameters λ_t and λ_r (see Equation (6)). To obtain the impact of the pricing of inflation trend shocks, I recompute the counterfactual ELB Arrow-Debreu price after imposing that $\lambda_t^{(\pi^*)} = 0$. In the same fashion, I obtain the counterfactual price without inflation volatility pricing by restricting $\lambda_t^{(\sigma)} = 0$. For both cases, I also impose that $\lambda_r = 0$ to avoid having pricing of inflation

components through short-rate shocks. Denoting the counterfactual ELB risk premia by $\text{RP}_{elb,t}^{(-\pi^*,n)}$ and $\text{RP}_{elb,t}^{(-\sigma,n)}$ respectively, I obtain the contribution of each component by:[10]

$$\text{RP}_{elb,t}^{(\pi^*,n)} = \text{RP}_{elb,t}^{(n)} - \text{RP}_{elb,t}^{(-\pi^*,n)} \qquad \text{and} \qquad \text{RP}_{elb,t}^{(\sigma,n)} = \text{RP}_{elb,t}^{(n)} - \text{RP}_{elb,t}^{(-\sigma,n)}. \quad (19)$$

[Insert Figure 8 about here.]

I present the decomposition of the ELB risk premium at the 1y and 5y maturity on panels (a) and (b) of Figure 8, respectively. Two striking features emerge from the picture. First, the risk premium associated to inflation trend shocks always contribute negatively to the ELB risk premium, both for the 1y and 5y series and consistently throughout the ELB period. Second, the pricing of inflation volatility shocks contributes negatively to the ELB risk premium before late 2011, and positively afterwards, with an order of magnitude at least twice bigger than the contribution of inflation trend. This is particularly blatant for the 5y maturity (panel (b) of Figure 8) where the inflation volatility contribution grows positive after the tapering of 2014. Up to late 2011, the two components contribute to nearly half of the observed negative ELB premium.

This result indicates that lifting-off is associated with adverse inflation trend outcomes during the entire ELB period, and adverse inflation outcomes up until late 2011, date at which the fact that the ELB will be binding for at least a year becomes perfectly anchored. Thus, a monetary policy embracing the ELB seems in line with the way investors priced inflation shocks at least until late 2011. Past that date, there are term structure effects at play. Lifting-

[10] Note that the physical probabilities are not impacted by this change in the prices of risk. The computation performed in Equation (19) is equivalent to computing $\frac{1}{n}\log\left(\frac{\mathbb{Q}_t(r_{t+1:t+n}=0)}{\widetilde{\mathbb{Q}}_t(r_{t+1:t+n}=0)}\right)$, where $\widetilde{\mathbb{Q}}_t$ is the alternative risk-neutral probability.

off during the next year is still associated with adverse inflation volatility outcomes whereas lifting-off before the next five years is not.

5.3 Liftoff shocks as destabilizing

Since liftoff shocks are at least partly associated with adverse inflation outcomes in the observed data, I derive impulse-response functions to observe the effect of an exogenous liftoff shock on inflation components and asset prices in the economy. Note that the model inherently embeds nonlinear dynamics through the short rate specification (4). Both magnitude and sign of impulse-responses thus critically depend on the starting state. This property is conform with the fact that the ELB represents a fundamentally different regime and that the reaction of asset prices to the exact same shocks can be different in normal times and during the ELB (see e.g. Lansing (2020)). A key advantage of the framework is that impulse-responses for each of these variables of interest are obtained in closed-form, so there is no need for simulations.

I perform impulse-responses resulting from a tightening monetary policy shock starting from each date in the sample. To make sure that the liftoff shock is independent from inflation shocks, I impose that it is fully reflected by shocks to the yield-specific factors y_t. The size of the shock is equal to the conditional volatility of the short-term interest rate at the starting date. These tightening/liftoff shocks range from 1bps to 17bps, and average 12bps before the ELB-binding period, and about 3bps afterwards. For ease of presentation, I group the IRFs over three sub-periods: *(i)* pre-ELB, *(ii)* unanchored ELB-binding [2009-2011] and *(iii)* anchored ELB-binding [2012-2015], and compute both the median, min and max responses over these sub-periods. The entire methodology is detailed in internet Appendix B.9.

[Insert Figure 9 about here.]

Figure 9 presents the results of this exercise. These IRFs show different features depending on the considered subsample. In normal times, a tightening monetary policy shock tends to be accompanied by further increases up to 30bps after a year, and slowly decays afterwards. This shock raises the term structure mostly through the expectation component so the yield curve flattens. Inflation expectations increase by 1bp, while both short and long-run inflation risk premia go down by 2bps, and inflation volatility slightly decrease. These are fairly moderate effects with respect to the size of the initial tightening policy shock. This shock has virtually no impact on ELB probabilities as such a situation is very unlikely during the first part of the sample.

A binding ELB produces two distinct effects that are present during the unanchored and anchored periods. The former produces qualitatively the same effects as when the ELB is not binding, but has a wider uncertainty. The size of the initial shock produces a maximum of 20bps on the short-term interest rate. All the median effects on inflation components are virtually the same as in normal times but for some starting conditions the magnitude becomes twice bigger (+2bps of inflation trend, −4bps of 1y IRP). Probabilities to go back to a binding ELB go down by 15 percentage points and the effect on ELB risk premium is positive, emphasizing that agents were not expecting the ELB to be binding for long.

The second type of effects can be observed during the anchored ELB period, where most effects are either dampened or reversed. An initial tightening shock of a few basis points quickly goes back to an undershooting of the short-term by up to 15bps. Long-term yields go down as well by about 10bps, mostly through the expectation component, creating a steepening of the curve. This

shock produces deflationary pressure up to −2bps, and effects on inflation risk premia are reversed as well. Inflation volatility goes up persistently up to 12bps annualized after 5 years, emphasizing the higher inflation uncertainty. Last, ELB probabilities overshoot after 1y by up to 15 percentage points, and ELB risk premia become negative emphasizing the ELB desirability.

These findings are consistent with the ELB desirability observed empirically during the crisis. The IRFs reveal that liftoff shocks are destabilizing, even though the magnitude of the monetary tightening is dampened when the ELB is binding. In this case, the effects on inflation components strongly depend on the state of the economy. These results also provide evidence that the ELB-binding period is not homogeneous and the effects of a tightening monetary policy shock depend on whether the expectations to stay at the ELB are well-anchored.

5.4 Unconventional monetary policy at the ELB

I complement the previous analysis by performing an event study around unconventional monetary policy (UMP) episodes, as represented by large scale asset purchases announcements.[11] I ask whether UMP transformed investors' perception of the ELB and the associated risks.

Regarding inflation pricing during the ELB, it is clear from Figure 4 that all UMP episodes except the tapering lead to lower short- and long-run deflation fears by pushing the IRP component upwards. Most notably, QE2 contributed to reduce the 1-y inflation premium from −100bps to approximately 0bps in a few months. Looking at Figures 7-8, we see that these UMP contribute to

[11] UMP event considered here are QE1 and its extension (2008-m12, 2009-m4), QE2 (2010-m11), Operation Twist (2011-m10), QE3 (2012-m10), the Taper Tantrum (2013-m5) and the actual tapering (2013-m12).

push down the ELB risk premia, reflecting a higher willingness of investors to stay at the ELB. Both the extension of QE1 and QE2 stand out as making this premium from positive to negative in just a few months. Overall, this shows that UMP episodes were efficient in *(i)* reducing concerns in the central bank's ability to control deflation risk, and *(ii)* making the liftoff event more undesirable thus enforcing its credibility to investors.

These combined effects can explain why UMP are not always relevant to reduce long-term sovereign yields. Indeed, by reducing deflation fears, the inflation premium component plays against possible signaling effects lowering down the expectation component of nominal yields. Additionally, by making the ELB more desirable, the central bank makes any deviation from its current ELB policy detrimental for investors, thus contributing to a higher premium associated with interest rate risk, driving up the nominal risk premium as well.

Last, the impulse response experiment showed that late 2011 represented a shift in the interdependence between monetary policy shocks and inflation components. Two unconventional monetary policy events are particularly noticeable around that date, namely the start of calendar-based forward guidance (Aug. 2011) and Operation Twist (Oct. 2011) – a sterilized buying of long-term bonds by select short-run maturities. These policies produced both the anchoring of a binding ELB and a resurgence in ELB desirability (see Figures 7). By enforcing the ELB, it contributed to change endogenous responses macroeconomic variables to monetary policy shocks as well as the perception of inflation volatility shocks (see Figure 8).

This analysis suggests that unconventional monetary policies can have effects on both financial and economic outcomes, both through investors expectations and risk premium. Second, some of the desired effects of these policies on long-run yields can be attenuated by adverse reactions of risk pre-

mia. Third, these policies can change endogenous responses of macroeconomic variables to conventional monetary policy shocks, which can influence the real impact of lifting off from the ELB.

6 Conclusion

In this paper, I investigate how asset prices can reveal information about inflation shocks during the effective lower bound period. To achieve such a goal, I provide a new way of modeling both nominal and real yield curves in an affine framework, which allows for the presence of inflation trend and volatility and is consistent with a persistent lower bound on nominal yields. Relying on a combination of quadratic term structure models and the gamma-zero distribution, the model is able to generate a short-term nominal rate stuck at the ELB for several periods. I show that the model provides closed-form formulas for nominal and real interest rates, interest rate forecasts, inflation forecasts, impulse-response functions, and liftoff probabilities under both physical and risk-neutral measure.

I provide empirical estimates of inflation components at the ELB, and study their interactions with monetary policy shocks in the U.S.. The ELB-consistent estimation combined with bond prices reveal that the ELB coincides with adverse inflation outcomes, i.e. persistently low inflation trend and high inflation volatility. These outcomes have a large influence on asset prices, and I show that they generate substantial long-run nominal term premia and short-run deflation fears. Second, I show that monetary policy embracing the ELB is beneficial from the investors perspective, since the liftoff is considered as a bad state of the world. Indeed, an impulse-response exercise reveals that lifting-off can create a wide variety of responses depending on the state of the economy

and whether investors expectations of a binding ELB are well-anchored. Unconventional monetary policies thus turn out to be a key monetary policy tool during the ELB for shaping these effects of the liftoff.

Acknowledgements

The author thanks Yakov Amihud, Daniel Andrei, Patrick Augustin, David Backus, Laurent Barras, Sebastien Bétermier, Mikhail Chernov, Antonio Diez De Los Rios, Robert Engle, Andras Fulop, Bruno Feunou, Jean-Sébastien Fontaine, Xavier Gabaix, René Garcia, Joseph Haubrich, Leonardo Iania, Eric Mengus, Alain Monfort, Sarah Mouabbi, Fulvio Pegoraro, Florian Pelgrin, Eric Renault, Jean-Paul Renne, Glenn Rudebusch, Olivier Scaillet, Christopher Sims, Robert Whitelaw, Jonathan Wright. The author also thanks participants to the 7^{th} Bundesbank term structure workshop, 12^{th} ESWC conference in Montreal, the 9^{th} CFE international conference, 9^{th} annual SoFiE conference, Barcelona Graduate School of Economics Summer Forum in time series, 69^{th} Econometric society European summer meeting, 3^{rd} Econometric society European winter meeting, NYU-Stern QFE seminar, Brown University econometrics seminar, CREST financial econometrics seminar, Banque de France seminar, students' finance, macroeconomics and econometrics seminars at NYU, and students' finance seminar at Columbia.

References

Abrahams, M., T. Adrian, R. Crump, E. Moench, and R. Yu. 2016. "Decomposing Real and Nominal Yield Curve". *Journal of Monetary Economics*.

Adrian, T., and H. Wu. 2009. *The Term Structure of Inflation Expectations*. Staff Reports 362. Federal Reserve Bank of New York.

Ahn, D.-H., R. F. Dittmar, and A. R. Gallant. 2002. "Quadratic Term Structure Models: Theory and Evidence". *Review of Financial Studies* 15, no. 1 (): 243–288.

Anderson, N., and J. Sleath. 2001. *New Estimates of the U.K. Real and Nominal Yield Curves*. Working Paper. Bank of England.

Andreasen, M., and A. Meldrum. 2011. *Likelihood Inference in Non-Linear Term Structure Models: The importance of the Zero Lower Bound*. Tech. rep.

— . 2015. *Market Beliefs about the UK Monetary Policy lift-off Horizon: A No-Arbitrage Shadow-Rate Term Structure Model Approach*. Tech. rep.

Andreasen, M., and A. Meldrum. 2018. "A Shadow Rate or a Quadratic Policy Rule? The Best Way to Enforce the Zero Lower Bound in the United States". *Journal of Financial and Quantitative Analysis*.

Ang, A., G. Bekaert, and M. Wei. 2008. "The Term Structure of Real Rates and Expected Inflation". *Journal of Finance* 63, no. 2 (): 797–849.

Ang, A., J. Boivin, S. Dong, and R. Loo-Kung. 2011. "Monetary Policy Shifts and the Term Structure". *Review of Economic Studies* 78, no. 2 (): 429–457.

Ang, A., and M. Piazzesi. 2003. "A No-Arbitrage Vector Autoregression of Term Structure Dynamics with Macroeconomic and Latent Variables". *Journal of Monetary Economics* 50, no. 4 (): 745–787.

Backus, D. K., S. Foresi, and C. I. Telmer. 2001. "Affine Term Structure Models and the Forward Premium Anomaly". *Journal of Finance* 56, no. 1 (): 279–304.

Barr, D., and J. Y. Campbell. 1997. "Inflation, Real Interest Rates, and the Bond Market: A Study of U.K. Nominal and Index-Linked Bond Prices". *Journal of Monetary Economics* 39:361–383.

Bauer, M. D., and G. D. Rudebusch. 2016. "Monetary Policy Expectations at the Zero Lower Bound". *Journal of Money, Credit and Banking*.

Black, F. 1995. "Interest Rates as Options". *Journal of Finance* 50, no. 5 (): 1371–76.

Branger, N., C. Schlag, I. Shaliastovich, and D. Song. 2016. *Macroeconomic Bond Risks at the Zero Lower Bound*. Tech. rep.

Breach, T., S. D'amico, and A. Orphanides. 2020. "The Term Structure and Inflation Uncertainty". *Journal of Financial Economics (forthcoming)*.

Camba-Mendez, G., and T. Werner. 2017. *The Inflation Risk Premium in the Post-Lehman Period*. Tech. rep. ECB.

Campbell, J. Y., and R. J. Shiller. 1991. "Yield Spreads and Interest Rate Movements: A Bird's Eye View". *The Review of Economic Studies* 58 (3): 495–514.

Campbell, J. Y., A. Sunderam, and L. M. Viceira. 2017. "Inflation Bets or Deflation Hedges? The Changing Risk of Nominal Bonds". *Critical Finance Review*, no. 6: 263–301.

Carriero, A., S. Mouabbi, and E. Vangelista. 2018. "UK Term Structure Decompositions at the Zero Lower Bound". *Journal of Applied Econometrics* 33 (5): 643–661.

Cheng, P., and O. Scaillet. 2007. "Linear-Quadratic Jump-Diffusion Modeling". *Mathematical Finance* 17 (4): 575–698.

Chernov, M., and P. Mueller. 2012. "The Term Structure of Inflation Expectations". *Journal of Financial Economics*, no. 106: 367–394.

Christensen, J. H., and G. Rudebusch. 2015. "Estimating Shadow-Rate Term Structure Models with Near-Zero Yields". *Journal of Financial Econometrics* 13 (2): 226–259.

Christensen, J. H. E., and J. M. Gillan. 2012. *Could the U.S. Treasury Benefit from Issuing More TIPS*. Tech. rep. Federal Reserve Bank of San Francisco.

Christiano, L. 2017. *Comment on Cochrane, Michelson-Morley, Fisher and Occam: The Radical Implications of Stable Quiet Inflation at the Zero Bound*. Tech. rep. Northwestern University.

Cochrane, J. H. 2017. "Michelson-Morley, Fisher, and Occam: The Radical Implications of Stable Quiet Inflation at the Zero Bound". In *NBER Macroeconomics Annual 2017, volume 32*, **by** M. Eichenbaum and J. A. Parker, 113–226. University of Chicago Press.

Cogley, T., G. Primiceri, and T. Sargent. 2010. "Inflation-Gap Persistence in the U.S." *American Economic Journal: Macroeconomics* 2, no. 1 (): 43–69.

D'Amico, S., D. H. Kim, and M. Wei. 2018. "Tips from TIPS: The Informational Content of Treasury Inflation-Protected Security Prices". *Journal of Financial and Quantitative Analysis* 53 (1): 395–436.

Dai, Q., and K. J. Singleton. 2002. "Expectation Puzzles, Time-varying Risk Premia, and Affine Models of the Term Structure". *Journal of Financial Economics* 63, no. 3 (): 415–441.

— . 2000. "Specification Analysis of Affine Term Structure Models". *Journal of Finance* 55, no. 5 (): 1943–1978.

Darolles, S., C. Gourieroux, and J. Jasiak. 2006. "Structural Laplace Transform and Compound Autoregressive Models". *Journal of Time Series Analysis* 27, no. 4 (): 477–503.

Debortoli, D., J. Gali, and L. Gambetti. 2020. "On the Empirical (Ir)Relevance of the Zero Lower Bound Constraint". *NBER Macroeconomics Annual*.

Driessen, J. 2004. "Is Default Event Risk Priced in Corporate Bonds?" *Review of Financial Studies*.

Duffee, G. R. 2002. "Term Premia and Interest Rate Forecasts in Affine Models". *Journal of Finance* 57 (1): 405–443.

Ehling, P., M. Gallmeyer, and C. Heyerdahl-Larsen. 2018. "Disagreement about inflation and the yield curve". *Journal of Financial Economics* 127:459–484.

Engle, R. 1982. "Autoregressive Conditional Heteroscedasticity with Estimates of the Variance of United Kingdom Inflation". *Econometrica* 50, no. 4 (): 987–1007.

Evans, M. D. D. 1998. "Real Rates, Expected Inflation and Inflation Risk Premia". *The Journal of Finance* 53, no. 1 ().

Feunou, B., J. Fontaine, A. Le, and C. Lundblad. 2015. *Term Structure Modeling when Monetary Policy is Unconventional: A New Approach*. Tech. rep.

Feunou, B., and J.-S. Fontaine. 2014. "Non-Markov Gaussian Term Structure Models: The Case of Inflation". *Review of Finance* 18:1953–2001.

Filipovic, D., M. Larsson, and A. Trolle. 2017. "Linear-Rational Term Structure Models". *Journal of Finance* 72 (2): 655–704.

Fleckenstein, M., F. A. Longstaff, and H. Lustig. 2017. "Deflation Risk". 30 (8): 2719–2760.

Fleckenstein, M., F. A. Longstaff, and H. Lustig. 2014. "The TIPS Treasury Bond Puzzle". *Journal of Finance* 69 (5): 2151–2197.

Gali, J. 2018. "The State of New Keynesian Economics: A Partial Assessment". *Journal of Economic Perspectives* 32 (3): 87–112.

Gallant, A., P. Rossi, and G. Tauchen. 1993. "Nonlinear Dynamic Structures". *Econometrica* 61 (4): 871–907.

Garcia, J.-A., and A. Poon. 2018. *Trend Inflation and Inflation Compensation*. Tech. rep. IMF.

Gouriéroux, C., and J. Jasiak. 2006. "Autoregressive Gamma Processes". *Journal of Forecasting* 25:129–152.

Gourio, F., and P. Ngo. 2020. *Risk Premia at the ZLB: A Macroeconomic Interpretation*. Tech. rep. Chicago Fed.

Grischenko, O. V., and J.-Z. Huang. 2013. "The Inflation Bond Risk Premium: Evidence From the TIPS Market". *The Journal of Fixed Income*.

Gurkaynak, R. S., B. Sack, and J. H. Wright. 2010. "The TIPS Yield Curve and Inflation Compensation". *American Economic Journal: Macroeconomics* 2 (1): 70–92.

— . 2007. "The U.S. Treasury yield curve: 1961 to the Present". *Journal of Monetary Economics* 54, no. 8 (): 2291–2304.

Haubrich, J., G. Pennacchi, and P. Ritchken. 2012. "Inflation Expectations, Real Rates, and Risk Premia: Evidence from Inflation Swaps". *Review of Financial Studies* 25 (5).

Joslin, S., M. Priebsch, and K. Singleton. 2014. "Risk Premiums in Dynamic Term Structure Models with Unspanned Macro Risks". *Journal of Finance* 69, no. 3 (): 1197–1233.

Joslin, S., K. J. Singleton, and H. Zhu. 2011. "A New Perspective on Gaussian Dynamic Term Structure Models". *Review of Financial Studies* 24 (3): 926–970.

Kim, D. H., and A. Orphanides. 2012. "Term Structure Estimation with Survey Data on Interest Rate Forecasts". *Journal of Financial and Quantitative Analysis* 47, no. 01 (): 241–272.

Kim, D. H., and M. Priebsch. 2013. *Estimation of Multi-Factor Shadow-Rate Term Structure Models*. Federal Reserve Board Discussion Paper Series. Federal Reserve Board.

Kim, D. H., and K. J. Singleton. 2012. "Term Structure Models and the Zero Bound: An Empirical Investigation of Japanese Yields". *Journal of Econometrics* 170 (1): 32–49.

King, T. 2019. "Expectation and Duration at the Effective Lower Bound". *Journal of Financial Economics* 134 (3): 736–760.

Kitsul, Y., and J. H. Wright. 2013. "The Economics of Options-Implied Inflation Probability Density Functions". *Journal of Financial Economics* 110 (3): 696–711.

Koop, G., H. Pesaran, and S. Potter. 1996. "Impulse Response Analysis in Nonlinear Multivariate Models". *Journal of Econometrics* 74 (1): 119–147.

Lansing, K. 2020. "Endogenous Forecast Switching Near the Zero Lower Bound". *Journal of Monetary Economics* forthcoming.

Leippold, M., and L. Wu. 2007. "Design and Estimation of Multi-Currency Quadratic Models". *Review of Finance* 11, no. 2 (): 167–207.

Lemke, W., and A. Vladu. 2016. *Below the zero lower bound a shadow-rate term structure model for the euro area*. Tech. rep.

Mertens, T., and J. Williams. 2018. *What to Expect from the Lower Bound on Interest Rates: Evidence from Derivatives Prices*. Tech. rep. FRBSF.

Moench, E., and A. Vladu. 2018. *A Fine Term Structure Model for Real and Nominal Bonds*. Tech. rep. Bundesbank (mimeo).

Monfort, A., and F. Pegoraro. 2012. "Asset pricing with Second-Order Esscher Transforms". *Journal of Banking & Finance* 36, no. 6 (): 1678–1687.

Monfort, A., F. Pegoraro, J.-P. Renne, and G. Roussellet. 2020. "Affine Modeling of Credit Risk, Pricing of Credit Events and Contagion". *Management Science (forthcoming)*.

— . 2017. "Staying at Zero with Affine Processes: A New Dynamic Term Structure Model". *Journal of Econometrics* 201 (2): 348–366.

Monfort, A., J.-P. Renne, and G. Roussellet. 2015. "A Quadratic Kalman Filter". *Journal of Econometrics* 187, no. 1 (): 43–56.

Pericoli, M., and M. Taboga. 2015. *Understanding Policy Rates at the Zero Lower Bound: Insights from a Bayesian Shadow Rate Model*. Tech. rep. Bank of Italy.

Pflueger, C. E., and L. M. Viceira. 2013. *Return Predictability in the Treasury Market: Real Rates, Inflation, and Liquidity*. Working Paper. Harvard Business School.

Priebsch, M. 2013. *Computing Arbitrage-Free Yields in Multi-Factor Gaussian Shadow-Rate Term Structure Models*. Tech. rep. FRB.

Renne, J.-P. 2014. "A Model of the Euro-Area Yield Curve with Discrete Policy Rates". *Studies in Nonlinear Dynamics and Econometrics* 21 (1).

Roussellet, G. 2015. "Non-Negativity, Zero Lower Bound and Affine Interest Rate Models". PhD thesis, Dauphine University.

Sack, B., and R. Elasser. 2004. *Treasury Inflation-Indexed Debt: A Review of the U.S. Experience*. Economic Policy Review. Federal Reserve Bank of New York.

Shen, P. 2006. *Liquidity Risk Premia and Breakeven Inflation Rates*. Economic Review. Federal Reserve Bank of Kansas City.

Stock, J. H., and M. W. Watson. 2007. "Has Inflation Become Harder to Forecast?" *Journal of Money, Credit and Banking* 39 (1): 3–34.

Swanson, E. T., and J. C. Williams. 2014. "Measuring the effect of the zero lower bound on Medium- and Longer-Term Interest Rates". *American Economic Review*, no. 104 (10): 3154–3185.

Williams, J. 2009. "Heeding Daedalus: Optimal Inflation and the Zero Lower Bound". *Brookings Papers on Economic Activity*: 1–37.

Wu, J. C., and F. D. Xia. 2016. "Measuring the Macroeconomic Impact of Monetary Policy at the Zero Lower Bound". *Journal of Money, Credit and Banking* 48 (2-3): 253–291.

Figures and Tables

Figure 1 – Nominal and real term structures and inflation data

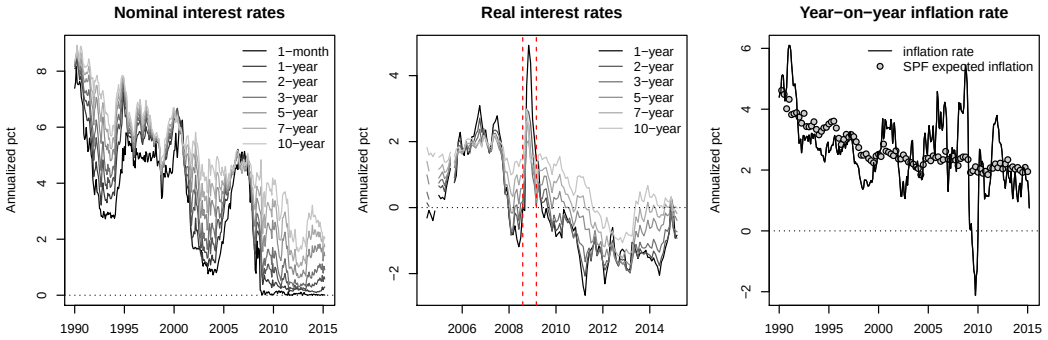

Notes: The left plot presents the time-series of the nominal term structure of interest rates from January 1990 to March 2015. Maturities range from 1 month to 10 years. The middle plot presents the term structure of real rates built as the difference between the nominal zero-coupon interest rates and the inflation swap rates of the same maturity. Observations start in July 2004 and run to March 2015. The vertical red dashed lines indicate the beginning and end of a reduced market liquidity period, that we treat as missing data in the estimation. The right plot presents the realized year-on-year inflation lagged of 3 months (black solid line). The dots superimpose the expected average inflation rate over the next year as measured by the survey of professional forecasters.

Figure 2 – Fitted series of survey data

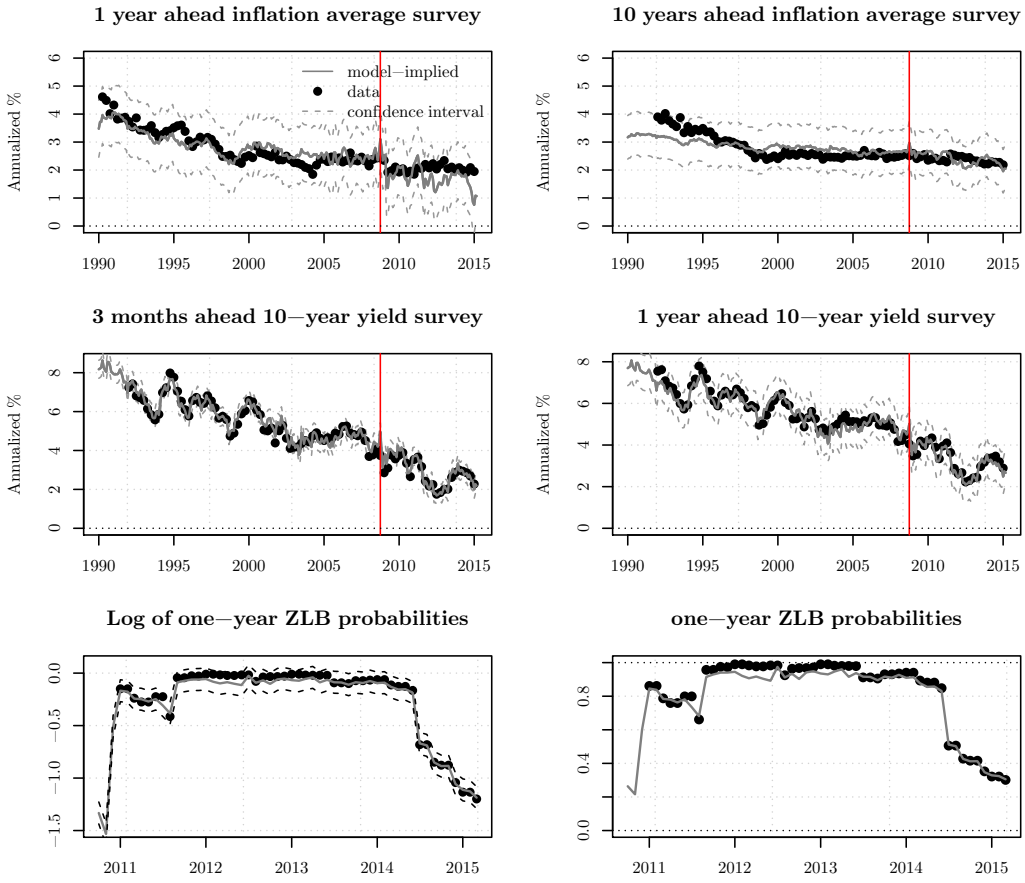

Notes: The black dots correspond to observed forecast data. The grey solid lines correspond to the model-implied forecasted values. Top graphs correspond respectively to the one-year ahead and 10-year ahead inflation average surveys. Medium graphs correspond respectively to the three-months ahead and one-year ahead 10-year yield survey. Units are in annualized percentage points. Bottom graphs correspond respectively to the fitted natural logarithm of ZLB probabilities, and of the exponential of the latter. Confidence intervals computed using the measurement errors standard deviations are plotted in grey dashed lines. The red vertical line delimits the beginning of the zero lower bound period.

Figure 3 – Filtered factors

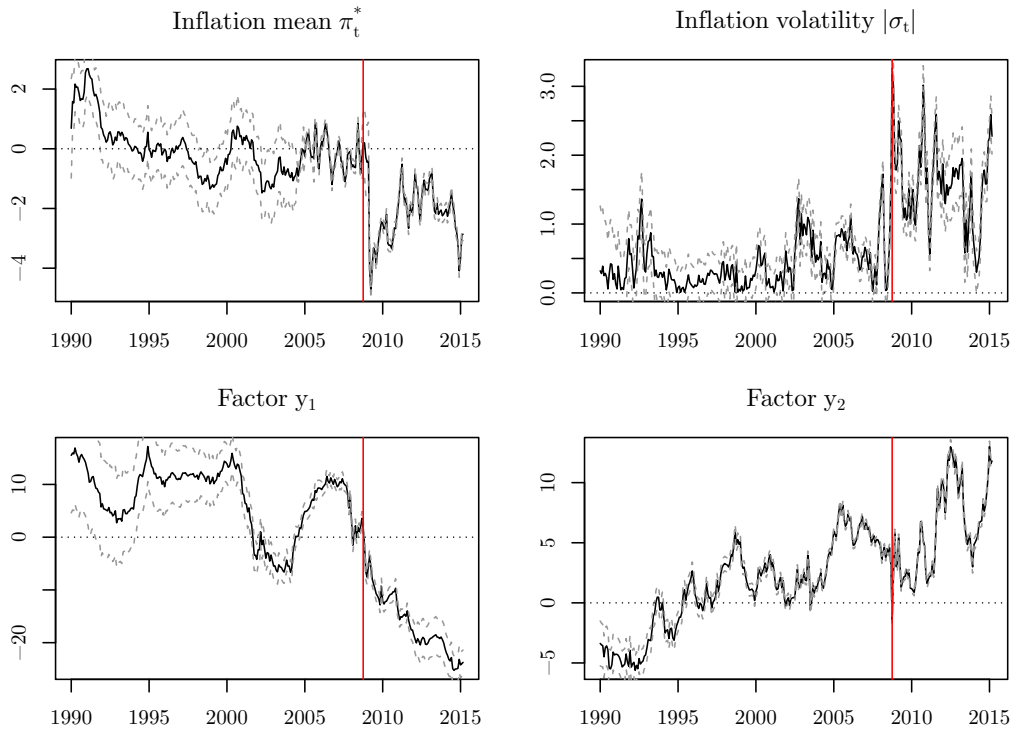

Notes: The unit for inflation central tendency π_t^* and inflation volatility σ_t is in percentage points. Grey dashed lines are 95% confidence bands. The red vertical line delimits the beginning of the zero lower bound period.

Figure 4 – Decomposition of interest rates

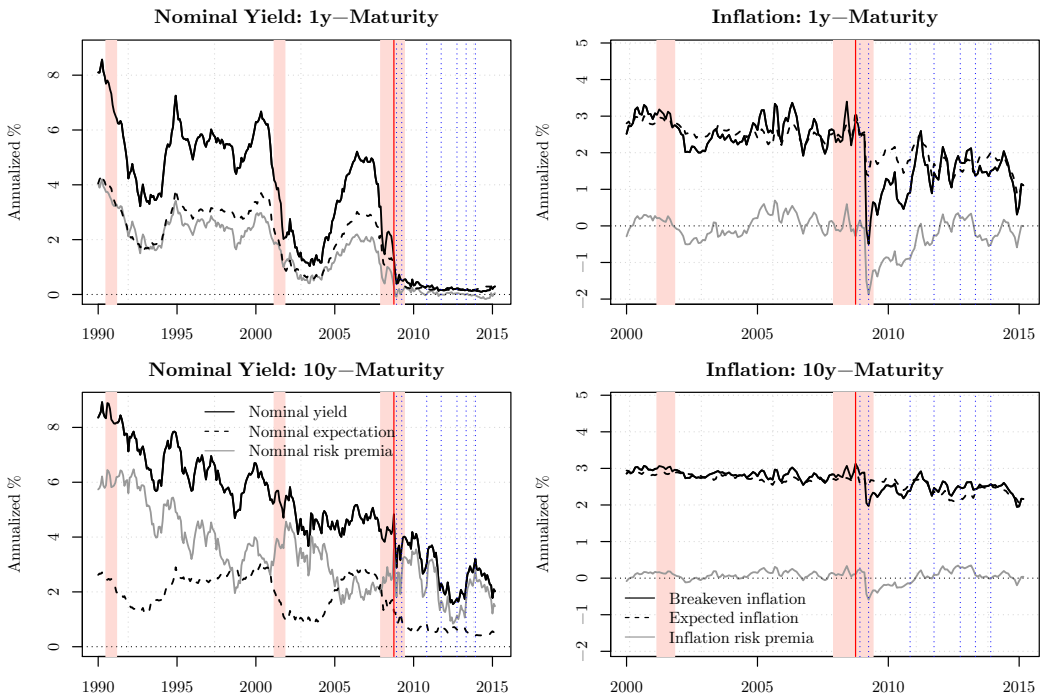

Notes: The first column presents results for the nominal yields components, whereas the second column presents results for the inflation components. The first row presents to the observed data (black solid line), the risk premia (grey solid line), and the expected component (black dashed line) at the one year maturity. The second row presents the same components at the 10 year maturity. Units are in annualized percentage points. The red vertical line delimits the beginning of the zero lower bound period. Pink shaded areas are NBER recession periods. The blue dashed lines are the different unconventional monetary policy episodes, namely: QE1, QE1-extension, QE2, Operation Twist, QE3, Taper tantrum, and the Tapering.

Figure 5 – Factors loadings of yields

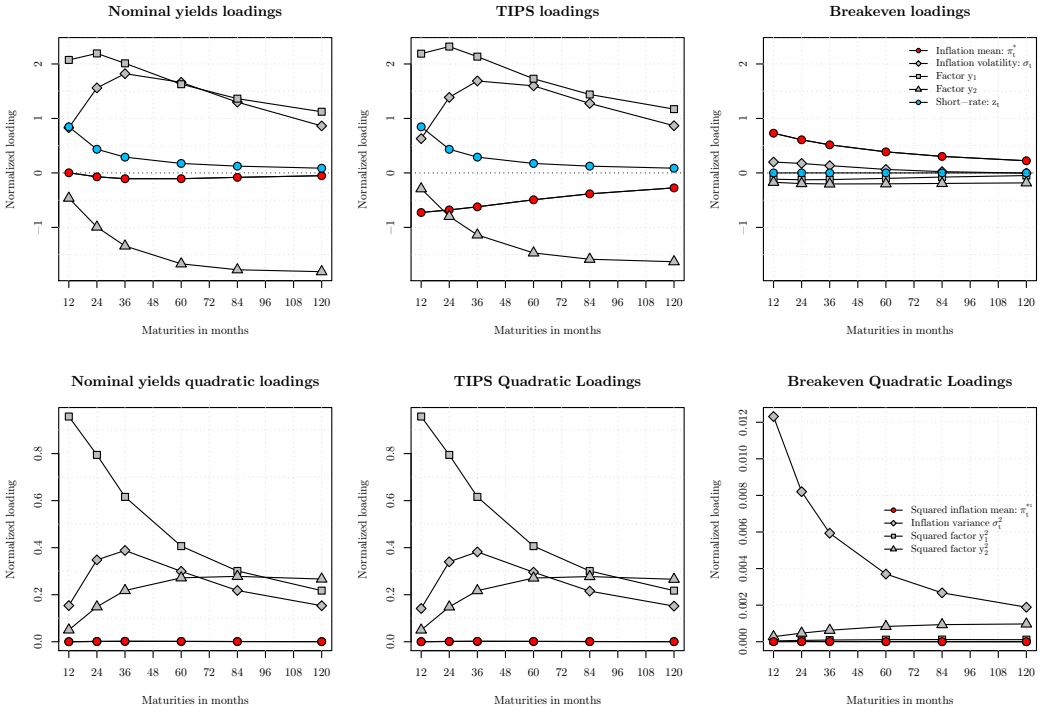

Notes: This plot gathers the linear loadings of the nominal interest rates, of the real rates, and the quadratic loadings with respect to maturity. These loadings are normalized by the in-sample standard deviation of the corresponding filtered factor to be comparable with each other.

Figure 6 – Factors loadings of yields components

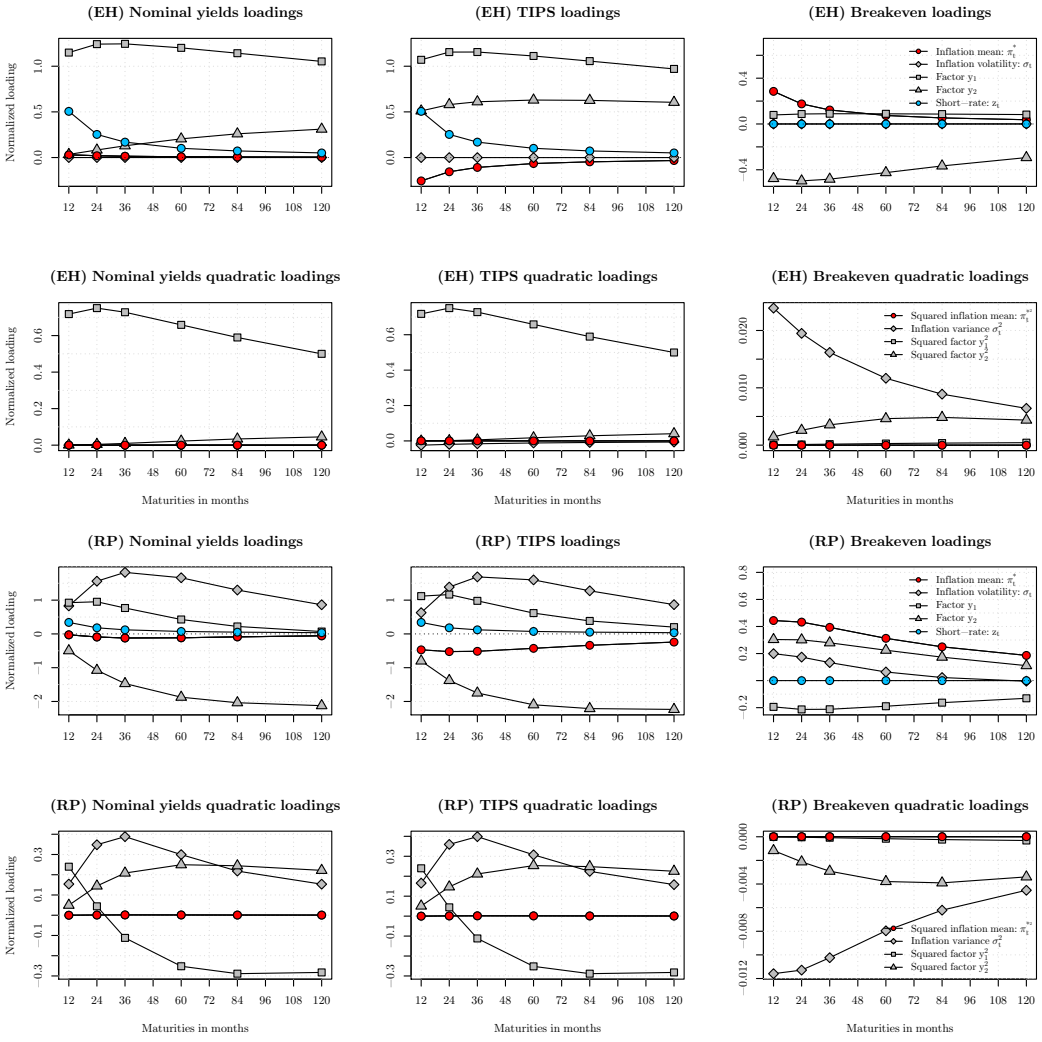

Notes: This plot gathers the linear loadings of the nominal interest rates expectation and risk premia components, of the real rates expectation and risk premia components, and the respective quadratic loadings with respect to maturity. These loadings are normalized by the in-sample standard deviation of the corresponding filtered factor to be comparable with each other.

Figure 7 – Physical and risk-neutral liftoff probabilities

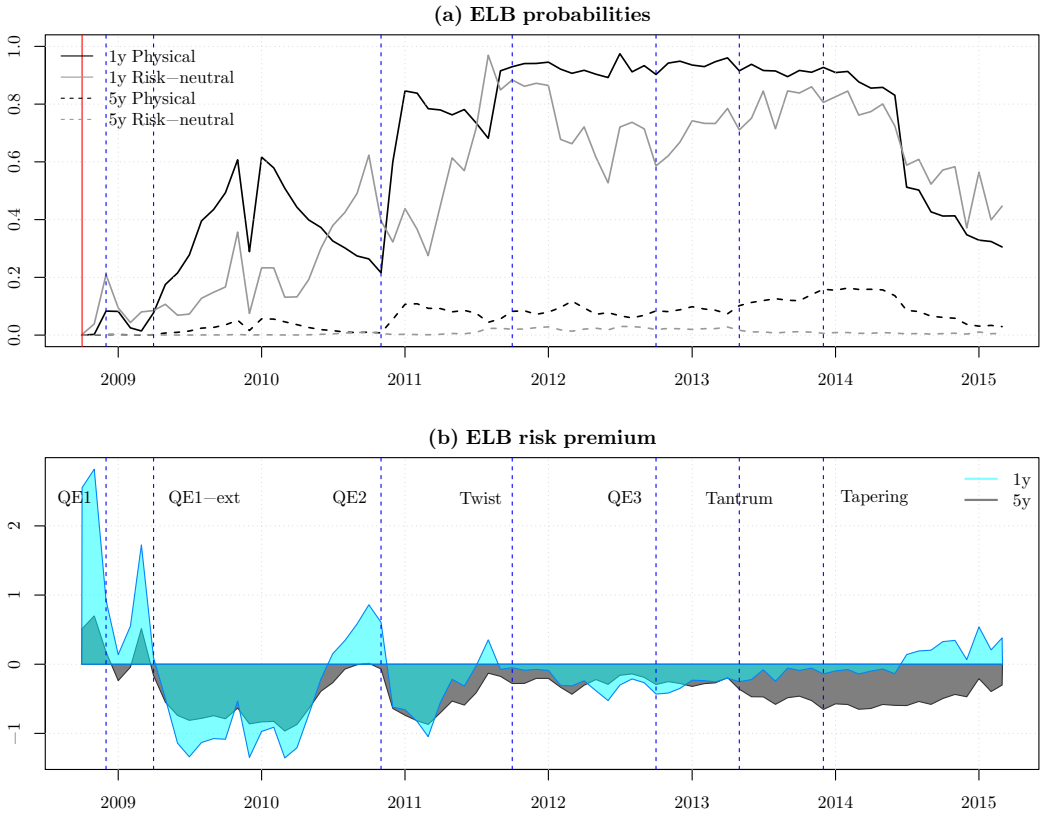

Notes: On panel (a), $\mathbb{P}$- and $\mathbb{Q}$-probabilities are respectively represented with black and grey lines, solid for 1y and dashed for 5y. Panel (b) presents the ELB risk premium as defined by Equation (18), blue for 1y and grey for 5y. All quantities are computed before applying corrections on the factors. The red vertical bar delimits the beginning of the ELB period. The blue dashed lines are the different unconventional monetary policy episodes, namely: QE1, QE1-extension, QE2, Operation Twist, QE3, Taper tantrum, and the Tapering.

Figure 8 – Physical and risk-neutral liftoff probabilities without inflation premia

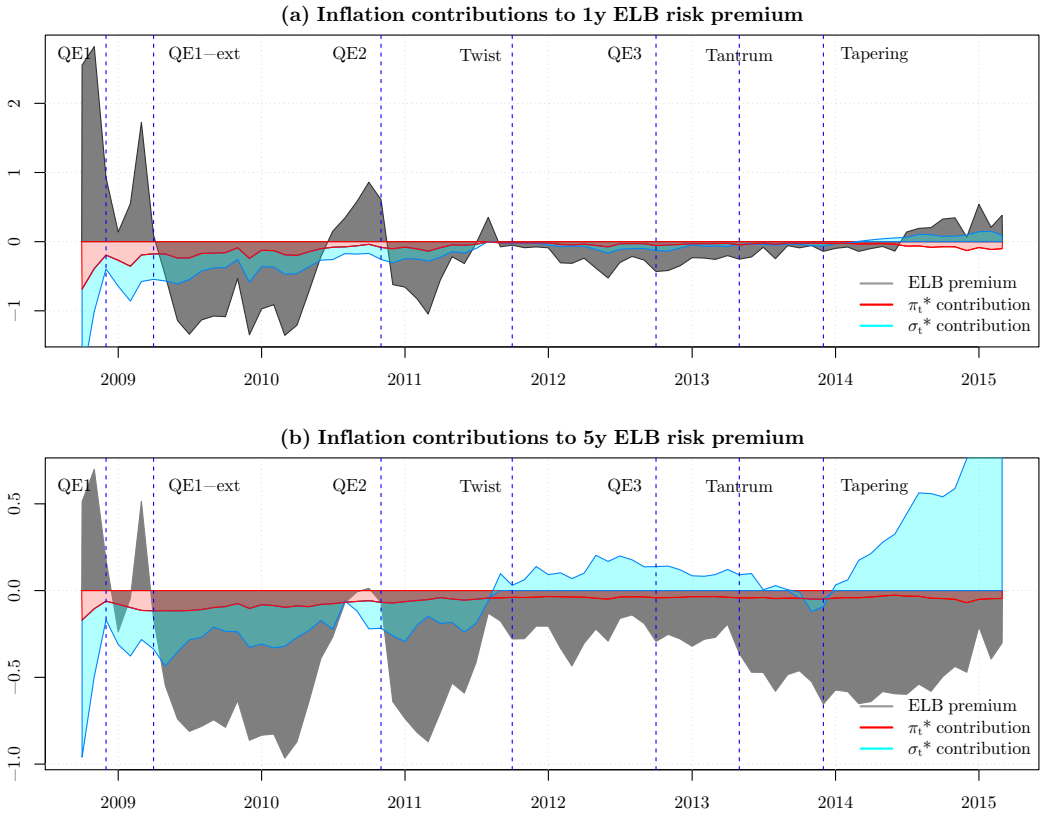

Notes: Both panels presents the ELB risk premium as defined by Equation (18). The red and blue components are the contributions of the inflation trend and volatility to the risk premium. Panel (a) and (b) present the results for the 1y and 5y maturities, respectively. All quantities are computed before applying corrections on the factors. The red vertical bar delimits the beginning of the ELB period. The blue dashed lines are the different unconventional monetary policy episodes, namely: QE1, QE1-extension, QE2, Operation Twist, QE3, Taper tantrum, and the Tapering.

Figure 9 – Impulse-response functions: liftoff shock

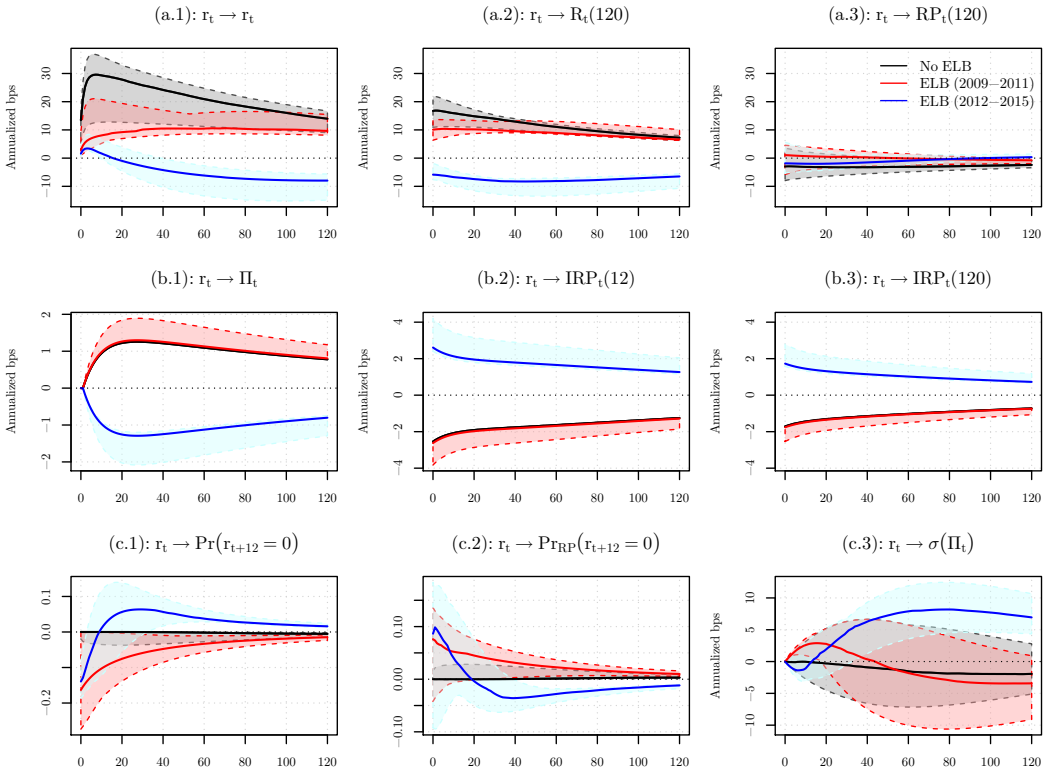

Notes: These graphs present the IRFs of an increase in the short-term nominal interest rate. Panel (a) presents the effect on the nominal side of the term structure, namely the short-term interest rate (a.1), the 10y yield (a.2) and the 10y risk premium (a.3). On panel (b), we find the effects on inflation components, namely inflation itself (b.1), 1y inflation risk premium (b.2) and 10y inflation risk premium (b.3). Panel (c) presents the effects on the 1y ZLB probability (c.1), the 1y ZLB risk premium (c.2) and the inflation volatility (c.3). Grey- and red-shaded areas represent the 50% range of possible outcomes given the different initial values respectively starting from a non-ZLB or a ZLB state. solid lines of the same color are the associated median responses. Green dashed-dotted lines and blue dashed-plus lines respresent the effects of the same shock on particular sample dates, namely on QE2 date and on March 2015 which is the last date of the sample. Units are in annualized basis points.

Table 1 – Descriptive statistics

	Nominal rates (1990-2015)						
	1-month	1-year	2-year	3-year	5-year	7-year	10-year
mean	2.883	3.375	3.642	3.893	4.336	4.699	5.103
sd	2.228	2.382	2.351	2.272	2.098	1.952	1.800
$\rho(1)$	0.981	0.986	0.985	0.984	0.982	0.980	0.979
	Inflation	Real rates (2004-2015)					
	y-o-y	1-year	2-year	3-year	5-year	7-year	10-year
mean	2.607	-0.071	-0.100	-0.034	0.234	0.532	0.909
mean (excl. crisis)		-0.221	-0.206	-0.111	0.174	0.473	0.855
sd	1.237	1.592	1.423	1.312	1.153	1.069	0.954
sd (excl. crisis)		1.431	1.362	1.286	1.146	1.055	0.936
$\rho(1)$	0.942	0.938	0.963	0.964	0.969	0.962	0.956
		Breakeven inflation rates (2004-2015)					
		1-year	2-year	3-year	5-year	7-year	10-year
mean		1.676	1.858	2.025	2.263	2.421	2.577
mean (excl. crisis)		1.859	1.997	2.130	2.335	2.477	2.615
sd		1.274	0.950	0.759	0.540	0.418	0.303
sd (excl. crisis)		0.886	0.685	0.564	0.414	0.318	0.245
$\rho(1)$		0.855	0.881	0.878	0.877	0.847	0.812

Notes: All units are annualized percentage points. 'mean' are sample averages, 'sd' are sample standard deviations, and '$\rho(1)$' are autocorrelation of order 1. The 'excl. crisis' rows present descriptive statistics calculated on the TIPS data excluding the period from September 2008 to February 2009.

Table 2 – Model fit and characteristics

Maturities (months)	1	12	24	36	60	84	120
Nominal rates RMSE (bps)	5.39	4.82	3.60	3.09	2.97	2.61	2.15
Real rates RMSE (bps)	-	17.16	6.02	7.82	10.04	10.61	10.72
Probabilities (in %)	$\mathbb{P}(r_t = \underline{r}) = 27.59$			$\mathbb{P}(r_t = \underline{r} \vert r_{t-1} = \underline{r}) = 74.48$			

Note: Probabilities are calculated with simulated paths of length 100,000.

Parameter Estimates

Table 3 – Parameter estimates: X_t dynamics

	estimates	std.		estimates	std.
μ_{π^*}	0.0158^{**}	(0.0072)	$\mu^{\mathbb{Q}}_{\pi^*}$	0.0171^{***}	(0.007)
μ_{σ}	0	–	$\mu^{\mathbb{Q}}_{\sigma}$	0	–
μ_{y_1}	0	–	$\mu^{\mathbb{Q}}_{y_1}$	0.5376^{***}	(0.1683)
μ_{y_2}	0.0217^{**}	(0.0112)	$\mu^{\mathbb{Q}}_{y_2}$	0.0217^{**}	(0.0112)
Φ_{π^*}	0.8855^{***}	(0.0194)	$\Phi^{\mathbb{Q}}_{\pi^*}$	0.9629^{***}	(0.0015)
Φ_{σ,π^*}	0	–	$\Phi^{\mathbb{Q}}_{\sigma,\pi^*}$	0.0043^{***}	(0.0012)
Φ_{y_1,π^*}	0	–	$\Phi^{\mathbb{Q}}_{y_1,\pi^*}$	-0.1256^{***}	(0.0232)
Φ_{y_2,π^*}	0	–	$\Phi^{\mathbb{Q}}_{y_2,\pi^*}$	-0.0195^{***}	(0.0054)
$\Phi_{\pi^*,\sigma}$	0	–	$\Phi^{\mathbb{Q}}_{\pi^*,\sigma}$	0.0169^{***}	(0.0035)
Φ_{σ}	0.9810^{***}	(0.0058)	$\Phi^{\mathbb{Q}}_{\sigma}$	0.9537^{***}	(0.0028)
$\Phi_{y_1,\sigma}$	0	–	$\Phi^{\mathbb{Q}}_{y_1,\sigma}$	0.5023^{***}	(0.0323)
$\Phi_{y_2,\sigma}$	0	–	$\Phi^{\mathbb{Q}}_{y_2,\sigma}$	0.083^{***}	(0.0158)
Φ_{π^*,y_1}	0.0009^{*}	$(5 \cdot 10^{-4})$	$\Phi^{\mathbb{Q}}_{\pi^*,y_1}$	-0.0012^{***}	$(2 \cdot 10^{-4})$
Φ_{σ,y_1}	-0.0006^{***}	$(2 \cdot 10^{-4})$	$\Phi^{\mathbb{Q}}_{\sigma,y_1}$	-0.0006^{***}	$(2 \cdot 10^{-4})$
Φ_{y_1}	0.9944^{***}	(0.001)	$\Phi^{\mathbb{Q}}_{y_1}$	0.9552^{***}	(0.0039)
Φ_{y_2,y_1}	0	–	$\Phi^{\mathbb{Q}}_{y_2,y_1}$	-0.005^{***}	$(8 \cdot 10^{-4})$
Φ_{π^*,y_2}	-0.0142^{***}	(0.0035)	$\Phi^{\mathbb{Q}}_{\pi^*,y_2}$	-0.0043^{***}	$(5 \cdot 10^{-4})$
Φ_{σ,y_2}	0.0078^{***}	(0.002)	$\Phi^{\mathbb{Q}}_{\sigma,y_2}$	0.0036^{***}	$(6 \cdot 10^{-4})$
Φ_{y_1,y_2}	0.0198^{***}	(0.0034)	$\Phi^{\mathbb{Q}}_{y_1,y_2}$	-0.1009^{***}	(0.0065)
Φ_{y_2}	0.9848^{***}	(0.0031)	$\Phi^{\mathbb{Q}}_{y_2}$	0.9848^{***}	(0.0031)
Σ_{π^*}	0.1674^{***}	(0.022)	$\Sigma^{\mathbb{Q}}_{\pi^*}$	0.1674^{***}	(0.022)
Σ_{σ,π^*}	0	–	$\Sigma^{\mathbb{Q}}_{\sigma,\pi^*}$	0	–
Σ_{y_1,π^*}	0	–	$\Sigma^{\mathbb{Q}}_{y_1,\pi^*}$	0.0001^{***}	(0)
Σ_{y_2,π^*}	0	–	$\Sigma^{\mathbb{Q}}_{y_2,\pi^*}$	0	–
Σ_{σ}	0.0999^{***}	(0.0098)	$\Sigma^{\mathbb{Q}}_{\sigma}$	0.0999^{***}	(0.0098)
$\Sigma_{y_1,\sigma}$	0	–	$\Sigma^{\mathbb{Q}}_{y_1,\sigma}$	0	–
$\Sigma_{y_2,\sigma}$	0	–	$\Sigma^{\mathbb{Q}}_{y_2,\sigma}$	0	–
Σ_{y_1}	1	–	$\Sigma^{\mathbb{Q}}_{y_1}$	1.0008^{***}	$(2 \cdot 10^{-4})$
Σ_{y_2,y_1}	0	–	$\Sigma^{\mathbb{Q}}_{y_2,y_1}$	0	–
Σ_{y_2}	1	–	$\Sigma^{\mathbb{Q}}_{y_2}$	1	–

Notes: Standard deviations are in parentheses and are calculated using the outer-product Hessian approximation. The '–' sign indicates that the parameter has been calibrated hence does not possess any standard deviation. Significance level: * <0.1, ** <0.05, *** <0.01.

Table 4 – Parameter estimates: short-rate and the prices of risk

	r_t dynamics *(parameters are divided by 1,200 except c, $\bar{\pi}$ and $\underline{r}$)*				
	estimates	std.		estimates	std.
α	1.3317***	(0.4427)	$\alpha^{\mathbb{Q}}$	1.5411***	(0.5345)
β_{π^*}	0.0535***	(0.0165)	$\beta^{\mathbb{Q}}_{\pi^*}$	0.0576***	(0.0176)
β_{σ}	0	–	$\beta^{\mathbb{Q}}_{\sigma}$	0	–
β_{y_1}	0.0901***	(0.0099)	$\beta^{\mathbb{Q}}_{y_1}$	0.0969***	(0.0108)
β_{y_2}	0	–	$\beta^{\mathbb{Q}}_{y_2}$	0	–
κ	1.7071***	(0.2606)	$\kappa^{\mathbb{Q}}$	1.8365***	(0.2928)
ϕ	1.0113***	(0.0894)	$\phi^{\mathbb{Q}}$	1.1704***	(0.0912)
$c \cdot 1200$	0.5471***	(0.0425)	$c^{\mathbb{Q}} \cdot 1200$	0.6331***	(0.0478)
$\underline{r} \cdot 1200$	0.1463***	(0.0035)	$\bar{\pi} \cdot 100$	2.8399***	(0.0601)
	Prices of risk and measurement errors standard deviations				
	estimates	std.		estimates	std.
λ_{0,π^*}	0	–	λ_{0,y_1}	0.524***	(0.1714)
$\lambda_{0,\sigma}$	0	–	λ_{0,y_2}	0	–
λ_{1,π^*}	0.4627***	(0.1045)	λ_{1,π^*,y_1}	−0.0129***	(0.0032)
λ_{1,σ,π^*}	0.0432***	(0.0114)	λ_{1,σ,y_1}	0	–
λ_{1,y_1,π^*}	−0.1259***	(0.0231)	λ_{1,y_1}	−0.0399***	(0.0038)
λ_{1,y_2,π^*}	−0.0195***	(0.0054)	λ_{1,y_2,y_1}	−0.005***	$(8 \cdot 10^{-4})$
$\lambda_{1,\pi^*,\sigma}$	0.1008***	(0.0239)	λ_{1,π^*,y_2}	0.0591***	(0.02)
$\lambda_{1,\sigma}$	−0.273***	(0.0653)	λ_{1,σ,y_2}	−0.0412**	(0.0207)
$\lambda_{1,y_1,\sigma}$	0.5019***	(0.0323)	λ_{1,y_1,y_2}	−0.1206***	(0.0082)
$\lambda_{1,y_2,\sigma}$	0.083***	(0.0158)	λ_{1,y_2}	0	–
λ_r	0.2484***	(0.0588)			
σ_R	0.0208***	$(4 \cdot 10^{-4})$	σ^*_R	0.1184***	(0.0025)
$\sigma^{(12)}_{\pi}$	0.509	–	$\sigma^{(120)}_{\pi}$	0.389	–
$\sigma^{(3)}_{S_R}$	0.231	–	$\sigma^{(12)}_{S_R}$	0.422	–
σ_{ZLB}	0.0522	–			

Notes: Standard deviations are in parentheses and are calculated using the outer-product Hessian approximation. The '–' sign indicates that the parameter has been calibrated hence does not possess any standard deviation. Significance level: * <0.1, ** <0.05, *** <0.01.

A Appendix

A.1 The Gamma-zero (γ_0) distribution

The gamma-zero autoregressive process was introduced by Monfort et al. (2017) as a generalization of the autoregressive gamma process of Gouriéroux and Jasiak (2006). Let $\mathfrak{I}_t = \mathfrak{I}(X_t, z_{t-1})$ be a non-negative process which is a function of the risk factors X_t and z_{t-1}, and j_t be a Poisson variable with intensity $\mathfrak{I}_t$. z_t is conditionally gamma-zero distributed if:

$$j_t|\underline{X_t}, \underline{z_{t-1}} \sim \mathcal{P}\left(\mathfrak{I}(\underline{X_t}, \underline{z_{t-1}})\right) \quad \text{and} \quad z_t|j_t \sim \text{Gamma}_{j_t}(c) \ , \tag{20}$$

that is, conditionally on the Poisson mixing variable, z_t has a gamma distribution with shape (or degree of freedom) parameter j_t and a scale parameter c. When $j_t = 0$, the conditional distribution of z_t converges to a Dirac point mass at zero. Integrating with respect to j_t, we obtain the conditional distribution of z_t given X_t and z_{t-1} that is called gamma-zero, encompassing a zero point mass. The conditional distribution of z_t given X_t and its past can be expressed with its conditional Laplace transform:

$$\mathbb{E}\left[\exp(u_z z_t)\middle|\underline{X_t}, \underline{z_{t-1}}\right] = \exp\left(\frac{u_z c}{1 - u_z c}\mathfrak{I}_t\right) \ , \tag{21}$$

In this paper, we consider an intensity which is a linear-quadratic function of X_t and a linear function of z_{t-1} (see Equation (4)). We thus have:

$$\mathbb{E}\left[\exp(u_z z_t)\middle|\underline{X_t}, \underline{z_{t-1}}\right] = \exp\left(\frac{u_z c}{1 - u_z c}\left(\alpha + \phi z_{t-1} + \kappa\beta' X_t + (\beta' X_t)^2\right)\right) \ .$$

The properties of the gamma-zero are such that its first two conditional moments are linear in its underlying intensity $\mathfrak{I}_t$. We thus have:

$$\mathbb{E}\left(z_t \middle| \underline{X_t}, \underline{z_{t-1}}\right) = c\,\mathfrak{I}_t \quad \text{and} \quad \mathbb{V}\left(z_t \middle| \underline{X_t}, \underline{z_{t-1}}\right) = 2\,c^2\,\mathfrak{I}_t\,.$$

We can expand the function of X_t in the intensity:

$$\begin{aligned}
\kappa\beta' X_t + (\beta' X_t)^2 &= \kappa\beta'\left(\mu + \Phi X_{t-1} + v_t\right) + \left[\beta'\left(\mu + \Phi X_{t-1} + v_t\right)\right]^2 \\
&= \kappa\beta'\left(\mu + \Phi X_{t-1} + v_t\right) + \left\{\left[\beta'\left(\mu + \Phi X_{t-1}\right)\right]^2 + \left(\beta' v_t\right)^2 + 2\beta'\left(\mu + \Phi X_{t-1}\right)\beta' v_t\right\} \\
&= \kappa\beta'\mu + \left(\beta'\mu\right)^2 + \beta'\Sigma\beta \\
&\quad + \kappa\beta'\Phi X_{t-1} + \left(\beta'\Phi X_{t-1}\right)^2 + 2\left(\beta'\mu\right)\left(\beta'\Phi X_{t-1}\right) \\
&\quad + \kappa\beta' v_t + \left[\left(\beta' v_t\right)^2 - \beta'\Sigma\beta\right] + 2\left(\mu + \Phi X_{t-1}\right)'\beta\beta' v_t
\end{aligned}$$

Using the conditional moments of linear-quadratic Gaussian processes (see technical Appendix B.5), the last row has zero conditional mean given the information available at $t-1$. We can then express the intensity as:

$$\begin{aligned}
\mathfrak{I}_t &= \alpha + \phi z_{t-1} + \left(\kappa + \beta'\mu\right)\beta'\mu + \beta'\Sigma\beta + \left(\kappa + 2\mu'\beta\right)\beta'\Phi X_{t-1} + \left(\beta'\Phi X_{t-1}\right)^2 \\
&\quad + \kappa\beta' v_t + \left[\left(\beta' v_t\right)^2 - \beta'\Sigma\beta\right] + 2\left(\mu + \Phi X_{t-1}\right)'\beta\beta' v_t\,,
\end{aligned}$$

and the short-rate is given by:

$$\begin{aligned}
r_t &= \underline{r} + c\,\mathfrak{I}_t + \varepsilon_t^z \\
&= \underline{r} + c\,\mathbb{E}_{t-1}\left(\mathfrak{I}_t\right) + \varepsilon_t^r \\
&= \underline{r} + c\left[\alpha + \phi z_{t-1} + \left(\kappa + \beta'\mu\right)\beta'\mu + \beta'\Sigma\beta + \left(\kappa + 2\mu'\beta\right)\beta'\Phi X_{t-1} + \left(\beta'\Phi X_{t-1}\right)^2\right] + \varepsilon_t^r \\
&= \underline{r} + \underbrace{c\left[\alpha + \left(\kappa + \beta'\mu\right)\beta'\mu + \beta'\Sigma\beta\right]}_{=\alpha^*} + \underbrace{c\phi}_{=\phi^*} z_{t-1} + c\left(\kappa + 2\mu'\beta\right)\beta'\Phi X_{t-1} + c\left(\beta'\Phi X_{t-1}\right)^2 + \varepsilon_t^r\,,
\end{aligned}$$

and by definition we obtain:

$$r_t = (1-\phi^*)\underline{r} + \alpha^* + \phi^* r_{t-1} + c\left(\kappa + 2\mu'\beta\right)\beta'\Phi X_{t-1} + c\left(\beta'\Phi X_{t-1}\right)^2 + \varepsilon_t^r\,, \quad (22)$$

and

$$\varepsilon_t^r = c\left[\kappa\beta' v_t + \left[\left(\beta' v_t\right)^2 - \beta'\Sigma\beta\right] + 2\left(\mu + \Phi X_{t-1}\right)'\beta\beta' v_t\right] + \varepsilon_t^z\,. \quad (23)$$

This shock is a zero-mean martingale difference with respect to the information set available at $t-1$. For conditional variance, we have:

$$\begin{aligned}
\mathbb{V}_{t-1}\left(r_t\right) &= \mathbb{V}_{t-1}\left(\varepsilon_t^r\right) \\
&= c^2\mathbb{V}_{t-1}\left[\left(\kappa + 2\left(\mu + \Phi X_{t-1}\right)'\beta\right)\beta' v_t + \left(\left(\beta' v_t\right)^2 - \beta'\Sigma\beta\right)\right] + \mathbb{V}_{t-1}\left(\varepsilon_t^z\right) \\
&= c^2\left(\left[\kappa + 2\left(\mu + \Phi X_{t-1}\right)'\beta\right]^2\beta'\Sigma\beta + 2\left(\beta'\Sigma\beta\right)^2\right) \\
&\quad + \quad 2c^2\left(\alpha + \phi z_{t-1} + \left(\kappa + \beta'\mu\right)\beta'\mu + \beta'\Sigma\beta + \left(\kappa + 2\mu'\beta\right)\beta'\Phi X_{t-1} + \left(\beta'\Phi X_{t-1}\right)^2\right)\,,
\end{aligned}$$

which is a linear-quadratic function of X_{t-1}.

A.2 Risk-neutral affine property

To derive the risk-neutral conditional Laplace transform of f_t given $\underline{f_{t-1}}$, we use the transition formulas provided in Roussellet (2015), Chapter 4. Using the block recursive affine structure of f_t, the risk-neutral conditional Laplace transform of z_t given X_t and $\underline{f_{t-1}}$ is given by:

$$\mathbb{E}^{\mathbb{Q}}\left(\exp\{u_z z_t\}\middle| X_t,\, \underline{f_{t-1}}\right) = \frac{\mathbb{E}\left(\exp\left\{\left[u_z + \lambda_r\right] z_t\right\}\middle| X_t,\, \underline{f_{t-1}}\right)}{\mathbb{E}\left(\exp\left\{\lambda_r z_t\right\}\middle| X_t,\, \underline{f_{t-1}}\right)} \quad (24$$

$$= \exp\left\{\left(\frac{(u_z+\lambda_r)c}{1-(u_z+\lambda_r)c} - \frac{\lambda_r c}{1-\lambda_r c}\right)(\alpha + \kappa\beta' X_t + X_t'\beta\beta' X_t + \phi z_{t-1})\right\}$$

where $\mathbb{E}^{\mathbb{Q}}(\cdot)$ is the expectation operator under the risk-neutral measure. The difference of ratios can be simplified as follows.

$$\begin{aligned}\frac{(u_z+\lambda_r)c}{1-(u_z+\lambda_r)c} - \frac{\lambda_r c}{1-\lambda_r c} &= \frac{(1-\lambda_r c)(u_z+\lambda_r)c - [1-(u_z+\lambda_r)c]\lambda_r c}{[1-\lambda_r c][1-(u_z+\lambda_r)c]} \\ &= c\frac{u_z - \lambda_r u_z c + u_z\lambda_r c}{[1-\lambda_r c][1-(u_z+\lambda_r)c]} = \frac{u_z c}{[1-\lambda_r c][1-(u_z+\lambda_r)c]}.\end{aligned}$$

Define now $c^{\mathbb{Q}} = \dfrac{c}{1-\lambda_r c}$, that is $c = \dfrac{c^{\mathbb{Q}}}{1+\lambda_r c^{\mathbb{Q}}}$. We obtain:

$$\frac{u_z c}{1-(u_z+\lambda_r)c} = \frac{u_z \frac{c^{\mathbb{Q}}}{1+\lambda_r c^{\mathbb{Q}}}}{1-(u_z+\lambda_r)\frac{c^{\mathbb{Q}}}{1+\lambda_r c^{\mathbb{Q}}}} = \frac{1+\lambda_r c^{\mathbb{Q}}}{1-u_z c^{\mathbb{Q}}} \times \frac{u_z c^{\mathbb{Q}}}{1+\lambda_r c^{\mathbb{Q}}} = \frac{u_z c^{\mathbb{Q}}}{1-u_z c^{\mathbb{Q}}}.$$

Hence the conditional Laplace transform of Equation (24) is given by:

$$\begin{aligned}\mathbb{E}^{\mathbb{Q}}\left(\exp\{u_z z_t\}\middle| X_t, \underline{f_{t-1}}\right) &= \exp\left\{\frac{u_z c^{\mathbb{Q}}}{1-u_z c^{\mathbb{Q}}} \times \frac{\alpha + \kappa\beta' X_t + X_t'\beta\beta' X_t + \phi z_{t-1}}{1-\lambda_r c}\right\} \\ &=: \exp\left\{\frac{u_z c^{\mathbb{Q}}}{1-u_z c^{\mathbb{Q}}}\left(\alpha^{\mathbb{Q}} + \kappa^{\mathbb{Q}}\beta^{\mathbb{Q}\prime} X_t + X_t'\beta^{\mathbb{Q}}\beta^{\mathbb{Q}\prime} X_t + \phi^{\mathbb{Q}} z_{t-1}\right)\right\}.\end{aligned}$$

z_t is therefore conditionally gamma-zero distributed given X_t and its past, where the risk-neutral parameters are given by:

$$\alpha^{\mathbb{Q}} = \frac{\alpha}{1-\lambda_r c}, \quad \beta^{\mathbb{Q}} = \frac{\beta}{\sqrt{1-\lambda_r c}}, \quad \kappa^{\mathbb{Q}} = \frac{\kappa}{\sqrt{1-\lambda_r c}}, \quad \phi^{\mathbb{Q}} = \frac{\phi}{1-\lambda_r c}, \quad c^{\mathbb{Q}} = \frac{c}{1-\lambda_r c}$$

We turn now to the computation of the risk-neutral conditional Laplace transform of $(X_t', \mathrm{Vec}(X_t X_t')')'$ given $\underline{f_{t-1}}$. Again, using the property in Roussellet

(2015) Chapter 4, we have:

$$\mathbb{E}^{\mathbb{Q}}\left(\exp\left\{u_x' X_t + X_t' U_x X_t\right\} \middle| \underline{f_{t-1}}\right) = \frac{\mathbb{E}\left[\exp\left\{(u_x + \widetilde{\lambda}_{t-1})' X_t + X_t'(U_x + \widetilde{\lambda}_r) X_t\right\} \middle| \underline{f_{t-1}}\right)}{\mathbb{E}\left[\exp\left\{\widetilde{\lambda}_{t-1}' X_t + X_t'(U_x + \widetilde{\lambda}_r) X_t\right\} \middle| \underline{f_{t-1}}\right)},$$

where $\widetilde{\lambda}_{t-1}$ and $\widetilde{\lambda}_r$ are given by:

$$\widetilde{\lambda}_{t-1} = \lambda_0 + \beta \frac{\kappa \lambda_r c}{1 - \lambda_r c} + \lambda_1 X_{t-1}, \quad \widetilde{\lambda}_r = \frac{\lambda_r c}{1 - \lambda_r c} \beta\beta'.$$

The transition between the physical and risk-neutral dynamics of X_t are as if the SDF was exponential-quadratic, with adjusted prices of risk $\widetilde{\Lambda}_{t-1}$ and $\widetilde{\lambda}_r$. Since $\widetilde{\lambda}_r$ the price associated to $\text{Vec}(X_t X_t')$ is constant through time, we can rely on the results of Monfort and Pegoraro (2012). We obtain that X_t follows a Gaussian VAR(1) under the risk-neutral measure and:

$$X_t = \mu^{\mathbb{Q}} + \Phi^{\mathbb{Q}} X_{t-1} + v_t^{\mathbb{Q}},$$

where $v_t^{\mathbb{Q}} \overset{i.i.d.}{\sim} \mathcal{N}\left(0, \Sigma^{\mathbb{Q}}\right)$ is a Gaussian white noise, and $\mu^{\mathbb{Q}}$, $\Phi^{\mathbb{Q}}$ and $\Sigma^{\mathbb{Q}}$ are given by:

$$\begin{aligned}
\mu^{\mathbb{Q}} &= \left(I_K - 2\frac{\lambda_r c}{1 - \lambda_r c}\Sigma\beta\beta'\right)^{-1}\left(\mu + \Sigma\lambda_0 + \frac{\kappa\lambda_r c}{1 - \lambda_r c}\Sigma\beta\right) \\
\Phi^{\mathbb{Q}} &= \left(I_K - 2\frac{\lambda_r c}{1 - \lambda_r c}\Sigma\beta\beta'\right)^{-1}\left(\Phi + \Sigma\lambda_1\right) \\
\Sigma^{\mathbb{Q}} &= \left(I_K - 2\frac{\lambda_r c}{1 - \lambda_r c}\Sigma\beta\beta'\right)^{-1}\Sigma.
\end{aligned}$$

The class of distributions are thus the same under the physical and the risk-neutral measure. Transforming Formula (33), the risk-neutral Laplace trans-

form of f_t given $\underline{f_{t-1}}$ is given by:

$$
\begin{aligned}
& \mathbb{E}^{\mathbb{Q}}\left[\exp\left(u' f_t\right) | \underline{f_{t-1}}\right] \\
= \; & \exp\left\{ \frac{u_z c^{\mathbb{Q}}}{1-u_z c^{\mathbb{Q}}} \left(\alpha^{\mathbb{Q}} + \phi^{\mathbb{Q}} z_{t-1}\right) - \frac{1}{2}\log\left| I_K - 2\Sigma^{\mathbb{Q}}\left(U_x + \frac{u_z c^{\mathbb{Q}}}{1-u_z c^{\mathbb{Q}}}\beta^{\mathbb{Q}}\beta^{\mathbb{Q}\prime}\right)\right| \right. \\
+ \; & \left(u_x + \frac{\kappa^{\mathbb{Q}} u_z c^{\mathbb{Q}}}{1-u_z c^{\mathbb{Q}}}\beta^{\mathbb{Q}}\right)' \left[I_K - 2\Sigma^{\mathbb{Q}}\left(U_x + \frac{u_z c^{\mathbb{Q}}}{1-u_z c^{\mathbb{Q}}}\beta^{\mathbb{Q}}\beta^{\mathbb{Q}\prime}\right)\right]^{-1} \left[\mu^{\mathbb{Q}} + \frac{1}{2}\Sigma^{\mathbb{Q}}\left(u_x + \frac{\kappa^{\mathbb{Q}} u_z c^{\mathbb{Q}}}{1-u_z c^{\mathbb{Q}}}\beta^{\mathbb{Q}}\right)\right] \\
+ \; & \mu^{\mathbb{Q}\prime}\left(U_x + \frac{u_z c^{\mathbb{Q}}}{1-u_z c^{\mathbb{Q}}}\beta^{\mathbb{Q}}\beta^{\mathbb{Q}\prime}\right)\left[I_K - 2\Sigma^{\mathbb{Q}}\left(U_x + \frac{u_z c^{\mathbb{Q}}}{1-u_z c^{\mathbb{Q}}}\beta^{\mathbb{Q}}\beta^{\mathbb{Q}\prime}\right)\right]^{-1}\mu^{\mathbb{Q}} \\
+ \; & \left[\left(u_x + \frac{\kappa^{\mathbb{Q}} u_z c^{\mathbb{Q}}}{1-u_z c^{\mathbb{Q}}}\beta^{\mathbb{Q}}\right)' + 2\mu^{\mathbb{Q}\prime}\left(U_x + \frac{u_z c^{\mathbb{Q}}}{1-u_z c^{\mathbb{Q}}}\beta^{\mathbb{Q}}\beta^{\mathbb{Q}\prime}\right)\right]\left[I_K - 2\Sigma^{\mathbb{Q}}\left(U_x + \frac{u_z c^{\mathbb{Q}}}{1-u_z c^{\mathbb{Q}}}\beta^{\mathbb{Q}}\beta^{\mathbb{Q}\prime}\right)\right]^{-1}\Phi^{\mathbb{Q}} X_{t-1} \\
+ \; & \left. X_{t-1}'\Phi^{\mathbb{Q}\prime}\left(U_x + \frac{u_z c^{\mathbb{Q}}}{1-u_z c^{\mathbb{Q}}}\beta^{\mathbb{Q}}\beta^{\mathbb{Q}\prime}\right)\left[I_K - 2\Sigma^{\mathbb{Q}}\left(U_x + \frac{u_z c^{\mathbb{Q}}}{1-u_z c^{\mathbb{Q}}}\beta^{\mathbb{Q}}\beta^{\mathbb{Q}\prime}\right)\right]^{-1}\Phi^{\mathbb{Q}} X_{t-1}\right\}. \qquad (25)
\end{aligned}
$$

This conditional Laplace transform is an exponential-affine function of f_{t-1}. (f_t) is therefore an affine process under the risk-neutral measure. Combined with the fact that both r_t and π_t are affine functions of f_t augmented with the idiosyncratic inflation shocks ε_t^{π}, this is sufficient to define an affine term structure model (ATSM) (see e.g. Dai and Singleton (2000) or Darolles et al. (2006)).

A.3 Pricing recursions

In this Section, we derive the pricing recursions for nominal bonds and TIPS. By no-arbitrage, we have:

$$
P_t^{(n)} = \mathbb{E}_t^{\mathbb{Q}}\left[e^{-r_t} P_{t+1}^{(n-1)}\right] \quad \text{and} \quad P_t^{(n)^*} = \mathbb{E}_t^{\mathbb{Q}}\left[e^{-r_t} P_{t+1}^{(n-1)^*}\frac{\mathcal{I}_{t+1}}{\mathcal{I}_t}\right]
$$

We postulate the form given by Equation (13), that is:

$$
\begin{aligned}
P_t^{(n)} &= \exp\left(\mathcal{A}_n + \mathcal{B}_n' X_t + X_t' \mathcal{C}_n X_t + \mathcal{D}_n z_t\right), \\
P_t^{(n)^*} &= \exp\left(\mathcal{A}_n^* + \mathcal{B}_n^{*\prime} X_t + X_t' \mathcal{C}_n^* X_t + \mathcal{D}_n^* z_t\right),
\end{aligned}
$$

Focusing first on nominal bonds, we obtain:

$$\mathcal{A}_n + \mathcal{B}_n' X_t + X_t' \mathcal{C}_n X_t + \mathcal{D}_n z_t = -\underline{r} - z_t + \mathcal{A}_{n-1} + \log \mathbb{E}_t^{\mathbb{Q}} \left[\exp \left(\mathcal{B}_{n-1}' X_{t+1} + X_{t+1}' \mathcal{C}_{n-1} X_{t+1} + \mathcal{D}_{n-1} z_{t+1} \right) \right]$$

Therefore, using the formulation of Equation (25), starting from initial conditions $\mathcal{A}_0 = 0$, $\mathcal{B}_0 = 0$, $\mathcal{C}_0 = 0$, $\mathcal{D}_0 = 0$, we get:

$$\begin{aligned}
\mathcal{A}_n &= -\underline{r} + \mathcal{A}_{n-1} + \frac{\mathcal{D}_{n-1} c^{\mathbb{Q}}}{1 - \mathcal{D}_{n-1} c^{\mathbb{Q}}} \alpha^{\mathbb{Q}} - \frac{1}{2} \log \left| I_K - 2\Sigma^{\mathbb{Q}} \left(\mathcal{C}_{n-1} + \frac{\mathcal{D}_{n-1} c^{\mathbb{Q}}}{1 - \mathcal{D}_{n-1} c^{\mathbb{Q}}} \beta^{\mathbb{Q}} \beta^{\mathbb{Q}\prime} \right) \right| \\
&+ \left(\mathcal{B}_{n-1} + \frac{\kappa^{\mathbb{Q}} \mathcal{D}_{n-1} c^{\mathbb{Q}}}{1 - \mathcal{D}_{n-1} c^{\mathbb{Q}}} \beta^{\mathbb{Q}} \right)' \left[I_K - 2\Sigma^{\mathbb{Q}} \left(\mathcal{C}_{n-1} + \frac{\mathcal{D}_{n-1} c^{\mathbb{Q}}}{1 - \mathcal{D}_{n-1} c^{\mathbb{Q}}} \beta^{\mathbb{Q}} \beta^{\mathbb{Q}\prime} \right) \right]^{-1} \left[\mu^{\mathbb{Q}} + \frac{1}{2} \Sigma^{\mathbb{Q}} \left(\mathcal{B}_{n-1} + \frac{\kappa^{\mathbb{Q}} \mathcal{D}_{n-1} c^{\mathbb{Q}}}{1 - \mathcal{D}_{n-1} c^{\mathbb{Q}}} \beta^{\mathbb{Q}} \right) \right] \\
&+ \mu^{\mathbb{Q}\prime} \left(\mathcal{C}_{n-1} + \frac{\mathcal{D}_{n-1} c^{\mathbb{Q}}}{1 - \mathcal{D}_{n-1} c^{\mathbb{Q}}} \beta^{\mathbb{Q}} \beta^{\mathbb{Q}\prime} \right) \left[I_K - 2\Sigma^{\mathbb{Q}} \left(\mathcal{C}_{n-1} + \frac{\mathcal{D}_{n-1} c^{\mathbb{Q}}}{1 - \mathcal{D}_{n-1} c^{\mathbb{Q}}} \beta^{\mathbb{Q}} \beta^{\mathbb{Q}\prime} \right) \right]^{-1} \mu^{\mathbb{Q}} \\
\mathcal{B}_n &= \Phi^{\mathbb{Q}\prime} \left[I_K - 2\Sigma^{\mathbb{Q}} \left(\mathcal{C}_{n-1} + \frac{\mathcal{D}_{n-1} c^{\mathbb{Q}}}{1 - \mathcal{D}_{n-1} c^{\mathbb{Q}}} \beta^{\mathbb{Q}} \beta^{\mathbb{Q}\prime} \right) \right]^{-1\prime} \\
&\times \left[\left(\mathcal{B}_{n-1} + \frac{\kappa^{\mathbb{Q}} \mathcal{D}_{n-1} c^{\mathbb{Q}}}{1 - \mathcal{D}_{n-1} c^{\mathbb{Q}}} \beta^{\mathbb{Q}} \right) + 2 \left(\mathcal{C}_{n-1} + \frac{\mathcal{D}_{n-1} c^{\mathbb{Q}}}{1 - \mathcal{D}_{n-1} c^{\mathbb{Q}}} \beta^{\mathbb{Q}} \beta^{\mathbb{Q}\prime} \right)' \mu^{\mathbb{Q}} \right] \\
\mathcal{C}_n &= \Phi^{\mathbb{Q}\prime} \left(\mathcal{C}_{n-1} + \frac{\mathcal{D}_{n-1} c^{\mathbb{Q}}}{1 - \mathcal{D}_{n-1} c^{\mathbb{Q}}} \beta^{\mathbb{Q}} \beta^{\mathbb{Q}\prime} \right) \left[I_K - 2\Sigma^{\mathbb{Q}} \left(\mathcal{C}_{n-1} + \frac{\mathcal{D}_{n-1} c^{\mathbb{Q}}}{1 - \mathcal{D}_{n-1} c^{\mathbb{Q}}} \beta^{\mathbb{Q}} \beta^{\mathbb{Q}\prime} \right) \right]^{-1} \Phi^{\mathbb{Q}} \\
\mathcal{D}_n &= \frac{\mathcal{D}_{n-1} c^{\mathbb{Q}}}{1 - \mathcal{D}_{n-1} c^{\mathbb{Q}}} \phi^{\mathbb{Q}} - 1 .
\end{aligned}$$

Now, turning to TIPS, there is a slight subtlety associated with the fact that π_{t+1} defines the year-on-year inflation and not the monthly inflation rate. The simplest case arises for maturities that are multiple of 12, (yearly maturities), which we have in the observables. In this case, the price of a TIPS with maturity $n = 12\widetilde{n}$ is given by:

$$P_t^{(12\widetilde{n})^*} = \mathbb{E}_t^{\mathbb{Q}} \left[\exp \left(- \sum_{i=0}^{12\widetilde{n}-1} r_{t+i} \right) \frac{\mathcal{I}_{t+12\widetilde{n}}}{\mathcal{I}_t} \right] = \mathbb{E}_t^{\mathbb{Q}} \left[\exp \left(- \sum_{i=0}^{12\widetilde{n}-1} r_{t+i} \right) \exp \left(\sum_{j=1}^{\widetilde{n}} \pi_{t+12j} \right) \right] .$$

The pricing formulas are still closed-form but rely on the recursions given by the multi-horizon Laplace transform of the vector $f_t^{(aug)} = \left(X_t^{(aug)\prime}, X_t^{(aug)\prime} \otimes X_t^{(aug)\prime}, z_t \right)$

and $X_t^{(aug)} = \left(X_t', \varepsilon_t^{\pi}, \pi_{t-1}^{*}\right)'$. We obtain:

$$P_t^{(12\widetilde{n})^*} = \exp\left(\widetilde{n}\bar{\pi} - 12\widetilde{n}\underline{r} - z_t\right) \mathbb{E}_t^{\mathbb{Q}}\left[\exp\left(\sum_{i=1}^{12\widetilde{n}} u_i' f_{t+i}^{(aug)}\right)\right], \tag{26}$$

where

$$u_{12\widetilde{n}} = \begin{pmatrix} \iota'_{K+2,K+2} & \iota'_{K+1,(K+2)^2} & 0 \end{pmatrix}' \tag{27}$$

$$u_i = \begin{pmatrix} \mathbf{0}'_{K+2} & \mathbf{0}'_{(K+2)^2} & -1 \end{pmatrix}' \quad \text{for} \quad i < 12\widetilde{n} \quad \text{and} \quad i/12 \neq \lfloor i/12 \rfloor \tag{28}$$

$$u_i = \begin{pmatrix} \iota'_{K+2,K+2} & \iota'_{K+1,(K+2)^2} & -1 \end{pmatrix}' \quad \text{for} \quad i < 12\widetilde{n} \quad \text{and} \quad i/12 = \lfloor i/12 \rfloor \tag{29}$$

where $\iota_{i,j}$ is the ith column of the identity matrix of size j. The recursions for the multi-horizon Laplace transform is detailed in the technical Appendix B.4.

A.4 Liftoff probabilities

Using the properties of the gamma-zero process presented in Monfort et al. (2017), the probabilities for the short-term interest rate to stay at its lower bound for n periods are given by the following:

$$\begin{aligned} \mathbb{P}\left(r_{t+1:t+n} = \underline{r} \middle| \underline{f}_t\right) &= \mathbb{P}\left(z_{t+1:t+n} = 0 \middle| \underline{f}_t\right) = \lim_{v \to -\infty} \mathbb{E}\left[\exp\left(\sum_{i=1}^{n} v z_{t+i}\right) \middle| \underline{f}_t\right] \\ \mathbb{Q}\left(r_{t+1:t+n} = \underline{r} \middle| \underline{f}_t\right) &= \mathbb{Q}\left(z_{t+1:t+n} = 0 \middle| \underline{f}_t\right) = \lim_{v \to -\infty} \mathbb{E}^{\mathbb{Q}}\left[\exp\left(\sum_{i=1}^{n} v z_{t+i}\right) \middle| \underline{f}_t\right] \end{aligned} \tag{30}$$

Notice that it is as if we were computing the n-maturity bond price and its respective expected component for a modified short-rate process. If our short-term nominal rate was given by $-vz_t$, this would be exactly the case. We thus

only have to use the same pricing recursions as in Appendix A.3 but putting $\underline{r} = 0$ and replacing $c^{\mathbb{Q}}$ by $v \to +\infty$. We obtain:

$$\begin{aligned}
\mathbb{Q}\left(r_{t+1:t+n} = \underline{r} \middle| \underline{f}_t\right) &= \exp\left(\mathcal{A}_n^{(\text{zlb})} + \mathcal{B}_n^{(\text{zlb})\prime} X_t + X_t' \mathcal{C}_n^{(\text{zlb})} X_t + \mathcal{D}_n^{(\text{zlb})} z_t\right) \\
\mathbb{P}\left(r_{t+1:t+n} = \underline{r} \middle| \underline{f}_t\right) &= \exp\left(\mathcal{A}_n^{\mathbb{P},(\text{zlb})} + \mathcal{B}_n^{\mathbb{P},(\text{zlb})\prime} X_t + X_t' \mathcal{C}_n^{\mathbb{P},(\text{zlb})} X_t + \mathcal{D}_n^{\mathbb{P},(\text{zlb})} z_t\right).
\end{aligned}$$

where the loadings follow the recursion:

$$\begin{aligned}
\mathcal{A}_n^{(\text{zlb})} &= \mathcal{A}_{n-1}^{(\text{zlb})} - \alpha^{\mathbb{Q}} - \frac{1}{2}\log\left|I_K - 2\Sigma^{\mathbb{Q}}\left(\mathcal{C}_{n-1}^{(\text{zlb})} - \beta^{\mathbb{Q}}\beta^{\mathbb{Q}\prime}\right)\right| \\
&+ \left(\mathcal{B}_{n-1}^{(\text{zlb})} - \kappa^{\mathbb{Q}}\beta^{\mathbb{Q}}\right)' \left[I_K - 2\Sigma^{\mathbb{Q}}\left(\mathcal{C}_{n-1}^{(\text{zlb})} - \beta^{\mathbb{Q}}\beta^{\mathbb{Q}\prime}\right)\right]^{-1} \left[\mu^{\mathbb{Q}} + \frac{1}{2}\Sigma^{\mathbb{Q}}\left(\mathcal{B}_{n-1}^{(\text{zlb})} - \kappa^{\mathbb{Q}}\beta^{\mathbb{Q}}\right)\right] \\
&+ \mu^{\mathbb{Q}\prime}\left(\mathcal{C}_{n-1}^{(\text{zlb})} - \beta^{\mathbb{Q}}\beta^{\mathbb{Q}\prime}\right)\left[I_K - 2\Sigma^{\mathbb{Q}}\left(\mathcal{C}_{n-1}^{(\text{zlb})} - \beta^{\mathbb{Q}}\beta^{\mathbb{Q}\prime}\right)\right]^{-1}\mu^{\mathbb{Q}} \\
\mathcal{B}_n^{(\text{zlb})} &= \Phi^{\mathbb{Q}\prime}\left[I_K - 2\Sigma^{\mathbb{Q}}\left(\mathcal{C}_{n-1}^{(\text{zlb})} - \beta^{\mathbb{Q}}\beta^{\mathbb{Q}\prime}\right)\right]^{-1'}\left[\left(\mathcal{B}_{n-1}^{(\text{zlb})} - \kappa^{\mathbb{Q}}\beta^{\mathbb{Q}}\right) + 2\left(\mathcal{C}_{n-1}^{(\text{zlb})} - \beta^{\mathbb{Q}}\beta^{\mathbb{Q}\prime}\right)'\mu^{\mathbb{Q}}\right] \\
\mathcal{C}_n^{(\text{zlb})} &= \Phi^{\mathbb{Q}\prime}\left(\mathcal{C}_{n-1}^{(\text{zlb})} - \beta^{\mathbb{Q}}\beta^{\mathbb{Q}\prime}\right)\left[I_K - 2\Sigma^{\mathbb{Q}}\left(\mathcal{C}_{n-1}^{(\text{zlb})} - \beta^{\mathbb{Q}}\beta^{\mathbb{Q}\prime}\right)\right]^{-1}\Phi^{\mathbb{Q}} \\
\mathcal{D}_n^{(\text{zlb})} &= -\phi^{\mathbb{Q}}.
\end{aligned}$$

For the physical probabilities, the recursions are the same replacing the risk-neutral parameters by the physical ones. We deduce the liftoff probabilities, i.e. to see the first interest rate hike in exactly $n+1$ periods.

$$\mathbb{P}\left(r_{t+1:t+n} = \underline{r}, r_{t+n+1} > \underline{r} \middle| \underline{f}_t\right) = \mathbb{P}\left(r_{t+1:t+n} = \underline{r} \middle| \underline{f}_t\right) - \mathbb{P}\left(r_{t+1:t+n+1} = \underline{r} \middle| \underline{f}_t\right).$$

B Internet Appendix (not for publication)

B.1 Dynamics for a general model

This Section shows how to easily generalize our assumed inflation dynamics for incorporating any number of macroeconomic variables. We assume that the dynamics of a $K \times 1$ vector of risk factors X_t are given by the following vector autoregression:

$$X_{t+1} = \mu + \Phi X_t + v_{t+1}\,, \tag{31}$$

where $v_{t+1} \overset{i.i.d.}{\sim} \mathcal{N}(0, \Sigma)$. This state vector contains three sets of variables, such that $X_{t+1} = \left(m^*_{t+1},\, \sigma_{t+1},\, y'_{t+1}\right)'$ where m^*_{t+1} and σ_{t+1} are vectors of size $K_m \times 1$ and $K_\sigma \times 1$ respectively and y_t is a vector of yield-specific risk factors of size $K_y \times 1$ ($K = K_m + K_\sigma + K_y$).

Let us consider a set of $K_\chi \times 1$ macroeconomic variables χ_t. We assume that the dynamics of the macroeconomic variables are given by:

$$\chi_t = \overline{\chi} + \Upsilon_m m^*_t + \Upsilon_\sigma \operatorname{diag}(\sigma_{t+1})\, \varepsilon^\chi_{t+1}\,, \tag{32}$$

where $\varepsilon^\chi_{t+1} \overset{i.i.d.}{\sim} \mathcal{N}(0, I_{K_\chi})$ and is uncorrelated with v_{t+1}, $\overline{\chi}$ is a $K_\chi \times 1$ vector, Υ_m is a $K_\chi \times K_m$ matrix and Υ_σ is a $K_\chi \times K_\sigma$ matrix.

This formulation still allows to discriminate between macroeconomic trends and volatility factors, which can eventually be of smaller dimension than the number of macroeconomic variables. The remaining pieces of the model write exactly the same as in Section 2 and all pricing and statistical properties remain intact.

B.2 Affine $\mathbb{P}$-property

In this Section, we show that our physical dynamics are affine. Define $u = [u_x', \text{Vec}(U_x)', u_z']'$, where the blocks have respective size K, K^2 and 1. We first introduce the following Lemma.

Lemma B.1 *The conditional Laplace transform of* $[X_t', \text{Vec}(X_t X_t')']'$ *given its past is given by:*

$$\begin{aligned}
& \mathbb{E}\left[\exp\left(u_x' X_t + X_t' U_x X_t\right) \middle| \underline{X_{t-1}}\right] \\
= \; & \exp\left\{ u_x'(I_K - 2\Sigma U_x)^{-1}\left(\mu + \frac{1}{2}\Sigma u_x\right) + \mu' U_x (I_K - 2\Sigma U_x)^{-1}\mu - \frac{1}{2}\log\left|I_K - 2\Sigma U_x\right| \right. \\
+ \; & \left. (u_x + 2U_x\mu)'(I_K - 2\Sigma U_x)^{-1}\Phi X_{t-1} + X_{t-1}\Phi' U_x (I_K - 2\Sigma U_x)^{-1}\Phi X_{t-1} \right\}
\end{aligned}$$

Proof See Cheng and Scaillet (2007). ■

Let us now calculate the conditional Laplace transform of $f_t := [X_t', \text{Vec}(X_t X_t')', z_t]$ given $\underline{f_{t-1}}$.

$$\begin{aligned}
& \mathbb{E}\left[\exp\left(u' f_t\right) \middle| \underline{f_{t-1}}\right] = \mathbb{E}\left[\exp\left(u_x' X_t + X_t' U_x X_t + u_z z_t\right) \middle| \underline{f_{t-1}}\right] \\
= \; & \mathbb{E}\left\{\mathbb{E}\left[\exp\left(u_x' X_t + X_t' U_x X_t + u_z z_t\right) \middle| \underline{f_{t-1}}, X_t\right] \middle| \underline{f_{t-1}}\right\} \\
= \; & \mathbb{E}\left[\exp\left\{u_x' X_t + X_t' U_x X_t + \frac{u_z c}{1 - u_z c}\left[\alpha + \kappa\beta' X_t + X_t'\beta\beta' X_t + \phi z_{t-1}\right]\right\} \middle| \underline{f_{t-1}}\right], \\
= \; & \exp\left(\frac{u_z c}{1 - u_z c}(\alpha + \phi z_{t-1})\right) \mathbb{E}\left[\exp\left\{\left(u_x + \frac{\kappa u_z c}{1 - u_z c}\beta\right)' X_t + X_t'\left(U_x + \frac{u_z c}{1 - u_z c}\beta\beta'\right) X_t\right\} \middle| \underline{f_{t-1}}\right],
\end{aligned}$$

We hence obtain the conditional Laplace transform of $[X_t', \text{Vec}(X_t X_t')']'$ applied in the two arguments $\left[\left(u_x + \kappa\frac{u_z c}{1-u_z c}\beta\right)'; \text{Vec}\left(U_x + \frac{u_z c}{1-u_z c}\beta\beta'\right)'\right]'$. Using Lemma B.1, we have:

$$
\begin{aligned}
& \mathbb{E}\left[\exp\left(u' f_t\right) \middle| \underline{f_{t-1}}\right] \\
= \; & \exp\left\{ \frac{u_z c}{1-u_z c}(\alpha + \phi z_{t-1}) + \left(u_x + \frac{\kappa u_z c}{1-u_z c}\beta\right)' \left[I_K - 2\Sigma\left(U_x + \frac{u_z c}{1-u_z c}\beta\beta'\right)\right]^{-1} \left[\mu + \frac{1}{2}\Sigma\left(u_x + \frac{\kappa u_z c}{1-u_z c}\beta\right)\right] \right. \\
+ \; & \mu'\left(U_x + \frac{u_z c}{1-u_z c}\beta\beta'\right)\left[I_K - 2\Sigma\left(U_x + \frac{u_z c}{1-u_z c}\beta\beta'\right)\right]^{-1}\mu - \frac{1}{2}\log\left|I_K - 2\Sigma\left(U_x + \frac{u_z c}{1-u_z c}\beta\beta'\right)\right| \\
+ \; & \left[\left(u_x + \frac{\kappa u_z c}{1-u_z c}\beta\right)' + 2\mu'\left(U_x + \frac{u_z c}{1-u_z c}\beta\beta'\right)\right]\left[I_K - 2\Sigma\left(U_x + \frac{u_z c}{1-u_z c}\beta\beta'\right)\right]^{-1}\Phi X_{t-1} \\
+ \; & \left. X_{t-1}'\Phi'\left(U_x + \frac{u_z c}{1-u_z c}\beta\beta'\right)\left[I_K - 2\Sigma\left(U_x + \frac{u_z c}{1-u_z c}\beta\beta'\right)\right]^{-1}\Phi X_{t-1}\right\}. \qquad (33)
\end{aligned}
$$

This conditional Laplace transform is an exponential-affine function of f_{t-1}. (f_t) is therefore an affine process under the physical measure. ■

B.3 Convexity adjustment for the pricing kernel

We now turn our interest to the derivation of the convexity adjustment in the pricing kernel given by Equation (6). By no-arbitrage, we have that:

$$
\mathbb{E}_{t-1}\left(M_t\right) = e^{-r_{t-1}} \Longleftrightarrow \mathbb{E}_{t-1}\left[\exp\left(\lambda_{t-1}' v_t + \lambda_r \varepsilon_t^r\right)\right] = \exp\left(\xi_{t-1}\right).
$$

To come back to the formulation of Equation (33), it is sufficient to multiply the left- and right-hand side of the previous Equation:

$$
\begin{aligned}
& \mathbb{E}_{t-1}\left[\exp\left(\lambda_{t-1}' v_t + \lambda_r \varepsilon_t^r\right)\right] = \exp\left(\xi_{t-1}\right) \\
\Longleftrightarrow \; & \mathbb{E}_{t-1}\left[\exp\left(\lambda_{t-1}' X_t + \lambda_r z_t\right)\right] = \exp\left[\xi_{t-1} + \lambda_{t-1}'\left(\mu + \Phi X_{t-1}\right) + \lambda_r \mathbb{E}_{t-1}\left(z_t\right)\right].
\end{aligned}
$$

Thus, using the result of Equation (33), we obtain:

$$
\xi_{t-1} = -\lambda_{t-1}'\left(\mu + \Phi X_{t-1}\right) - \lambda_r \mathbb{E}_{t-1}\left(z_t\right) + \frac{\lambda_r c}{1-\lambda_r c}(\alpha + \phi z_{t-1})
$$

$$
\begin{aligned}
&+ \quad \left(\lambda_{t-1} + \frac{\kappa\lambda_r c}{1-\lambda_r c}\beta\right)' \left[I_K - 2\Sigma\left(\frac{\lambda_r c}{1-\lambda_r c}\beta\beta'\right)\right]^{-1} \left[\mu + \frac{1}{2}\Sigma\left(\lambda_{t-1} + \frac{\kappa\lambda_r c}{1-\lambda_r c}\beta\right)\right] \\
&+ \quad \mu'\left(\frac{\lambda_r c}{1-\lambda_r c}\beta\beta'\right)\left[I_K - 2\Sigma\left(\frac{\lambda_r c}{1-\lambda_r c}\beta\beta'\right)\right]^{-1}\mu - \frac{1}{2}\log\left|I_K - 2\Sigma\left(\frac{\lambda_r c}{1-\lambda_r c}\beta\beta'\right)\right| \\
&+ \quad \left[\left(\lambda_{t-1} + \frac{\kappa\lambda_r c}{1-\lambda_r c}\beta\right)' + 2\mu'\left(\frac{\lambda_r c}{1-\lambda_r c}\beta\beta'\right)\right]\left[I_K - 2\Sigma\left(\frac{\lambda_r c}{1-\lambda_r c}\beta\beta'\right)\right]^{-1}\Phi X_{t-1} \\
&+ \quad X'_{t-1}\Phi'\left(\frac{\lambda_r c}{1-\lambda_r c}\beta\beta'\right)\left[I_K - 2\Sigma\left(\frac{\lambda_r c}{1-\lambda_r c}\beta\beta'\right)\right]^{-1}\Phi X_{t-1}\,.
\end{aligned}
$$

B.4 Multi-horizon Laplace transform

Using the notation:

$$
\mathbb{E}^{\mathbb{Q}}\left[\exp\left(u' f_t\right)\left|\underline{f_{t-1}}\right.\right] =: \exp\left\{\mathbb{A}^{\mathbb{Q}}(u) + \mathbb{B}^{\mathbb{Q}'}(u)X_{t-1} + X'_{t-1}\mathbb{C}^{\mathbb{Q}}(u)X_{t-1} + \mathbb{D}^{\mathbb{Q}}(u)z_{t-1}\right\},
$$

where:

$$
\begin{aligned}
\mathbb{A}^{\mathbb{Q}}(u) &= \frac{u_z c^{\mathbb{Q}}}{1-u_z c^{\mathbb{Q}}}\alpha^{\mathbb{Q}} - \frac{1}{2}\log\left|I_K - 2\Sigma^{\mathbb{Q}}\left(U_x + \frac{\kappa u_z c^{\mathbb{Q}}}{1-u_z c^{\mathbb{Q}}}\beta^{\mathbb{Q}}\beta^{\mathbb{Q}'}\right)\right| \\
&+ \left(u_x + \frac{u_z c^{\mathbb{Q}}}{1-u_z c^{\mathbb{Q}}}\beta^{\mathbb{Q}}\right)'\left[I_K - 2\Sigma^{\mathbb{Q}}\left(U_x + \frac{\kappa u_z c^{\mathbb{Q}}}{1-u_z c^{\mathbb{Q}}}\beta^{\mathbb{Q}}\beta^{\mathbb{Q}'}\right)\right]^{-1}\left[\mu^{\mathbb{Q}} + \frac{1}{2}\Sigma^{\mathbb{Q}}\left(u_x + \frac{u_z c^{\mathbb{Q}}}{1-u_z c^{\mathbb{Q}}}\beta^{\mathbb{Q}}\right)\right] \\
&+ \mu^{\mathbb{Q}'}\left(U_x + \frac{\kappa u_z c^{\mathbb{Q}}}{1-u_z c^{\mathbb{Q}}}\beta^{\mathbb{Q}}\beta^{\mathbb{Q}'}\right)\left[I_K - 2\Sigma^{\mathbb{Q}}\left(U_x + \frac{\kappa u_z c^{\mathbb{Q}}}{1-u_z c^{\mathbb{Q}}}\beta^{\mathbb{Q}}\beta^{\mathbb{Q}'}\right)\right]^{-1}\mu^{\mathbb{Q}} \\
\mathbb{B}^{\mathbb{Q}}(u) &= \Phi^{\mathbb{Q}'}\left[I_K - 2\Sigma^{\mathbb{Q}}\left(U_x + \frac{\kappa u_z c^{\mathbb{Q}}}{1-u_z c^{\mathbb{Q}}}\beta^{\mathbb{Q}}\beta^{\mathbb{Q}'}\right)\right]^{-1'}\left[\left(u_x + \frac{u_z c^{\mathbb{Q}}}{1-u_z c^{\mathbb{Q}}}\beta^{\mathbb{Q}}\right) + 2\left(U_x + \frac{\kappa u_z c^{\mathbb{Q}}}{1-u_z c^{\mathbb{Q}}}\beta^{\mathbb{Q}}\beta^{\mathbb{Q}'}\right)'\mu^{\mathbb{Q}}\right] \\
\mathbb{C}^{\mathbb{Q}}(u) &= \Phi^{\mathbb{Q}'}\left(U_x + \frac{\kappa u_z c^{\mathbb{Q}}}{1-u_z c^{\mathbb{Q}}}\beta^{\mathbb{Q}}\beta^{\mathbb{Q}'}\right)\left[I_K - 2\Sigma^{\mathbb{Q}}\left(U_x + \frac{\kappa u_z c^{\mathbb{Q}}}{1-u_z c^{\mathbb{Q}}}\beta^{\mathbb{Q}}\beta^{\mathbb{Q}'}\right)\right]^{-1}\Phi^{\mathbb{Q}} \\
\mathbb{D}^{\mathbb{Q}}(u) &= \frac{u_z c^{\mathbb{Q}}}{1-u_z c^{\mathbb{Q}}}\phi^{\mathbb{Q}}
\end{aligned}
$$

Since the one-period ahead conditional risk-neutral Laplace transform of f_t given $\underline{f_{t-1}}$ is exponential-affine in f_{t-1}, it is well-known that the condi-

tional multi-horizon risk-neutral Laplace transform of $(f_t, \ldots, f_{t+k})$ is also exponential-affine in f_{t-1} (see e.g. Darolles, Gourieroux, and Jasiak (2006)). We obtain:

$$\begin{aligned}\mathbb{E}^{\mathbb{Q}}\left[\exp\left(\sum_{i=0}^{k} u_i' f_{t+i}\right)\Big|\underline{f_{t-1}}\right] &= \exp\Big(\mathbb{A}_k^{\mathbb{Q}}(u_0,\ldots,u_k) + \mathbb{B}_k^{\mathbb{Q}'}(u_0,\ldots,u_k)X_{t-1} \\ &+ X_{t-1}'\mathbb{C}_k^{\mathbb{Q}}(u_0,\ldots,u_k)\,X_{t-1} + \mathbb{D}_k^{\mathbb{Q}}(u_0,\ldots,u_k)\,\mathfrak{r}_{t-1}\Big),\end{aligned}$$

where:

$$\begin{aligned}\mathbb{A}_k^{\mathbb{Q}}(u_0,\ldots,u_k) &:= \mathbb{A}_{k,k}^{\mathbb{Q}}(u_0,\ldots,u_k)\\ \mathbb{B}_k^{\mathbb{Q}}(u_0,\ldots,u_k) &:= \mathbb{B}_{k,k}^{\mathbb{Q}}(u_0,\ldots,u_k)\\ \mathbb{C}_k^{\mathbb{Q}}(u_0,\ldots,u_k) &:= \mathbb{C}_{k,k}^{\mathbb{Q}}(u_0,\ldots,u_k)\\ \mathbb{D}_k^{\mathbb{Q}}(u_0,\ldots,u_k) &:= \mathbb{D}_{k,k}^{\mathbb{Q}}(u_0,\ldots,u_k),\end{aligned}$$

with initial conditions $\mathbb{A}_{k,1}^{\mathbb{Q}}(u_0,\ldots,u_k) = \mathbb{A}^{\mathbb{Q}}(u_k)$, $\mathbb{B}_{k,1}^{\mathbb{Q}}(u_0,\ldots,u_k) = \mathbb{B}^{\mathbb{Q}}(u_k)$, $\mathbb{C}_{k,1}^{\mathbb{Q}}(u_0,\ldots,u_k) = \mathbb{C}^{\mathbb{Q}}(u_k)$ and $\mathbb{D}_{k,1}^{\mathbb{Q}}(u_0,\ldots,u_k) = \mathbb{D}^{\mathbb{Q}}(u_k)$, and $\forall i \in \{2,\ldots,k\}$,

$$\begin{aligned}\mathbb{A}_{k,i}^{\mathbb{Q}}(u_0,\ldots,u_k) &= \mathbb{A}_{k,i-1}^{\mathbb{Q}}(u_0,\ldots,u_k)\\ &+ \mathbb{A}^{\mathbb{Q}}\left(u_{k-i+1} + \left[\mathbb{B}_{k,i-1}^{\mathbb{Q}'}(u_0,\ldots,u_k), \mathrm{Vec}\left(\mathbb{C}_{k,i-1}^{\mathbb{Q}}(u_0,\ldots,u_k)\right)', \mathbb{D}_{k,i-1}^{\mathbb{Q}}(u_0,\ldots,u_k)\right]'\right)\\ \mathbb{B}_{k,i}^{\mathbb{Q}}(u_0,\ldots,u_k) &= \mathbb{B}^{\mathbb{Q}}\left(u_{k-i+1} + \left[\mathbb{B}_{k,i-1}^{\mathbb{Q}'}(u_0,\ldots,u_k), \mathrm{Vec}\left(\mathbb{C}_{k,i-1}^{\mathbb{Q}}(u_0,\ldots,u_k)\right)', \mathbb{D}_{k,i-1}^{\mathbb{Q}}(u_0,\ldots,u_k)\right]'\right)\\ \mathbb{C}_{k,i}^{\mathbb{Q}}(u_0,\ldots,u_k) &= \mathbb{C}^{\mathbb{Q}}\left(u_{k-i+1} + \left[\mathbb{B}_{k,i-1}^{\mathbb{Q}'}(u_0,\ldots,u_k), \mathrm{Vec}\left(\mathbb{C}_{k,i-1}^{\mathbb{Q}}(u_0,\ldots,u_k)\right)', \mathbb{D}_{k,i-1}^{\mathbb{Q}}(u_0,\ldots,u_k)\right]'\right)\\ \mathbb{D}_{k,i}^{\mathbb{Q}}(u_0,\ldots,u_k) &= \mathbb{D}^{\mathbb{Q}}\left(u_{k-i+1} + \left[\mathbb{B}_{k,i-1}^{\mathbb{Q}'}(u_0,\ldots,u_k), \mathrm{Vec}\left(\mathbb{C}_{k,i-1}^{\mathbb{Q}}(u_0,\ldots,u_k)\right)', \mathbb{D}_{k,i-1}^{\mathbb{Q}}(u_0,\ldots,u_k)\right]'\right).\end{aligned}$$

Since the conditional Laplace transform of f_t given $\underline{f_{t-1}}$ under the physical

measure is the same function as the risk-neutral one, but plugging in the physical parameters instead of the risk-neutral ones, we easily obtain:

$$\begin{aligned}
&\varphi_{t-1}(u_0, \ldots, u_k) = \mathbb{E}\left[\exp\left(\sum_{i=0}^{k} u_i' f_{t+i}\right) \Big| \underline{f_{t-1}}\right] \\
=: \;& \exp\left(\mathbb{A}_k(u_0, \ldots, u_k) + \mathbb{B}_k'(u_0, \ldots, u_k) X_{t-1} + X_{t-1}' \mathbb{C}_k(u_0, \ldots, u_k)\, X_{t-1} + \mathbb{D}_k(u_0, \ldots, u_k) \mathfrak{r}_{t-1}\right) \qquad (34)
\end{aligned}$$

where:

$$\begin{aligned}
\mathbb{A}_k(u_0, \ldots, u_k) &:= \mathbb{A}_{k,k}(u_0, \ldots, u_k) \\
\mathbb{B}_k(u_0, \ldots, u_k) &:= \mathbb{B}_{k,k}(u_0, \ldots, u_k) \\
\mathbb{C}_k(u_0, \ldots, u_k) &:= \mathbb{C}_{k,k}(u_0, \ldots, u_k) \\
\mathbb{D}_k(u_0, \ldots, u_k) &:= \mathbb{D}_{k,k}(u_0, \ldots, u_k),
\end{aligned}$$

with initial conditions $\mathbb{A}_{k,1}(u_0, \ldots, u_k) = \mathbb{A}(u_k)$, $\mathbb{B}_{k,1}(u_0, \ldots, u_k) = \mathbb{B}(u_k)$, $\mathbb{C}_{k,1}(u_0, \ldots, u_k) = \mathbb{C}(u_k)$ and $\mathbb{D}_{k,1}(u_0, \ldots, u_k) = \mathbb{D}(u_k)$, and $\forall i \in \{2, \ldots, k\}$,

$$\begin{aligned}
\mathbb{A}_{k,i}(u_0, \ldots, u_k) &= \mathbb{A}_{k,i-1}(u_0, \ldots, u_k) \\
&+ \mathbb{A}\left(u_{k-i+1} + \left[\mathbb{B}_{k,i-1}'(u_0, \ldots, u_k), \mathrm{Vec}\left(\mathbb{C}_{k,i-1}(u_0, \ldots, u_k)\right)', \mathbb{D}_{k,i-1}(u_0, \ldots, u_k)\right]'\right) \\
\mathbb{B}_{k,i}(u_0, \ldots, u_k) &= \mathbb{B}\left(u_{k-i+1} + \left[\mathbb{B}_{k,i-1}'(u_0, \ldots, u_k), \mathrm{Vec}\left(\mathbb{C}_{k,i-1}(u_0, \ldots, u_k)\right)', \mathbb{D}_{k,i-1}(u_0, \ldots, u_k)\right]'\right) \\
\mathbb{C}_{k,i}(u_0, \ldots, u_k) &= \mathbb{C}\left(u_{k-i+1} + \left[\mathbb{B}_{k,i-1}'(u_0, \ldots, u_k), \mathrm{Vec}\left(\mathbb{C}_{k,i-1}(u_0, \ldots, u_k)\right)', \mathbb{D}_{k,i-1}(u_0, \ldots, u_k)\right]'\right) \\
\mathbb{D}_{k,i}(u_0, \ldots, u_k) &= \mathbb{C}\left(u_{k-i+1} + \left[\mathbb{B}_{k,i-1}'(u_0, \ldots, u_k), \mathrm{Vec}\left(\mathbb{C}_{k,i-1}(u_0, \ldots, u_k)\right)', \mathbb{D}_{k,i-1}(u_0, \ldots, u_k)\right]'\right).
\end{aligned}$$

B.5 Conditional moments of f_t

From Monfort, Renne, and Roussellet (2015) the conditional first two moments of $(X_t', \text{Vec}(X_t X_t')')'$ given the past can be expressed as:

$$\mathbb{E}\left[\begin{pmatrix} X_t \\ \text{Vec}(X_t X_t') \end{pmatrix} \middle| \underline{f_{t-1}}\right] = \begin{pmatrix} \mu \\ \text{Vec}(\mu\mu' + \Sigma) \end{pmatrix} + \left(\begin{array}{c|c} \Phi & 0 \\ \hline \mu \otimes \Phi + \Phi \otimes \mu & \Phi \otimes \Phi \end{array}\right) \begin{pmatrix} X_{t-1} \\ \text{Vec}(X_{t-1} X_{t-1}') \end{pmatrix}$$

$$\mathbb{V}\left[\begin{pmatrix} X_t \\ \text{Vec}(X_t X_t') \end{pmatrix} \middle| \underline{f_{t-1}}\right] = \left(\begin{array}{c|c} \Sigma & \Sigma\Gamma_{t-1}' \\ \hline \Gamma_{t-1}\Sigma & \Gamma_{t-1}\Sigma\Gamma_{t-1}' + (I_{K^2} + \mathcal{K}_K)(\Sigma \otimes \Sigma) \end{array}\right).$$

where $\otimes$ is the standard Kronecker product, $\Gamma_{t-1} = [I_K \otimes (\mu + \Phi X_{t-1}) + (\mu + \Phi X_{t-1}) \otimes I_K]$, and $\mathcal{K}_K$ is the $(K^2 \times K^2)$ commutation matrix.

Given that we have conditional first two moments of z_t given f_{t-1} in Appendix A.1, we focus here on the conditional covariance between $(X_t',\ \text{Vec}(X_t X_t')')'$ and z_t:

$$\begin{aligned} \mathbb{C}ov\left[\begin{pmatrix} X_t \\ \text{Vec}(X_t X_t') \end{pmatrix},\ z_t \middle| \underline{f_{t-1}}\right] &= \mathbb{C}ov\left[\begin{pmatrix} X_t \\ \text{Vec}(X_t X_t') \end{pmatrix},\ c\left(\alpha + \kappa\beta' X_t + X_t'\beta\beta' X_t + \phi z_{t-1}\right) \middle| \underline{f_{t-1}}\right] \\ &= \begin{pmatrix} c\Sigma\beta\left[\kappa + 2\left(\mu + \Phi X_{t-1}\right)'\beta\right] \\ c\Gamma_{t-1}\Sigma\beta\left[\kappa + 2\left(\mu + \Phi X_{t-1}\right)'\beta\right] + 2c\text{Vec}(\Sigma\beta\beta'\Sigma) \end{pmatrix}. \end{aligned}$$

In the end, putting the previous results together, we obtain that f_t follows a semi-strong VAR of the form

$$f_t = \Psi_0 + \Psi f_{t-1} + \text{Vec}^{-1/2}(\Omega_0 + \Omega f_{t-1})\zeta_t \tag{35}$$

with parameters given by:

$$\Psi_0 = \begin{pmatrix} \mu \\ \text{Vec}(\mu\mu' + \Sigma) \\ c\left[\alpha + (\kappa + \beta'\mu)\,\beta'\mu + \beta'\Sigma\beta\right] \end{pmatrix},$$

$$\Psi = \left(\begin{array}{c|c|c} \Phi & 0 & 0 \\ \hline \mu \otimes \Phi + \Phi \otimes \mu & \Phi \otimes \Phi & 0 \\ \hline c\,(\kappa + 2\mu'\beta)\,\beta'\Phi & c\,(\beta'\Phi \otimes \beta'\Phi) & c\phi \end{array}\right),$$

and,

$$\text{Vec}^{-1}(\Omega_0 + \Omega f_{t-1}) =$$

$$\left(\begin{array}{c|c|l} \Sigma & \Sigma\Gamma'_{t-1} & c\Sigma\beta\left[\kappa + 2\left(\mu + \Phi X_{t-1}\right)'\beta\right] \\ \hline & \Gamma_{t-1}\Sigma\Gamma'_{t-1} + (I_{K^2} + \mathcal{K}_K)(\Sigma \otimes \Sigma) & c\Gamma_{t-1}\Sigma\beta\left[\kappa + 2\left(\mu + \Phi X_{t-1}\right)'\beta\right] + 2c\text{Vec}(\Sigma\beta\beta'\Sigma) \\ \hline & & c^2\left(\left[\kappa + 2\left(\mu + \Phi X_{t-1}\right)'\beta\right]^2\beta'\Sigma\beta + 2\left(\beta'\Sigma\beta\right)^2\right) \\ & & +\quad 2c^2\left(\alpha + \phi z_{t-1} + (\kappa + \beta'\mu)\,\beta'\mu + \beta'\Sigma\beta + (\kappa + 2\mu'\beta)\,\beta'\Phi X_{t-1} + \left(\beta'\Phi X_{t-1}\right)^2\right). \end{array}\right)$$

Looking at the Ψ matrix, we can easily see that the system is stationary as soon as the eigenvalues of Φ are inside the unit circle and that $c\phi$ is below one. In this case, $(I_{K+K^2+1} - \Psi)^{-1}$ exists, and we have:[12]

$$\mathbb{E}\left(f_{t+n}|\underline{f_t}\right) \;=\; \mathbb{E}\left(\Psi_0 + \Psi f_{t+n-1}|\underline{f_t}\right)$$

[12]The conditional moments formulas are given with the use of the matrix $(I_{K+K^2+1} - \Psi)^{-1}$ which is only invertible if the system is stationary. Note that the stationarity assumption is however not necessary and the same formulas can be expressed in the form of truncated sums.

$$= \sum_{i=0}^{n-1} \Psi^i \Psi_0 + \Psi^n f_t$$

Noting that:

$$\sum_{i=0}^{n-1} \Psi^i = \left(I_{K+K^2+1} - \Psi\right)^{-1} \left(I_{K+K^2+1} - \Psi^n\right) .$$

we obtain:

$$\begin{aligned} \mathbb{E}\left(f_{t+n}|\underline{f_t}\right) &= \left(I_{K+K^2+1} - \Psi\right)^{-1} \left(I_{K+K^2+1} - \Psi^n\right) \Psi_0 + \Psi^n f_t \\ \mathbb{E}\left(f_t\right) &= \left(I_{K+K^2+1} - \Psi\right)^{-1} \Psi_0 . \end{aligned}$$

For the conditional variance, we apply the law of total variance and obtain:

$$\begin{aligned} \mathbb{V}\left(f_{t+n}|\underline{f_t}\right) &= \mathbb{V}\left[\mathbb{E}\left(f_{t+n}|\underline{f_{t+n-1}}\right)|\underline{f_t}\right] + \mathbb{E}\left[\mathbb{V}\left(f_{t+n}|\underline{f_{t+n-1}}\right)|\underline{f_t}\right] \\ &= \mathbb{V}\left(\Psi f_{t+n-1}|\underline{f_t}\right) + \mathbb{E}\left[\mathrm{Vec}^{-1}\left(\Omega_0 + \Omega f_{t+n-1}\right)|\underline{f_t}\right] \\ &= \Psi \mathbb{V}\left(f_{t+n-1}|\underline{f_t}\right)\Psi' + \mathrm{Vec}^{-1}\left[\Omega_0 + \Omega\mathbb{E}\left(f_{t+n-1}|\underline{f_t}\right)\right] . \end{aligned}$$

Therefore,

$$\begin{aligned} \mathrm{Vec}\left[\mathbb{V}\left(f_{t+n}|\underline{f_t}\right)\right] &= (\Psi \otimes \Psi)\mathrm{Vec}\left[\mathbb{V}\left(f_{t+n-1}|\underline{f_t}\right)\right] + \\ &\qquad \left[\Omega_0 + \Omega\left\{\left(I_{K+K^2+1} - \Psi\right)^{-1}\left(I_{K+K^2+1} - \Psi^{n-1}\right)\Psi_0 + \Psi^{n-1} f_t\right\}\right] . \end{aligned}$$

A simple recursion gives the conditional variance as of function of the current

value of the factors:

$$\text{Vec}\left[\mathbb{V}\left(f_{t+n}\middle|\underline{f_t}\right)\right] = \sum_{i=0}^{n-1}\left(\Psi\otimes\Psi\right)^i\left(\Omega_0+\Omega\left[(I_{K+K^2+1}-\Psi)^{-1}(I_{K+K^2+1}-\Psi^{n-i-1})\Psi_0+\Psi^{n-i-1}f_t\right]\right)\,.$$

For the marginal variance, again using the law of total variance we have:

$$\begin{aligned}\mathbb{V}\left(f_t\right) &= \mathbb{V}\left[\mathbb{E}\left(f_t|\underline{f_{t-1}}\right)\right]+\mathbb{E}\left[\mathbb{V}\left(f_t|\underline{f_{t-1}}\right)\right]\\ &= \Psi\mathbb{V}\left(f_t\right)\Psi'+\text{Vec}^{-1}\left[\Omega_0+\Omega\mathbb{E}\left(f_t\right)\right]\,,\end{aligned}$$

Both first and second order conditional and unconditional moments of the extended vector f_t are thus closed form functions.

B.6 The Quadratic Kalman Filter

As in Cheng and Scaillet (2007), we stack together the linear and quadratic components of the risk factors. We denote by:

$$f_t^{(aug)} = \left(X_t^{(aug)'},\, X_t^{(aug)'}\otimes X_t^{(aug)'},\, z_t\right)'$$

We have shown that $f_t^{(aug)}$ is an affine process thus it possesses a semi-strong VAR form. Stacking together the transition and the measurement equations, we obtain:

$$\begin{aligned}f_t^{(aug)} &= \Psi_0^{(aug)}+\Psi^{(aug)}f_{t-1}^{(aug)}+\left[\text{Vec}^{-1}\left(\Omega_0^{(aug)}+\Omega^{(aug)}f_{t-1}^{(aug)}\right)\right]^{1/2}\zeta_t^{(aug)}\\ \mathcal{Y}_t^{(obs)} &=: \mathcal{A}+\widetilde{\mathcal{B}}'f_t^{(aug)}+\eta_t\,,\end{aligned}\tag{36}$$

where $\mathcal{A}$ and $\mathcal{B}$ stack respectively the intercepts and the loadings of the different observables. Notice that the transition Equation has been modified with

respect to the one presented in Appendix B.5 because of the addition of the idiosyncratic inflation shock ε_t^π to the system. Since extending the system is straightforward, we do not detail it here.

The Quadratic Kalman Filter (QKF) is particularly fitted to this class of models. The original filtering algorithm has been applied to state-space models where the transition dynamics are given by a Gaussian VAR and the measurement equations are linear-quadratic. This algorithm is slightly modified to incorporate z_t (which is non-Gaussian) and is detailed below.

Since the state-space model expressed with respect to f_t is affine, we can apply the Kalman filter algorithm. Using the notations $f_{t|t-1}^{(aug)} = \mathbb{E}(f_t^{(aug)}|\underline{\mathcal{Y}_{t-1}^{(obs)}})$, $P_{t|t-1} = \mathbb{V}(f_t^{(aug)}|\underline{\mathcal{Y}_{t-1}^{(obs)}})$, $f_{t|t}^{(aug)} = \mathbb{E}(f_t^{(aug)}|\underline{\mathcal{Y}_{t}^{(obs)}})$, $\mathcal{Y}_{t|t-1}^{(obs)} = \mathbb{E}(\mathcal{Y}_t^{(obs)}|\underline{\mathcal{Y}_{t-1}^{(obs)}})$, $M_{t|t-1} = \mathbb{V}(\mathcal{Y}_t^{(obs)}|\underline{\mathcal{Y}_{t-1}^{(obs)}})$, $P_{t|t} = \mathbb{V}(f_t^{(aug)}|\underline{\mathcal{Y}_{t}^{(obs)}})$, the steps in the algorithm are the following. Initialize the filter at $f_{0|0}^{(aug)} = \mathbb{E}(f_t^{(aug)})$ and $P_{0|0} = \mathbb{V}(f_t^{(aug)})$ using the results of Appendix B.5. Then, for each period t, predict the latent:

$$\begin{aligned} f_{t|t-1}^{(aug)} &= \Psi_0^{(aug)} + \Psi^{(aug)} f_{t-1|t-1}^{(aug)} \\ P_{t|t-1} &= \Psi^{(aug)} P_{t-1|t-1} \Psi^{(aug)\prime} + \text{Vec}^{-1}\left(\Omega_0^{(aug)} + \Omega^{(aug)} f_{t-1|t-1}^{(aug)}\right), \end{aligned}$$

predict the observable:

$$\begin{aligned} \mathcal{Y}_{t|t-1}^{(obs)} &= \mathcal{A} + \widetilde{\mathcal{B}}' f_{t|t-1}^{(aug)} \\ M_{t|t-1} &= \widetilde{\mathcal{B}}' P_{t|t-1} \widetilde{\mathcal{B}} + \mathbb{V}(\eta_t), \end{aligned}$$

update the prediction of the latent:

$$\begin{aligned} f_{t|t}^{(aug)} &= f_{t|t-1}^{(aug)} + P_{t|t-1} \widetilde{\mathcal{B}} M_{t|t-1}^{-1} \left(\mathcal{Y}_t^{(obs)} - \mathcal{Y}_{t|t-1}^{(obs)}\right) \\ P_{t|t} &= P_{t|t-1} - P_{t|t-1} \widetilde{\mathcal{B}} M_{t|t-1}^{-1} \widetilde{\mathcal{B}}' P_{t|t-1}, \end{aligned}$$

and compute the quasi log-likelihood assuming that the conditional distribution of $\mathcal{Y}_t^{(obs)}$ given $\underline{\mathcal{Y}_{t-1}^{(obs)}}$ is Gaussian with mean $\mathcal{Y}_{t|t-1}^{(obs)}$ and variance $M_{t|t-1}$.

$$\mathcal{L}_t = -\frac{1}{2}\left[K_{obs}\log(2\pi) + \log|M_{t|t-1}| + \left(\mathcal{Y}_t^{(obs)} - \mathcal{Y}_{t|t-1}^{(obs)}\right)' M_{t|t-1}^{-1}\left(\mathcal{Y}_t^{(obs)} - \mathcal{Y}_{t|t-1}^{(obs)}\right)\right] .$$

where K_{obs} is the dimension of the vector $\mathcal{Y}_t^{(obs)}$. In order to be consistent with the theoretical properties of the processes, two corrections are applied to the filtered values after storing the results. First, if the components of $z_{t|t}$ are negative, they are set to zero. Second, the filtered values of $\left(X^{(aug)} \otimes X^{(aug)}\right)_{t|t}$ are imposed to be exactly equal to $\left(X_{t|t}^{(aug)} \otimes X_{t|t}^{(aug)}\right)$.

As for the standard Kalman filter, the QKF provides a convenient way to handle missing data. One just has to adjust the size of the parameters in the measurement equations to predict only the variables that are observed. The measurement equation rewrites

$$\widetilde{\mathcal{Y}}_t^{(obs)} = E_t\left(\mathcal{A} + \widetilde{\mathcal{B}}' f_t^{(aug)} + \eta_t\right) =: \mathcal{A}_t + \widetilde{\mathcal{B}}_t' f_t^{(aug)} + E_t\eta_t ,$$

where $\widetilde{\mathcal{Y}}_t^{(obs)}$ is the subset of variables of Y_t that is observed, and E_t is a matrix selecting the corresponding rows. The prediction and update states remain the same using the adjusted parameters.

B.7 Primary Dealer Survey data

The primary dealer surveys (PDS) are publicly available from January 2011 on. They are conducted by the New York Fed to inform the FOMC members of primary dealer's expectation about the economy, monetary policy and financial markets developments. They are conducted on a regular basis, prior to the FOMC meetings (8 per year) in January, March, April, June, July,

September, October and December.[13] The questions and statistics collected have evolved to adapt to the economic environment, which makes it difficult to create homogeneous time-series on the probability to stay at the zero lower bound for a year.

We construct the conditional probabilities of staying at zero for a year using the question: *Of the possible outcomes below, please indicate the percent chance you attach to the timing of the first federal funds target rate increase.* (question #2 of each survey). The answer takes the form of a table associating the average of all participant answers per horizon. Table 5 provides two examples.

Table 5 – Examples of primary dealer survey answers

Panel(a): January 2011

	2011				2012				⩾ 2013
	Q1	Q2	Q3	Q4	Q1	Q2	Q3	Q4	Q1
Average	0%	1%	2%	11%	14%	13%	16%	17%	25%

Panel(b): March 2013

	2013		2014		2015		2016		2017	
	H1	H2	H1	H2	H1	H2	H1	H2	H1	⩾H2
Average	0%	1%	5%	10%	23%	27%	18%	8%	4%	4%

As can be seen on Table 5, the horizons of the question can be for next quarter or next semester. For all time periods where the horizons are quarterly or below, we aggregate the answers to get semi-annual horizons for homogeneity.

[13] See the survey results on https://www.newyorkfed.org/markets/primarydealer_survey_questions.html.

We then compute the probabilities as follow. Let $\mathcal{M}_t = \{1, \ldots, 12\}$ be the number of the current date-t month, $\mathcal{Y}_t$ the number of date-t year, and $\mathcal{H}_t = 1 + \mathbb{1}\{\mathcal{M}_t \in \{7, \ldots, 12\}\}$ the indicator of the semester. Let $p_t(\mathcal{H}_t, \mathcal{Y}_t)$ be the answer given in the survey. Our probabilities are given by:

$$\begin{aligned}
&[1 - p_t(\mathcal{H}_t, \mathcal{Y}_t)] \times [1 - p_t(\mathcal{H}_t + 1, \mathcal{Y}_t)] \times \left[1 - p_t(\mathcal{H}_t, \mathcal{Y}_t + 1)\, \tfrac{\mathcal{M}_t - 1}{12}\right] \qquad \text{if} \quad \mathcal{H}_t = 1 \\
&[1 - p_t(\mathcal{H}_t, \mathcal{Y}_t)] \times [1 - p_t(\mathcal{H}_t - 1, \mathcal{Y}_t + 1)] \times \left[1 - p_t(\mathcal{H}_t, \mathcal{Y}_t + 1)\, \tfrac{\mathcal{M}_t - 1}{12}\right] \quad \text{if} \quad \mathcal{H}_t = 2\,.
\end{aligned}$$

The previous formula assumes that inside the last semester considered, the timing of the first increase is uniformly distributed. For example, for the two panels of Table 5, we obtain the probabilities:

$$\begin{aligned}
2011 - 01 \quad &\rightarrow \quad [1 - (0 + 0.01)] \times [1 - (0.02 + 0.11)] \simeq 0.86 \\
2013 - 03 \quad &\rightarrow \quad (1 - 0) \times (1 - 0.01) \times \left(1 - \frac{3 - 1}{12} 0.05\right) \simeq 0.965\,.
\end{aligned}$$

Last, in order to avoid the fitted series to be too volatile, we fill out the missing data with the last available data point (step function) and impose that the measurement errors standard deviation is equal to 15% of the obtained series standard deviation.

B.8 Campbell-Shiller regression coefficients

The excess returns of any bond for k-holding periods can be defined as the return of a strategy consisting in buying the bond at time t and selling it at time $t + k$, minus the risk-less interest rate of maturity k. This k-period risk-less rate is equal to $R_t^{(k)}$ in the nominal world and $R_t^{(k)*}$ in the real world.

Proposition B.1 *The k-period nominal excess returns of nominal bonds and*

real excess returns of TIPS of maturity n are written:

$$\mathcal{XR}_{t+k} = \frac{n-k}{k}\left[R_t^{(n)} - R_{t+k}^{(n-k)}\right] + R_t^{(n)} - R_t^{(k)} \tag{37}$$

$$\mathcal{XR}^*_{t+k} = \frac{n-k}{k}\left[R_t^{(n)*} - R_{t+k}^{(n-k)*}\right] + R_t^{(n)*} - R_t^{(k)*}\,. \tag{38}$$

Corollary B.1.1 *The nominal and real expected excess returns of nominal bonds and TIPS at date t are affine functions of f_t computable in closed-form.*

Indeed, the one-year excess returns of holding a nominal bond of maturity n are given by:

$$\frac{1}{k}\log\left(\frac{P_{t+k}^{(n-k)}}{P_t^{(n)}}\right) - R_t^{(k)} = \frac{n}{k}R_t^{(n)} - \frac{n-k}{k}R_{t+k}^{(n-k)} - R_t^{(k)}\,.$$

For the excess returns of TIPS, I denote by $P_{t\to t+k}^{(n-k)*}$ the price at $t+k$ of the TIPS issued at time t of maturity n. Let $\mathcal{I}_t$ be the reference inflation index at date t.

$$P_{t\to t+k}^{(n-k)*} = \mathbb{E}\left[M_{t+k,t+n}\frac{\mathcal{I}_{t+n}}{\mathcal{I}_t}\Big|\underline{f_{t+k}}\right]\,, \tag{39}$$

where the principal is adjusted by the reference price-index variation between the inception and the maturity date (t and $t+n$). Rearranging formula (39), this price can be expressed with the price of a newly issued TIPS at date $t+k$.

$$P_{t\to t+k}^{(n-k)*} = \mathbb{E}\left[M_{t+k,t+n}\frac{\mathcal{I}_{t+n}}{\mathcal{I}_{t+k}}\Big|\underline{f_{t+k}}\right]\frac{\mathcal{I}_{t+k}}{\mathcal{I}_t} = P_{t+k}^{(n-k)*}\exp(\pi_{t:t+k})\,, \tag{40}$$

where $\pi_{t:t+k}$ is the inflation rate between t and $t+k$. Therefore, the excess returns of holding TIPS for k-holding periods are given by:

$$\frac{1}{k}\log\left(\frac{P_{t+k}^{(n-k)*}}{P_t^{(n)*}}\exp(\pi_{t:t+k})\right) - \frac{1}{k}\pi_{t:t+k} - R_t^{(k)*} = \frac{1}{k}\log\left(\frac{P_{t+k}^{(n-k)*}}{P_t^{(n)*}}\right) - R_t^{(k)*}$$

$$= \frac{n}{k} R_t^{(n)*} - \frac{n-k}{k} R_{t+k}^{(n-k)*} - R_t^{(k)*} .$$

These excess returns computations can be used to test whether the model is able to reproduce the deviations from the expectation hypothesis consistently with the data, and whether the model-implied predictions of excess returns are reasonable. These two tests are respectively called LPY-I and LPY-II in the terminology of Dai and Singleton (2002). Both LPY-I and LPY-II reformulates the excess returns in the form of the well-known Campbell and Shiller (1991) regressions (CS henceforth).

Proposition B.2 *The CS regressions are given by:*[14]

$$R_{t+k}^{(n-k)} - R_t^{(n)} = \alpha_{k,n} + \beta_{k,n} \frac{k}{n-k} \left(R_t^{(n)} - R_t^{(k)} \right) + \epsilon_{t+k,n} \tag{41}$$

$$R_{t+k}^{(n-k)*} - R_t^{(n)*} = \alpha_{k,n}^* + \beta_{k,n}^* \frac{k}{n-k} \left(R_t^{(n)*} - R_t^{(k)*} \right) + \epsilon_{t+k,n}^* . \tag{42}$$

All model-implied intercepts and slopes $\alpha_{k,n}$, $\alpha_{k,n}^*$, $\beta_{k,n}$, and $\beta_{k,n}^*$ are computable in closed-form.

Due to the similarities of the two specifications, we only present the computations of the coefficients for (41). By the properties of OLS estimator, the optimal slope of this regression is given by:

$$\beta_{k,n} = \frac{n-k}{k} \times \frac{\mathbb{C}ov \left[R_{t+k}^{(n-k)} - R_t^{(n)}, R_t^{(n)} - R_t^{(k)} \right]}{\mathbb{V} \left[R_t^{(n)} - R_t^{(k)} \right]} .$$

[14] The same formulations can be found in Haubrich et al. (2012). Evans (1998) formulates a slightly different regression with the Equation (20) of his paper. He expresses the expectation hypothesis equating the expected nominal excess returns of TIPS with the expected nominal excess returns of nominal bonds.

Using the notation $f_t = (X_t', X_t' \otimes X_t', z_t)'$,

$$R_t^{(n)} = \mathcal{A}_n + \mathcal{B}_n^{(R)'} f_t \,,$$

we obtain:

$$\beta_{k,n} = \frac{n-k}{k} \times \frac{\mathbb{C}ov\left[\mathcal{B}_{n-k}^{(R)'} f_{t+k} - \mathcal{B}_n^{(R)'} f_t, \mathcal{B}_n^{(R)'} f_t - \mathcal{B}_k^{(R)'} f_t\right]}{\mathbb{V}\left[\mathcal{B}_n^{(R)'} f_t - \mathcal{B}_k^{(R)'} f_t\right]},$$

which can be simplified using the semi-strong VAR form of Equation (35):

$$= \frac{n-k}{k} \times \frac{\mathbb{C}ov\left[\left(\mathcal{B}_{n-k}^{(R)'}\Psi^k - \mathcal{B}_n^{(R)'}\right) f_t, \left(\mathcal{B}_n^{(R)'} - \mathcal{B}_k^{(R)'}\right) f_t\right]}{\mathbb{V}\left[\left(\mathcal{B}_n^{(R)'} - \mathcal{B}_k^{(R)'}\right) f_t\right]}$$

$$= \frac{n-k}{k} \times \frac{\left[\left(\mathcal{B}_n^{(R)'} - \mathcal{B}_k^{(R)'}\right) \otimes \left(\mathcal{B}_{n-k}^{(R)'}\Psi^k - \mathcal{B}_n^{(R)'}\right)\right] \left(I_{(K+K^2+1)^2} - (\Psi \otimes \Psi)\right)^{-1} (\Omega_0 + \Omega\mathbb{E}(f_t))}{\left[\left(\mathcal{B}_n^{(R)'} - \mathcal{B}_k^{(R)'}\right) \otimes \left(\mathcal{B}_n^{(R)'} - \mathcal{B}_k^{(R)'}\right)\right] \left(I_{(K+K^2+1)^2} - (\Psi \otimes \Psi)\right)^{-1} (\Omega_0 + \Omega\mathbb{E}(f_t))},$$

where $\mathbb{E}(f_t) = (I_{K+K^2+1} - \Psi)^{-1}\Psi_0$. The proofs for the other regressions are of similar fashion, since all dependent and independent variables of all regressions can be expressed as affine functions of the process f_t.

If the expectation hypothesis was holding true, intercept and slopes would all be respectively equal to 0 and 1 and the corresponding excess return would average to zero. However, since the expectation hypothesis is largely violated in practice, the current slope of nominal/real interest rates can predict future excess returns. In practice, we consider $k = 12$ months. Testing LPY-I consists in estimating regressions (41-42) on the data for maturities ranging from 1 to 10 years, and comparing the estimated regression coefficients to the model-implied ones.[15] Testing LPY-II consists in performing the same regressions on the data

[15] To obtain the yields of nominal bonds and TIPS at all maturities for the whole sample

adding the corresponding model-implied expected excess returns series on the right-hand side of the regression. Adding the expected excess return should in theory correct the deviations from the expectation hypothesis.[16] A consistent model should be able to produce $\beta_{k,n}$ coefficients non significantly different from 1.

The results presented in Figure 10 show that all model-implied regression slope estimates are not statistically different (5% level) from the empirical estimates obtained directly from the data. We also perform joint F-tests considering not only the slopes of the regression but also the intercepts at the same time. Estimates gathered in Table 6 show that for all maturities we are not able to reject (I) the equality between model-implied and data-based intercepts and slopes in the first set of regressions, and (II) the equality of intercepts and slopes to (0,1) in the second set of regressions.

B.9 Impulse Response Methodology

The affine structure of the model makes it easy to perform an impulse response analysis. All the variables considered in this section can be expressed as linear combinations of f_t components.[17] Let us consider the impact of a shock of size s of variable v_2 on variable v_1, where $v_1 = e'_{v_1} f_t$ and $v_2 = e'_{v_2} f_t$, with e_{v_1} and e_{v_2} vectors weighting and selecting the right entries of f_t depending on the variables of interest. Let us also denote by $\mathcal{E}_v = (e_{v_3}, \cdots, e_{v_q})$ the matrix of $(q-2)$ weighting vectors that define variables $v_j = e'_{v_j} f_t$ that we do not want to shock at the initial period. The impulse response at horizon n, denoted by

period, we use the model-implied yield series reconstructed from the filtered factors and omit the measurement errors.

[16] We add the series of expected excess returns to the regressor so that we still estimate one regression slope.

[17] or equivalently, $f_t^{(aug)}$. we drop the superscript for ease of notation.

Figure 10 – Campbell-Shiller regression slopes

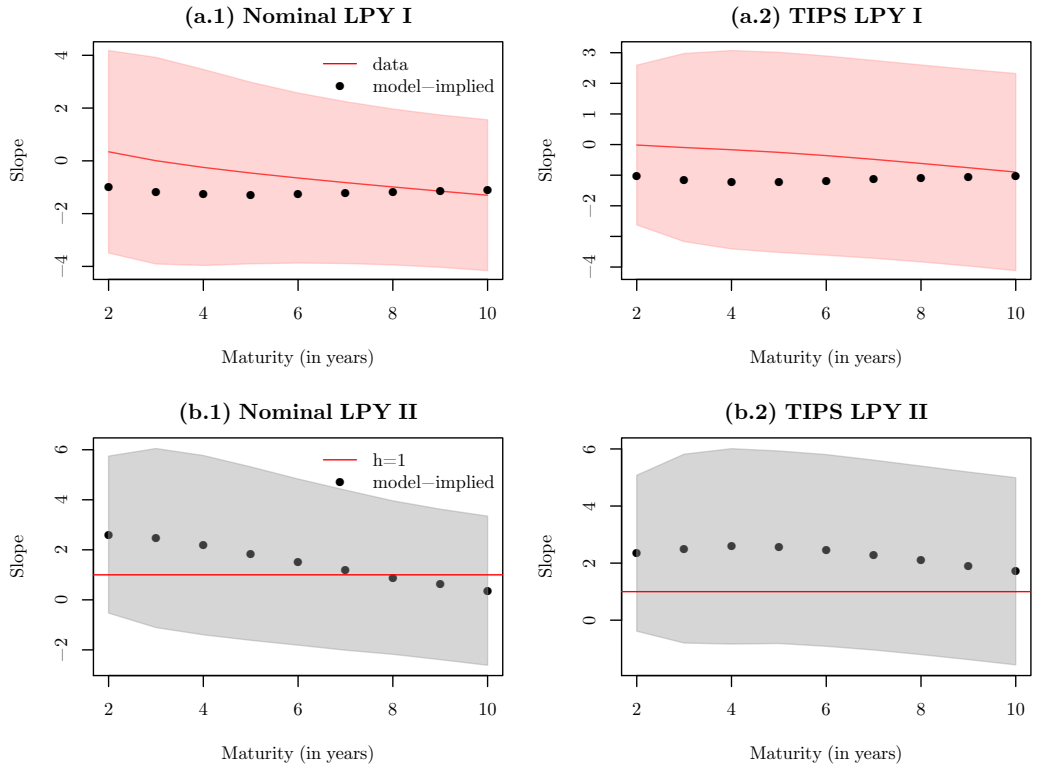

Notes: These graphs present the slopes of Campbell and Shiller regressions with a 12-months holding period. On panel (a), the red solid line gathers the slope estimates obtained with yields data. 95% Confidence intervals are computed using Newey-West robust estimators with automatically selected lag and are indicated with the red-shaded areas. Model-implied estimates are indicated with the black dots and computed with the yields and inflation expectation and variance formulas. On panel (b), the red solid line represents the theoretical values of the regression, namely one for all maturities. Model-implied estimates are indicated with the black dots and computed performing the Campbell and Shiller regressions where the dependent variable is adjusted by the model-implied expected excess returns. 95% Confidence intervals are computed using Newey-West robust estimators with automatically selected lag and are indicated with the grey-shaded areas.

$\mathcal{IRF}_{t,n}^{v_2 \to v_1}$ is given by:

$$\begin{aligned} \mathcal{IRF}_{t,n}^{v_2 \to v_1} &= \mathbb{E}\left(e_{v_1}' f_{t+n} \middle| \underline{f_{t-1}},\, e_{v_2}'[f_t - \mathbb{E}(f_t|\underline{f_{t-1}})] = s,\, \mathcal{E}_v'[f_t - \mathbb{E}(f_t|\underline{f_{t-1}})] = 0\right) \\ &- \mathbb{E}\left(e_{v_1}' f_{t+n} \middle| \underline{f_{t-1}},\, e_{v_2}'[f_t - \mathbb{E}(f_t|\underline{f_{t-1}})] = 0,\, \mathcal{E}_v'[f_t - \mathbb{E}(f_t|\underline{f_{t-1}})] = 0\right) \end{aligned} \tag{43}$$

Using the semi-strong VAR formulation of Equation (35), the impulse response function $\mathcal{IRF}_{t,n}^{v_2 \to v_1}$ is given by:

$$\begin{aligned} \mathcal{I}_{t,n}^{v_2 \to v_1} &= e_{v_1}' \Psi^n \Big[\mathbb{E}\left(f_t \middle| \underline{f_{t-1}},\, e_{v_2}'[f_t - \mathbb{E}(f_t|\underline{f_{t-1}})] = s,\, \mathcal{E}_v'[f_t - \mathbb{E}(f_t|\underline{f_{t-1}})] = 0 \right) \\ &- \mathbb{E}\left(f_t \middle| \underline{f_{t-1}},\, e_{v_2}'[f_t - \mathbb{E}(f_t|\underline{f_{t-1}})] = 0,\, \mathcal{E}_v'[f_t - \mathbb{E}(f_t|\underline{f_{t-1}})] = 0 \right) \Big], \end{aligned} \tag{44}$$

which only requires filtered values of the factor f_t given initial and observable conditions.

In our empirical exercise, we are in particular interested in shocking components of X_t itself for inflation central tendency or volatility shocks. The IRF of any variable v_1 to one of those structural shocks on $\iota_i' X_t$, ι_i selecting the i^{th} component of X_t is defined by:

$$\mathcal{IRF}_{t,n}^{v_2 \to v_1} = e_{v_1}' \Psi^n \begin{bmatrix} \Sigma^{1/2} & 0 \\ \Gamma_{t-1}\Sigma^{1/2} & \Sigma^{1/2} \otimes \Sigma^{1/2} \\ c\kappa\beta' & c(\beta \otimes \beta)' \end{bmatrix} \begin{bmatrix} s\iota_i \\ s^2 (\iota_i \otimes \iota_i) \end{bmatrix}, \tag{45}$$

where Γ_{t-1} is defined in Appendix B.5. For general linear functions of f_t, the QKF provides a natural procedure to obtain the most probable vector of shocks. Let $\widetilde{\mathcal{B}} = (e_{v_2},\, \mathcal{E}_v)$. The computable version of the IRF of Equation (44) is given by:

$$\mathcal{IRF}_{t,n}^{v_2 \to v_1} = e_{v_1}' \Psi^n \left[\mathrm{Vec}^{-1}(\Omega_0 + \Omega f_{t-1}) \widetilde{\mathcal{B}} \left(\widetilde{\mathcal{B}}' \left[\mathrm{Vec}^{-1}(\Omega_0 + \Omega f_{t-1}) \right] \widetilde{\mathcal{B}} \right)^{-1} \begin{pmatrix} s \\ 0 \end{pmatrix} \right]. \tag{46}$$

Again, the terms in the bracket are slightly modified such that $\text{Vec}(XX')_{t|t} = \text{Vec}(X_{t|t}X'_{t|t})$ and $z_{t|t} \geqslant 0$. To understand where Equation (46) comes from, consider the initial conditions f_{t-1} and the shocks are known without errors, so $P_{t-1,t-1} = 0$. Replacing the unknown quantities in Equation (44) by the values given by the QKF, the result is immediately obtained.

So far, we have only considered responses on variables that can be expressed as affine combinations of the extended vector of factors f_t. However, because of the closed-formedness of the conditional Laplace transform of f_t given its past, we can also compute the conditional expectation of any exponential-affine combination of f_t in closed-form. In general this requires the use of the multi-horizon conditional Laplace transform, which we detail in the technical Appendix B.4. In practice, we apply these formulas to obtain the responses of the ZLB probabilities and the corresponding premia.

The average IRF can be computed in two different ways. First, we can apply Formula (44) to the initial condition $f_{t-1} = \left[\bar{X}', \left(\bar{X} \otimes \bar{X}\right)', \bar{z}\right]'$, where $\bar{X} := \mathbb{E}(X_t)$ and $\bar{z} = \mathbb{E}(z_t)$.[18] Second, we can simulate many initial conditions f_{t-1} using its marginal distribution, compute the IRFs using Formula (44) for each initial condition, and average over the responses. The two approaches are not equivalent since they flip the order of integration (see for example Gallant et al. (1993) or Koop et al. (1996)). We rely on the latter method in Section 5.

B.10 Additional Tables and Figures from the benchmark ZLB model

[18] It is worth mentioning that the initial condition $f_{t-1} = [\bar{X}', \text{Vec}(\bar{X}\bar{X}')', \mathbb{E}(z_t)]'$ is different from $f_{t-1} = \mathbb{E}(f_{t-1})$ since $\mathbb{E}[XX'] \neq \mathbb{E}(X)\mathbb{E}(X')$. However, once conditioning by $X_{t-1} = \bar{X}$, it follows directly that $\text{Vec}(X_{t-1}X'_{t-1}) = \text{Vec}(\bar{X}\bar{X}')$ with probability one.

Figure 11 – Distribution of short-term interest rates and inflation

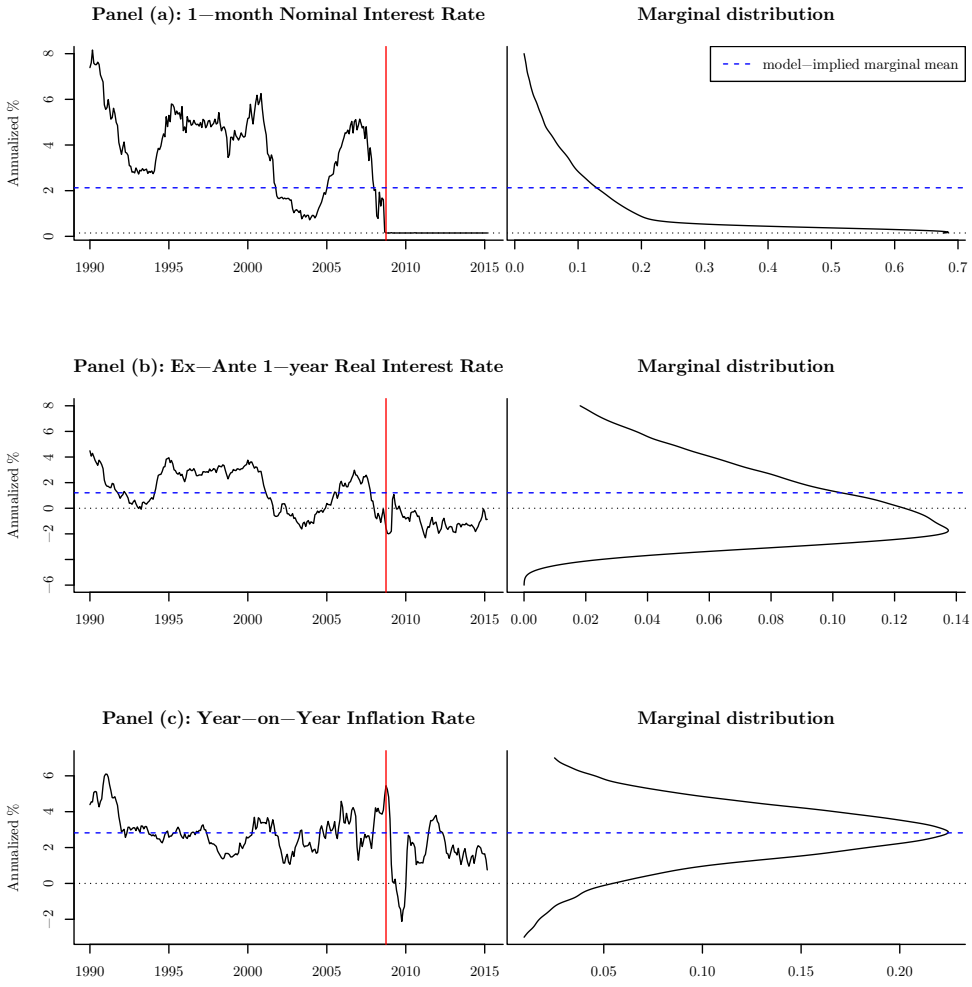

Notes: Marginal distributions on the right-hand side are computed with kernel density estimates on 100,000 simulations.

Table 6 – Campbell-Shiller regressions: 12 months holding period

		Panel (I): LPY-I regressions								
	Maturity (yrs)	2	3	4	5	6	7	8	9	10
Nominal bonds	$\hat{\alpha}_{12,n}^{(\text{model})}$	-0.341	-0.228	-0.231	-0.239	-0.235	-0.223	-0.208	-0.193	-0.179
	$\hat{\alpha}_{12,n}^{(\text{data})}$	-0.659	-0.548	-0.462	-0.385	-0.318	-0.260	-0.211	-0.169	-0.132
	$\sigma_{\text{NW}}\left(\hat{\alpha}_{12,n}^{(\text{data})}\right)$	(0.854)	(0.730)	(0.646)	(0.577)	(0.521)	(0.476)	(0.438)	(0.408)	(0.384)
	$\hat{\beta}_{12,n}^{(\text{model})}$	-1.011	-1.178	-1.266	-1.289	-1.268	-1.227	-1.185	-1.149	-1.122
	$\hat{\beta}_{12,n}^{(\text{data})}$	0.343	0.006	-0.248	-0.461	-0.649	-0.824	-0.989	-1.148	-1.302
	$\sigma_{\text{NW}}\left(\hat{\beta}_{12,n}^{(\text{data})}\right)$	(1.957)	(1.997)	(1.895)	(1.755)	(1.644)	(1.564)	(1.506)	(1.472)	(1.458)
	Joint p-val	0.78	0.84	0.86	0.88	0.91	0.94	0.98	0.99	0.99
Tips	$\hat{\alpha}_{12,n}^{*(\text{model})}$	-0.283	-0.169	-0.169	-0.178	-0.178	-0.170	-0.160	-0.150	-0.140
	$\hat{\alpha}_{12,n}^{*(\text{data})}$	-0.372	-0.366	-0.355	-0.331	-0.301	-0.268	-0.236	-0.206	-0.178
	$\sigma_{\text{NW}}\left(\hat{\alpha}_{12,n}^{*(\text{data})}\right)$	(0.479)	(0.461)	(0.447)	(0.432)	(0.413)	(0.393)	(0.374)	(0.356)	(0.341)
	$\hat{\beta}_{12,n}^{*(\text{model})}$	-1.013	-1.152	-1.208	-1.210	-1.176	-1.131	-1.085	-1.047	-1.017
	$\hat{\beta}_{12,n}^{*(\text{data})}$	-0.016	-0.097	-0.169	-0.255	-0.361	-0.483	-0.616	-0.756	-0.898
	$\sigma_{\text{NW}}\left(\hat{\beta}_{12,n}^{*(\text{data})}\right)$	(1.331)	(1.567)	(1.653)	(1.668)	(1.660)	(1.648)	(1.641)	(1.638)	(1.643)
	Joint p-val	0.75	0.79	0.82	0.85	0.89	0.92	0.96	0.98	0.99
		Panel (II): LPY-II regressions								
Nominal bonds	$\hat{\alpha}_{12,n}$	-0.348	-0.554	-0.566	-0.513	-0.442	-0.370	-0.305	-0.249	-0.200
	$\sigma_{\text{NW}}\left(\hat{\alpha}_{12,n}\right)$	(0.668)	(0.663)	(0.627)	(0.580)	(0.527)	(0.478)	(0.425)	(0.389)	(0.361)
	$\hat{\beta}_{12,n}$	2.608	2.470	2.186	1.850	1.509	1.187	0.890	0.617	0.366
	$\sigma_{\text{NW}}\left(\hat{\beta}_{12,n}\right)$	(1.601)	(1.826)	(1.8282	(1.769)	(1.694)	(1.632)	(1.565)	(1.534)	(1.521)
	Joint p-val.	0.59	0.68	0.66	0.63	0.59	0.53	0.45	0.39	0.34
Tips	$\hat{\alpha}_{12,n}^{*}$	0.162	-0.174	-0.320	-0.380	-0.393	-0.382	-0.361	-0.334	-0.307
	$\sigma_{\text{NW}}\left(\hat{\alpha}_{12,n}^{*}\right)$	(0.551)	(0.571)	(0.539)	(0.492)	(0.465)	(0.431)	(0.399)	(0.370)	(0.345)
	$\hat{\beta}_{12,n}^{*}$	2.346	2.508	2.587	2.556	2.444	2.282	2.097	1.905	1.714
	$\sigma_{\text{NW}}\left(\hat{\beta}_{12,n}^{*}\right)$	(1.394)	(1.688)	(1.746)	(1.721)	(1.713)	(1.697)	(1.685)	(1.676)	(1.673)
	Joint p-val.	0.25	0.58	0.65	0.66	0.67	0.67	0.66	0.63	0.60

Notes: This table presents the results of several Campbell-Shiller regressions for LPY-I and LPY-II conditions for excess returns of 12-months holding period (see Dai and Singleton (2002) and Technical Appendix B.8). Panel (I) presents values of intercepts and slopes for LPY-I regressions computed with model-implied parameters (subscript *model*) and with OLS on fitted data (subscript *data*). The joint p-value is the p-value associated with the F-statistic testing whether model-implied and data-implied quantities are equal. Panel (II) presents values of intercepts and slopes for LPY-II regressions computed with OLS on fitted data when the dependent variable is corrected from model-implied expected excess returns. The joint p-value is the p-value associated with the F-statistic testing whether intercepts and slopes are equal to $(0, 1)$.

Figure 12 – Expected liftoff date

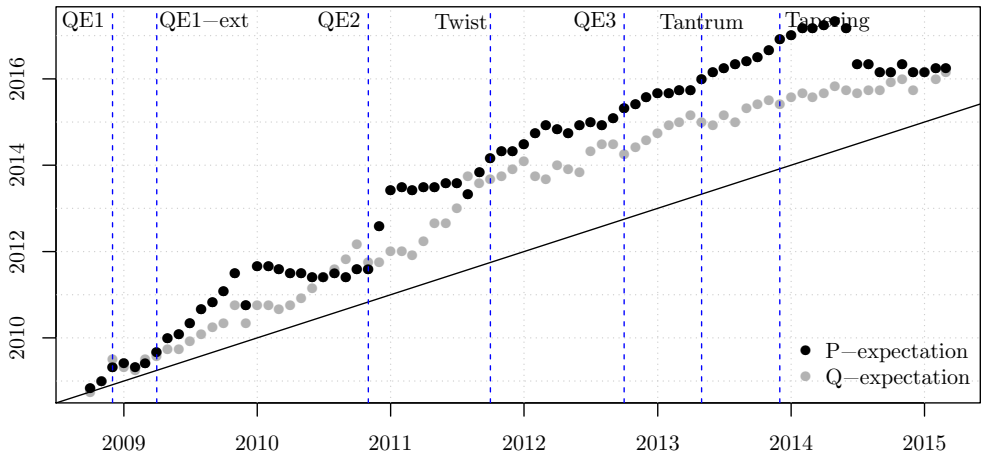

Notes: The black and grey dots represent respectively the physical and risk-neutral expectations of the future liftoff date. The black solid line is the 45 degree line. The blue dashed lines are the different unconventional monetary policy episodes, namely: QE1, QE1-extension, QE2, Operation Twist, QE3, Taper tantrum, and the Tapering.

B.11 QTSM estimates and results

Table 7 – Parameter estimates: X_t dynamics: Standard QTSM

	estimates	std.		estimates	std.
μ_{π^*}	0.0037	(0.0089)	$\mu^{\mathbb{Q}}_{\pi^*}$	0.0037	(0.0089)
μ_{σ}	0	–	$\mu^{\mathbb{Q}}_{\sigma}$	0	–
μ_{y_1}	0	–	$\mu^{\mathbb{Q}}_{y_1}$	0	–
μ_{y_2}	-0.3102^{***}	(0.0703)	$\mu^{\mathbb{Q}}_{y_2}$	-0.3102^{***}	(0.0703)
Φ_{π^*}	0.8724^{***}	(0.0177)	$\Phi^{\mathbb{Q}}_{\pi^*}$	0.9671^{***}	(0.0014)
Φ_{σ,π^*}	0	–	$\Phi^{\mathbb{Q}}_{\sigma,\pi^*}$	0	–
Φ_{y_1,π^*}	0	–	$\Phi^{\mathbb{Q}}_{y_1,\pi^*}$	0	–
Φ_{y_2,π^*}	0	–	$\Phi^{\mathbb{Q}}_{y_2,\pi^*}$	-0.0378^{***}	(0.0027)
$\Phi_{\pi^*,\sigma}$	-0.1136^{***}	(0.0236)	$\Phi^{\mathbb{Q}}_{\pi^*,\sigma}$	-0.1136^{***}	(0.0236)
Φ_{σ}	0.9922^{***}	(0.0022)	$\Phi^{\mathbb{Q}}_{\sigma}$	1.0254^{***}	(0.007)
$\Phi_{y_1,\sigma}$	0	–	$\Phi^{\mathbb{Q}}_{y_1,\sigma}$	1.2678^{***}	(0.262)
$\Phi_{y_2,\sigma}$	0	–	$\Phi^{\mathbb{Q}}_{y_2,\sigma}$	-0.1903^{***}	(0.0434)
Φ_{π^*,y_1}	0	–	$\Phi^{\mathbb{Q}}_{\pi^*,y_1}$	0.0206^{***}	(0.0036)
Φ_{σ,y_1}	-0.0033^{***}	(0.001)	$\Phi^{\mathbb{Q}}_{\sigma,y_1}$	-0.0058^{***}	(0.0014)
Φ_{y_1}	0.9188^{***}	(0.0195)	$\Phi^{\mathbb{Q}}_{y_1}$	0.7499^{***}	(0.0105)
Φ_{y_2,y_1}	0	–	$\Phi^{\mathbb{Q}}_{y_2,y_1}$	0.0198^{***}	(0.0063)
Φ_{π^*,y_2}	0	–	$\Phi^{\mathbb{Q}}_{\pi^*,y_2}$	0.0148^{***}	(0.0035)
Φ_{σ,y_2}	-0.0034^{***}	$(9{\cdot}10^{-4})$	$\Phi^{\mathbb{Q}}_{\sigma,y_2}$	-0.0034^{***}	$(9{\cdot}10^{-4})$
Φ_{y_1,y_2}	-0.0852^{***}	(0.0194)	$\Phi^{\mathbb{Q}}_{y_1,y_2}$	-0.1634^{***}	(0.0208)
Φ_{y_2}	0.9791^{***}	(0.0033)	$\Phi^{\mathbb{Q}}_{y_2}$	0.9791^{***}	(0.0033)
Σ_{π^*}	0.1892^{***}	(0.02)	$\Sigma^{\mathbb{Q}}_{\pi^*}$	0.1892^{***}	(0.02)
Σ_{σ,π^*}	0	–	$\Sigma^{\mathbb{Q}}_{\sigma,\pi^*}$	0	–
Σ_{y_1,π^*}	0	–	$\Sigma^{\mathbb{Q}}_{y_1,\pi^*}$	0	–
Σ_{y_2,π^*}	0	–	$\Sigma^{\mathbb{Q}}_{y_2,\pi^*}$	0	–
Σ_{σ}	0.0083^{***}	(0.0021)	$\Sigma^{\mathbb{Q}}_{\sigma}$	0.0083^{***}	(0.0021)
$\Sigma_{y_1,\sigma}$	0	–	$\Sigma^{\mathbb{Q}}_{y_1,\sigma}$	0	–
$\Sigma_{y_2,\sigma}$	0	–	$\Sigma^{\mathbb{Q}}_{y_2,\sigma}$	0	–
Σ_{y_1}	1	–	$\Sigma^{\mathbb{Q}}_{y_1}$	1	–
Σ_{y_2,y_1}	0	–	$\Sigma^{\mathbb{Q}}_{y_2,y_1}$	0	–
Σ_{y_2}	1	–	$\Sigma^{\mathbb{Q}}_{y_2}$	1	–

Notes: Standard deviations are in parentheses and are calculated using the outer-product Hessian approximation. The '–' sign indicates that the parameter has been calibrated hence does not possess any standard deviation. Significance level: * <0.1, ** <0.05, *** <0.01.

Table 8 – Parameter estimates: short-rate and the prices of risk: Standard QTSM

	r_t dynamics				
	estimates	std.		estimates	std.
α	0.0087***	(0.0013)	κ	0.1867***	(0.0134)
β_{π^*}	0	–	β_{y_1}	-0.0025***	($1{\cdot}10^{-4}$)
β_σ	-0.0122***	(0.0026)	β_{y_2}	0.001***	($2{\cdot}10^{-4}$)
$\underline{r} \cdot 1200$	0.0431***	(0.0103)	$\bar{\pi} \cdot 100$	3.1771***	(0.0946)
	Prices of risk and measurement errors standard deviations				
	estimates	std.		estimates	std.
λ_{0,π^*}	0	–	λ_{0,y_1}	0	–
$\lambda_{0,\sigma}$	0	–	λ_{0,y_2}	0	–
λ_{1,π^*} 0.5001***	(0.1027)		λ_{1,π^*,y_1} 0.109***	(0.0232)	
λ_{1,σ,π^*}	0	–	λ_{1,σ,y_1}	-0.3055***	(0.1203)
λ_{1,y_1,π^*}	0	–	λ_{1,y_1}	-0.169***	(0.0211)
λ_{1,y_2,π^*}	-0.0378***	(0.0027)	λ_{1,y_2,y_1}	0.0198***	(0.0063)
$\lambda_{1,\pi^*,\sigma}$	0	–	λ_{1,π^*,y_2}	0.0781***	(0.0213)
$\lambda_{1,\sigma}$	4.024***	(1.5329)	λ_{1,σ,y_2}	0	–
$\lambda_{1,y_1,\sigma}$	1.2678***	(0.262)	λ_{1,y_1,y_2}	-0.0782***	(0.0213)
$\lambda_{1,y_2,\sigma}$	-0.1903***	(0.0434)	λ_{1,y_2}	0	–
λ_r	0	–			
σ_R	0.0617***	($9{\cdot}10^{-4}$)	σ_R^*	0.1262***	(0.0034)
$\sigma_\pi^{(12)}$	0.509	–	$\sigma_\pi^{(120)}$	0.389	–
$\sigma_{S_R}^{(3)}$	0.231	–	$\sigma_{S_R}^{(12)}$	0.422	–
σ_{ZLB}	0.0522	–			

Notes: Standard deviations are in parentheses and are calculated using the outer-product Hessian approximation. The '–' sign indicates that the parameter has been calibrated hence does not possess any standard deviation. Significance level: * <0.1, ** <0.05, *** <0.01.

Table 9 – Model fit and characteristics: standard QTSM

Maturities (months)	1	12	24	36	60	84	120
Nominal rates RMSE (bps)	8.09	8.28	4.93	6.25	5.74	3.83	6.08
Real rates RMSE (bps)	-	17.87	7.76	7.94	11.66	10.67	9.42
Probabilities (in %)	$\mathbb{P}(r_t < 0.25\%) = 9.45$						

Note: Probabilities are calculated with simulated paths of length 100,000.

Figure 13 – Filtered factors: standard QTSM

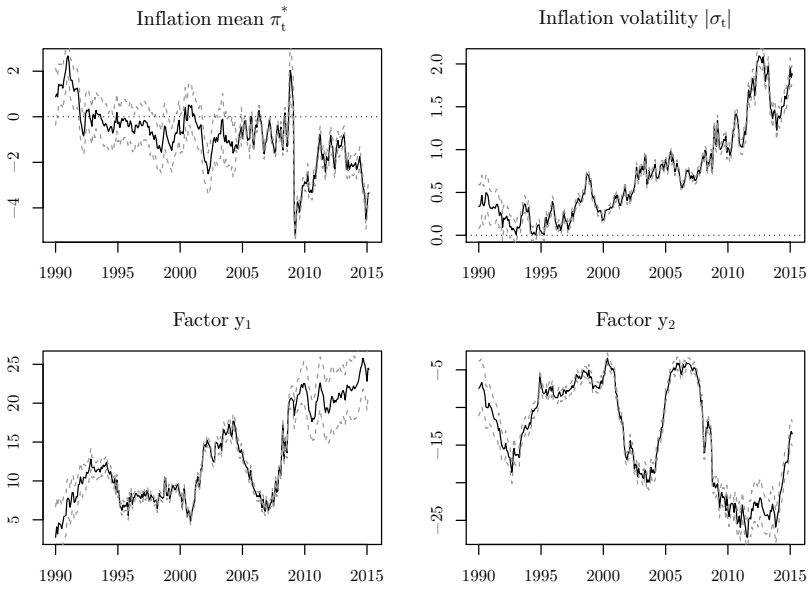

Notes: The unit for inflation central tendency π_t^* and inflation volatility σ_t is in percentage points. Grey dashed lines are 95% confidence bands. The red vertical line delimits the beginning of the zero lower bound period.

Figure 14 – Factors loadings of yields: standard QTSM

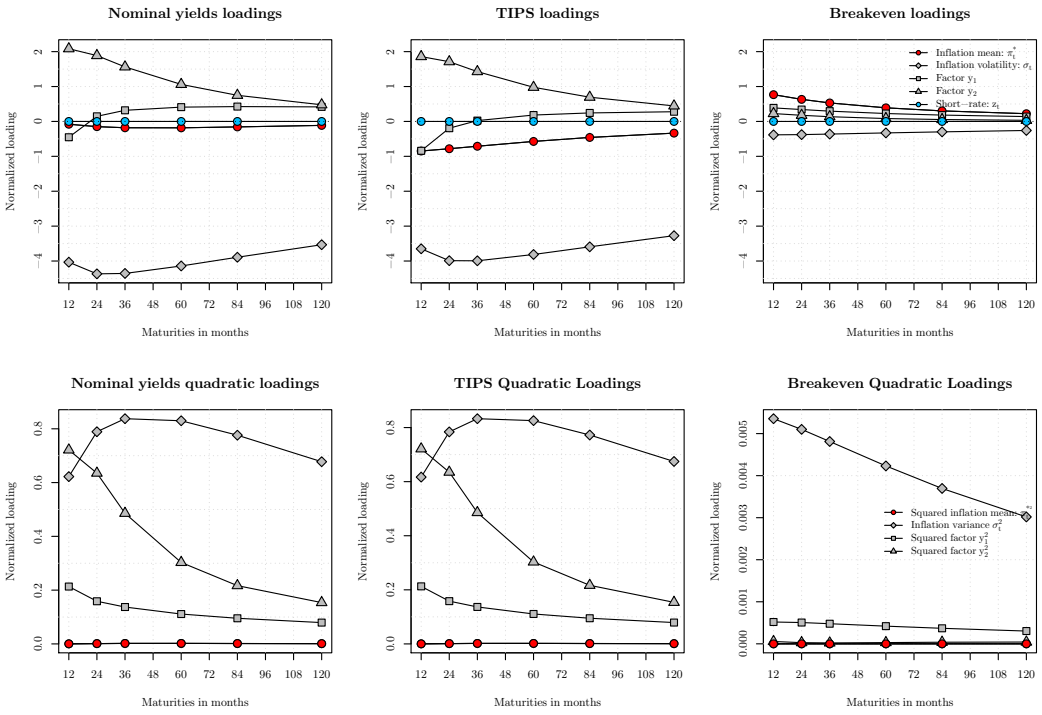

Notes: This plot gathers the linear loadings of the nominal interest rates, of the real rates, and the quadratic loadings with respect to maturity. These loadings are normalized by the in-sample standard deviation of the corresponding filtered factor to be comparable with each other.

Figure 15 – Fitted series of survey data: standard QTSM

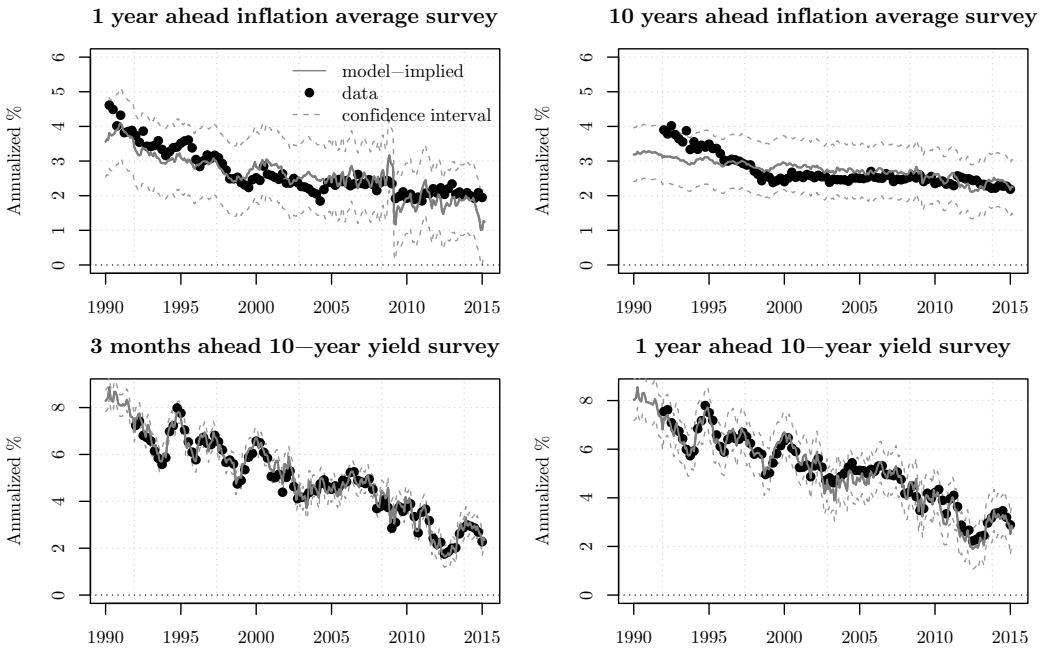

Notes: The black dots correspond to observed forecast data. The grey solid lines correspond to the model-implied forecasted values. Top graphs correspond respectively to the one-year ahead and 10-year ahead inflation average surveys. Medium graphs correspond respectively to the three-months ahead and one-year ahead 10-year yield survey. Units are in annualized percentage points. Bottom graphs correspond respectively to the fitted natural logarithm of ZLB probabilities, and of the exponential of the latter. Confidence intervals computed using the measurement errors standard deviations are plotted in grey dashed lines. The red vertical line delimits the beginning of the zero lower bound period.

Figure 16 – Distribution of short-term interest rates and inflation: standard QTSM

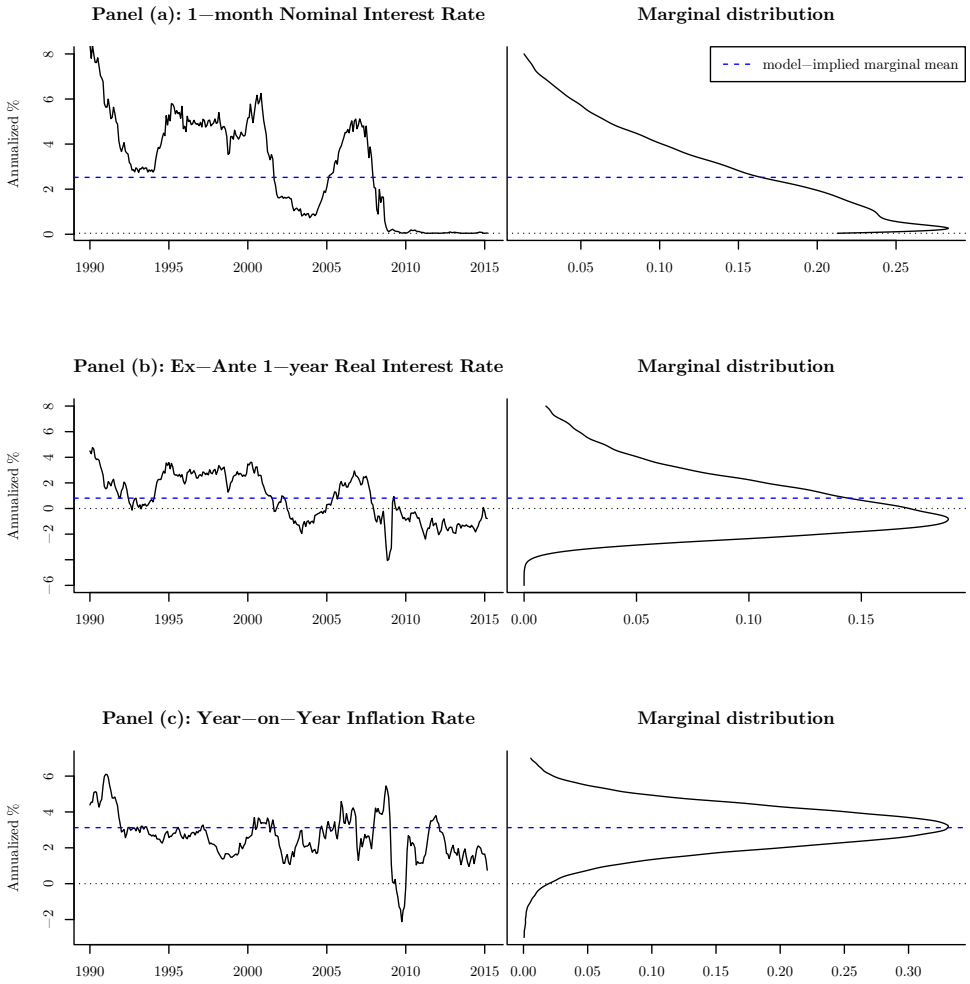

Notes: Marginal distributions on the right-hand side are compute with kernel density estimates on 100,000 simulations.

Figure 17 – Campbell-Shiller regression slopes: standard QTSM

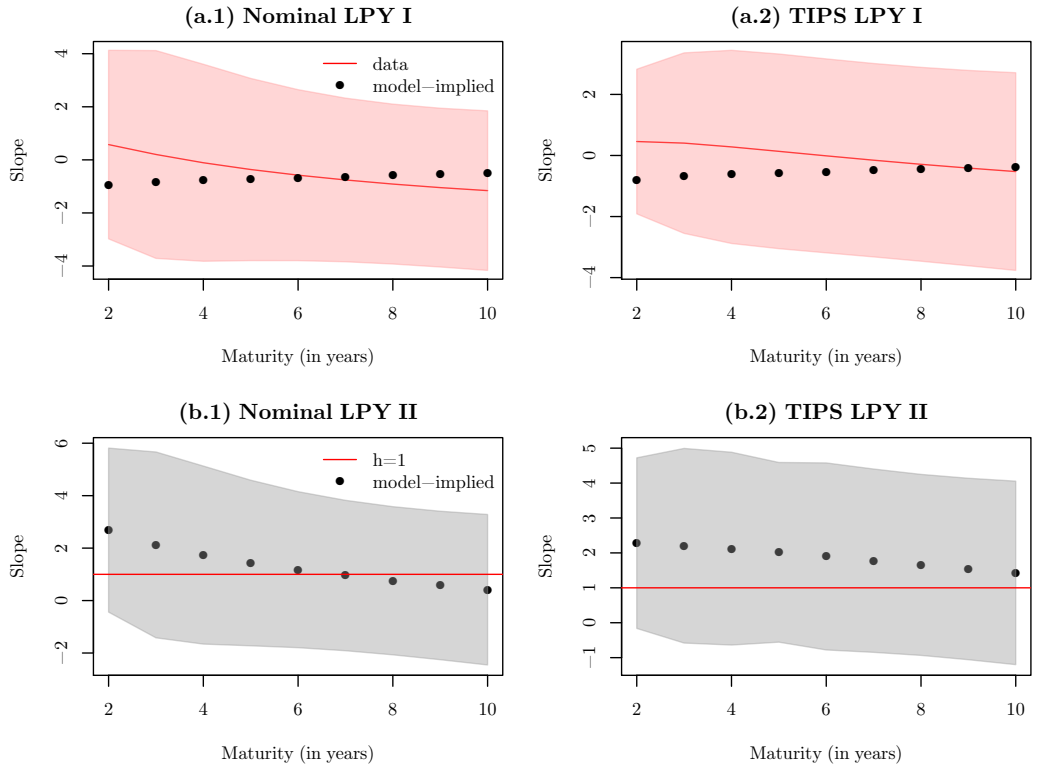

Notes: These graphs present the slopes of Campbell and Shiller regressions with a 12-months holding period. On panel (a), the red solid line gathers the slope estimates obtained with yields data. 95% Confidence intervals are computed using Newey-West robust estimators with automatically selected lag and are indicated with the red-shaded areas. Model-implied estimates are indicated with the black dots and computed with the yields and inflation expectation and variance formulas. On panel (b), the red solid line represents the theoretical values of the regression, namely one for all maturities. Model-implied estimates are indicated with the black dots and computed performing the Campbell and Shiller regressions where the dependent variable is adjusted by the model-implied expected excess returns. 95% Confidence intervals are computed using Newey-West robust estimators with automatically selected lag and are indicated with the grey-shaded areas.

Figure 18 – Decomposition of interest rates: standard QTSM

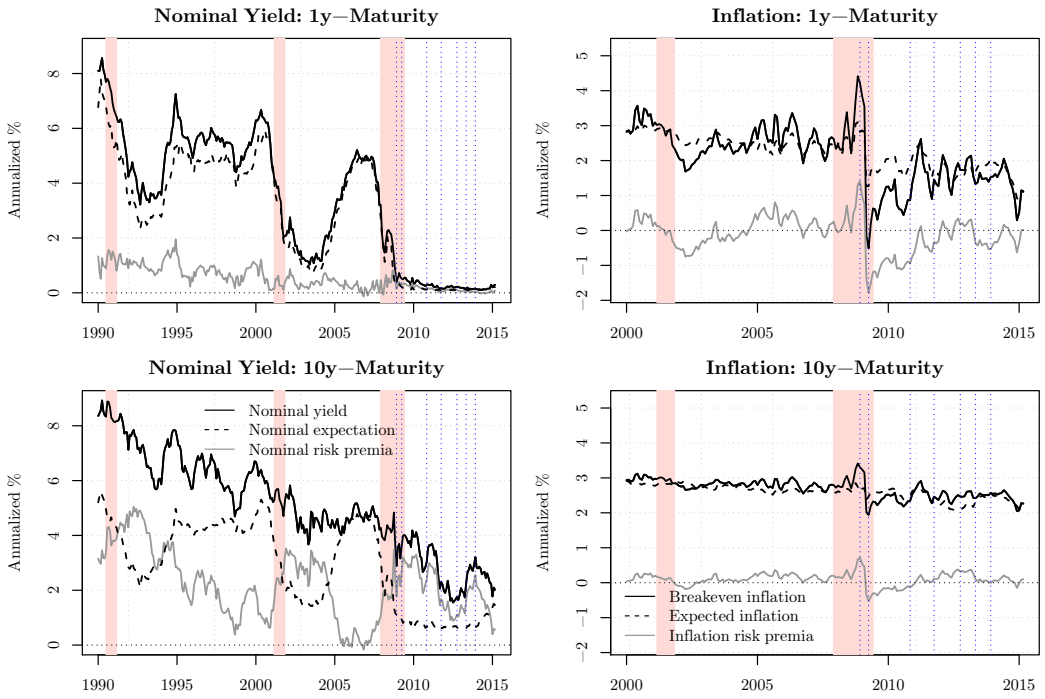

Notes: The first column presents results for the nominal yields components, whereas the second column presents results for the inflation components. The first row presents to the observed data (black solid line), the risk premia (grey solid line), and the expected component (black dashed line) at the one year maturity. The second row presents the same components at the 10 year maturity. Units are in annualized percentage points. The red vertical line delimits the beginning of the zero lower bound period. Pink shaded areas are NBER recession periods. The blue dashed lines are the different unconventional monetary policy episodes, namely: QE1, QE1-extension, QE2, Operation Twist, QE3, Taper tantrum, and the Tapering.